

The hydrographic structure along the 137° E line in the western North Pacific from 1990 to 2007

Lamona I. BERNAWIS^{1,2)}, Masao NEMOTO¹⁾ and Jiro YOSHIDA¹⁾

Abstract : We examined detailed hydrographic structures data along 137°E from 3°N to 34°N from 1990 to 2007 by using CTD. The general oceanic features found along this line agreed well with the results of previous studies using Nansen bottle data. We investigated the activity of double diffusive convection through the histogram plots of the density ratio (R_ρ) and the Turner angle (Tu) to detect the modification processes of water masses in more detail. The region where the stratification is favourable for the onset of salt finger convection ($R_\rho > 3.7$ and $45^\circ < Tu < 60^\circ$) is found just below the bottom half of North Pacific Equatorial Water (NPEW) and North Pacific Tropical Water (NPTW) extending to the upper half of North Pacific Intermediate Water (NPIW). This region existed isopycnally on the surface between $24.0 \sigma_\theta$ and $26.8 \sigma_\theta$ persistently along 137°E line. The mode value of R_ρ is 3.48, meaning that the activity of salt finger convection was not so high.

Keywords : JMA 137° E section, CTD, NPIW core, double diffusive convection, salt finger.

1. Introduction

The western Pacific Ocean is a region which dominates the dynamics of the climate system in the world. For example, the equatorial processes releasing heat by rain drives the so-called Walker Circulation, and then the equatorial currents redistribute heat. The inter-annual variability of currents and temperatures in the equatorial Pacific modulates the oceanic forcing to the atmosphere; El Niño, for example causes the biggest changes in the equatorial dynamics. In the mid- and high latitude regions, the subtropical and the subarctic gyres redistribute heat from the low latitude to moderate the weather system there (STEWART, 2005).

The current system in the western equatorial Pacific consists of at least four major cur-

rents: (1) the North Equatorial Current (NEC) flowing westward between about 20° and 8°N which corresponds to the southern rim of the subtropical gyre, (2) the South Equatorial Current (SEC) flowing westward from about 3°N to 10°S, (3) the narrower North Equatorial Counter Current (NECC) flowing eastward between them, and (4) the Equatorial Under Current (EUC) flowing eastward below the surface straddling the equator over 2°N~2°S. In the region between 20 and 26°N, there is an eastward flowing current known as the Subtropical Counter Current (STCC). The NEC bifurcates into the northward flowing Kuroshio and the southward flowing Mindanao Current. The Kuroshio flows along the Japanese coast, and changes its direction to east off the Joban and Sanriku coast of Japan to form the Kuroshio Extension (KE). The westward counter current known as the Kuroshio Counter Current (KCC) flows between 25 and 30°N. The KE continues to flow eastward as the North Pacific Current (NPC, the northern rim of the subtropical gyre). To the north of subtropical gyre, the subarctic gyre is formed having the

1) Department of Ocean Sciences, Tokyo University of Marine Science and Technology, 4-5-7 Konan, Minato-ku, Tokyo 108-8477, Japan

2) Bandung Institute of Technology, Gedung Labtek XI lt.1, Jl. Ganesha 10, Bandung 40132, Jawa Barat-Indonesia

Jiro YOSHIDA. E-mail: jiroy@kaiyodai.ac.jp

Oyashio as another western boundary current flowing from the eastern coast of Hokkaido to south.

Some major water masses exist in the western Pacific. The North Pacific Intermediate Water (NPIW) is a low salinity water (33.80~34.10) characterized as a vertical salinity minimum around the mid depth (300 m~800 m) originated from the subpolar region (e.g., SVERDRUP *et al.*, 1942) extending from 130°E~130°W and 10°N~45°N. Talley (1993) suggested that the Oyashio Winter Water is the source of NPIW, and in the mixed water region between the Kuroshio Extension and the Oyashio front it is modified through some mixing processes to acquire the characteristics of NPIW. This water intrudes into the subtropical gyre as a cross gyre flow and spreads into the mid-depth of the western North Pacific. REID (1965) pointed out that the salinity minimum could be traced on a 26.8 σ_θ surface. The Subtropical Mode Water (STMW) is a minimum of potential density gradient in the 100–400 db layer extending from 130~180°E and 20°N–40°N (MASUZAWA, 1969). The North Pacific Tropical Water (NPTW) is a subsurface salinity maximum (>35.0) water on a 24.0 σ_θ surface caused by excess evaporation over precipitation and by long residence of the surface water in the central Pacific in the 100–200 db layer extending from 130~180°E and 10~25°N (TSUCHIYA *et al.*, 1989). The North Pacific Central Water (NPCW) is a thermocline layer between the NPTW and the NPIW extending from 35°N to 15°N (e.g., SVERDRUP *et al.*, 1942). The North Pacific Equatorial Water (NPEW) is a subsurface salinity maximum (>35.4) at a depth of 150 db from the equator to the south of NPTW covering the whole equatorial Pacific Ocean (e.g., SVERDRUP *et al.*, 1942). The variability and modification of these water masses have been attractive subjects in this area.

Since 1967, the Japan Meteorological Agency (JMA) has been carrying out winter oceanographic surveys along the 137°E from the southern coast of Japan to the area off the New Guinea coast using the R/V Ryofu Maru and Keifu Maru. From 1972, summer observations have begun. Some studies have been conducted using this section to detect the variability of

current systems and major water masses cited above (e.g., MASUZAWA, 1969; SUGA *et al.*, 1989; QIU and JOYCE, 1992; Suga and Hanawa, 1995; SHUTO, 1996; BINGHAM *et al.*, 2002).

QIU and JOYCE (1992) extensively analysed the hydrographic features along 137°E observed from 1967 to 1988. Their main purpose was to identify the inter-annual fluctuations in the Kuroshio and KCC, and to understand their relation to the change of the path of the Kuroshio. They also discussed the inter-annual fluctuation in the low latitudes: fluctuation in the transport of NEC and NECC, the surface dynamic height anomalies and the upper mixed layer thickness associated with the ENSO events. Using an analytical model, they found that the inter-annual fluctuations of NEC and NECC were highly correlated with the Sverdrup transport fluctuations. They also discussed the variability of water masses cited above.

SHUTO (1996) used this section to analyse the inter-annual variability of temperature and salinity to discuss the relationship between these variations and the wind forcing. He showed that the temperature changes occurred in the equatorial region of the western North Pacific accompanied by El Niño and La-Niña events, which reached about 20°N where the inclination of isotherms across the NEC fluctuates there. The Empirical Orthogonal Function (EOF) analysis of the winter water temperature resulted in the interruption El Niño and La-Niña events as the first mode, and the decadal changes in SST in the North Pacific as the second mode.

The classical hydrographic observation had been conducted using reversing thermometers and Nansen casts, therefore, QIU and JOYCE (1992) and SHUTO (1996) were obliged to apply the cubic spline fit to vertical discrete data to obtain smooth profiles. Consequently, there were inherent difficulties in detailed analysis such as a variability of the modification process of water masses. This point has been improved by the introduction of CTD observation from 1988. CTD observation becomes as a routine base from 1990. Therefore, taking the advantage of successive CTD data, we try to make detailed water mass analysis using a density

ratio R_ρ (Turner angle: Tu) to grasp the modification processes of major water masses in the present study.

The density ratio or the Turner angle is an indicator of the activity of double diffusive convection (RUDDICK, 1983). The double diffusive convection has two forms; one is the salt finger convection that occurs when a layer of warm and salty water overlies on a layer of relatively cool and fresh water. Another is the diffusive oscillatory convection that occurs when a layer of cool and fresh water overlies on a layer of relatively warm and salty water. For both convections, a fluid layer is statically stable; however, due to the faster diffusion of heat than that of salt give rise to the onset of convection. In both cases, the lower layer becomes dense (up-gradient of density stratification) irrespective of the basic stable stratification. Then, the double diffusive convection should have a certain role in the modification of water masses.

From this point of view, FIGUEROA (1996) and YOU (2002) have investigated the distributions of the density ratio in the world ocean. They showed that double diffusive convection is not so active in the North Pacific ($R_\rho \approx 3\sim 4$) except at some places where the water masses having distinct contrasts in properties directly contact. The region off Joban-Kashima and Sanriku coast is such a place where the warm/salty Kuroshio and relatively cold/fresh Oyashio waters directly contact each other forming many temperature inversion layers and interleaving structures. Then, these regions are favourable for the onset of double diffusive convection. TALLEY and YUN (2001) and INOUE *et al.* (2003) focused their attention to this point and investigated the role of double diffusive convection on the modification process of NPIW. They both showed that cabling and double diffusive convection could explain the total increment of density of NPIW while it extends from the subarctic region to the Sanriku coast. As was mentioned above, various water masses exist along 137°E, and the double diffusive convection should occur in the area sandwiched with the NPTW and NPIW and that below the NPEW. Therefore, in the present paper, focusing on the activity of dou-

ble diffusive convection along 137°E, we will examine the role of these phenomena on the variability and modification of water masses along 137°E. We describe data analysis process in section 2, followed by hydrographic structures along 137°E from 1990 to 2007 in section 3. We show the characteristics of annual mean and seasonal structures and those associated with ENSO occasionally referring to the previous studies cited above. In section 4, histogram analysis of the density ratio (the Turner angle) is presented to investigate the activity of double diffusive convection. In section 5, we will summarize the results.

2. Data Analysis

We use 35 CTD data from summer and winter cruises (1990–2007) in this study. Basic data by CTD on temperature and salinity at 1 db interval are distributed in ASCII format through CD. Temperature data are converted into potential temperature (θ) and then, potential density is calculated. Stations are located from 34 to 3°N with 1° interval in latitude, except for 40' in the Kuroshio region between 34–32°N. We will use this basic data set for detecting the variability of hydrographic structures. We also use two types of data set: seasonal average data sets at each station and at each depth. The ENSO event average data set in which averaging was made for El Niño, La Niña and Normal periods according to the JMA's criterion of categorizing ENSO event. Since 2006, the JMA has changed the standard for the definition of ENSO event in a certain year from that based on the deviation from 30 years average of 1961~1990 to that of 30 years starting from the year before. Based on this, detailed ENSO events are as follows: El Niño: April 1991 – July 1992, April 1997 – May 1998, June 2002 – February 2003; La Niña: Jul 1995 – February 1996, August 1998 – April 2000, October 2005 – March 2006, February 2007 – March 2008. The other periods are categorized as “Normal”. Following QIU and JOYCE (1992), we divide the observational stations into seven bins (Area A – Area G) at an 5° interval (Fig.1).

Following Ruddick (1983), the density ratio and the Turner angle are defined :

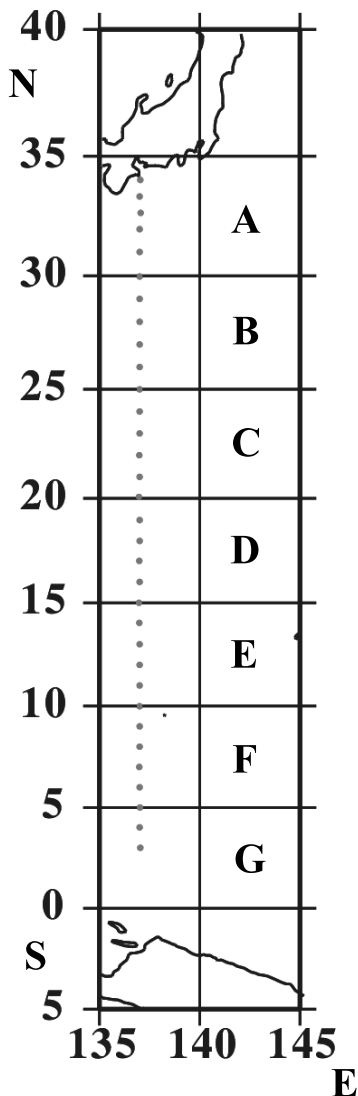


Fig. 1. CTD observation stations along 137°E. Seven areas from A – G are shown.

Density ratio $R_\rho = \frac{\overline{\alpha\theta_z}}{\beta\overline{S_z}}$, where $\alpha = \frac{1}{\rho} \frac{\partial\rho}{\partial\theta}$ and

$$\beta = \frac{1}{\rho} \frac{\partial\rho}{\partial S};$$

Turner angel $Tu = \tan^{-1} \left(\frac{R_\rho + 1}{R_\rho - 1} \right)$,

where $\overline{\theta_z}$ and $\overline{S_z}$ are mean vertical gradients of potential temperature and salinity, respectively. α and β are the thermal expansion and

haline contraction coefficients, respectively. The least square fit over 11 db data is adapted to obtain the mean temperature and salinity gradients. Note that the density ratio is defined as a ratio of temperature gradient on density divided by that of a salinity gradient. When R_ρ is larger than 1 (Tu ranges between 45 and 90°), the salt finger convection occurs, and when R_ρ ranged between 1 and 0 (Tu ranges between -45 and -90°), the diffusive convection occurs. The activity of both convection is intensified as R_ρ becomes unity. Especially, when R_ρ ranged between 1 and 2 (Tu ranges between 72° and 90°), the salt finger convection is so active that salt and heat are efficiently transported downwards and when R_ρ ranges between 0.5 and 1 (Tu ranges between -72 and -90°), diffusive convection is active to transport heat and salt effectively upward. In the present study, Tu is calculated down to 1000 db, because in the Pacific Ocean, the layer below 1000 db is usually statically stably stratified. Histogram plots of Turner angle is presented to know the activity of double diffusive convection. Tu is divided at one degree interval from -90° to 90°, and the number of Tu which falls into each one degree bin is counted, and is divided by the total data number to obtain the occurrence frequency. In this process no averaging was made at each station and at each depth.

3. Hydrographic structures along the 137°E section

3.1 Mean structures of currents and water masses

The basic hydrographic structures seen from the mean of summer/winter cruises are similar to those obtained by QIU and JOYCE (1992). The upheaval of thermocline at 8°N indicates the upwelling region that forms a boundary between the NEC and the NECC (Fig. 2 (a)). The 28°C isotherm at the surface layer marks one of the characteristics features of the western equatorial Pacific Ocean so-called warm pool. The variability of this warm pool is related to the ENSO event. Upward inclinations of isotherms toward north from the surface layer down to a depth of 300 db from 17°N to 25°N indicate the STCC. The thermocline rises sharply

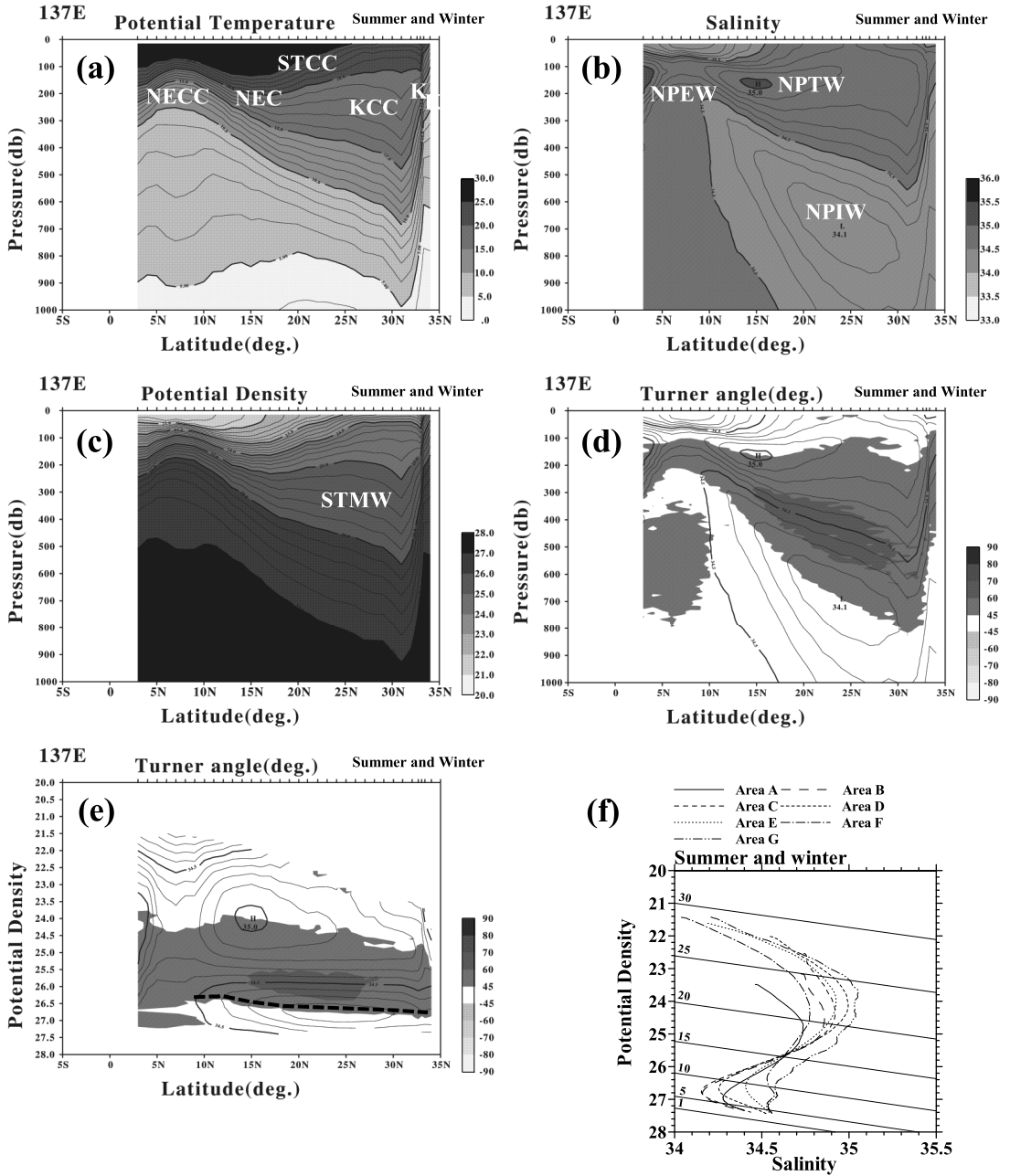


Fig. 2. Vertical cross sections in summer/winter average: (a) potential temperature (interval : 1°C), (b) salinity (interval : 0.1), (c) potential density (interval : 0.1 σ_θ), (d) Turner angle (interval: 10 degree) overlaid on salinity distribution, (e) Turner angle (interval: 10 degree) overlaid on salinity distribution taking σ_θ for the vertical axis and (f) potential density-salinity relation in each area. Solid curves in this figure show potential temperature. Dashed line in Fig.2 (e) indicates the extension of salinity minimum. K : Kuroshio, KCC : Kuroshio Counter Current, STCC : Sub-Tropical Counter Current, NEC : North Equatorial Current, NECC: North Equatorial Counter Current, NPIW : North Pacific Intermediate Water, NPTW : North Pacific Tropical Water, NPEW : North Pacific Equatorial Water, STMW : Sub-Tropical Mode Water.

from about 31°N to the Japanese coast, indicating the location of Kuroshio (here, abbreviated as K). The KCC flows westward between 27° N and 31°N.

Two shallow salinity maximums having distinct cores exist near the equator at 150 db and at around 15°N at 160 db (Fig. 2 (b)), respectively. The former corresponds to the NPEW with a salinity exceeding 35.09, and the latter to the NPTW with a salinity exceeding 35.02. The NPEW extends from 3°N to 5°N and its vertical extension is from 80 db to 250 db. QIU and JOYCE (1992) showed that the maximum salinity of the core of NPEW exceeds 35.4 and its location extends from the equator to 5°N. This means that only the northern fraction of NPEW is observed in Fig. 2 (b). In contrast to this limiting extension of NPEW, the NPTW extends broadly from 9°N to 25°N, and its core exist between 13°10'N and 16°40'N. The vertical extension of NPTW is from the surface (at about 25°N) to 300 db (at about 31°N). These two cores of salinity maximums are found roughly at the same isopycnal surface ($24.0\sigma_\theta$, Fig. 2 (e)); however, the NPEW exists on rather broad isopycnal layers between 22.6 and $25.9\sigma_\theta$, and the NPTW between 22.6 and $25.3\sigma_\theta$.

In the region from 20 to 30°N and between the depths of 160 and 400 db, the gradient of potential density is weak (Fig. 2 (c)). This water mass is the STMW. SUGA *et al.* (1989) pointed out that a major part of the STMW appearing in this section is formed in the previous winter, and is advected through the KCC.

We can see a broad extension of salinity minimum region from 30°N at a depth of 850 db steeply ascending towards 9°N to a depth of 200 db (Fig. 2 (b)). This salinity minimum water is the NPIW. The core of NPIW (salinity < 34.14) lies almost on the $26.8\sigma_\theta$ isopycnal surface indicating the extension of the NPIW is essentially an isopycnal process (Fig. 2 (e)); however, it should be noted that the density of salinity minimum become decreased to the south of 15°N.

The region where the stratification is favourable for the onset of salt finger convection ($R_\rho > 3.7$ and $45^\circ < Tu < 60^\circ$) is found in the bottom half of NPEW and NPTW (Fig. 2 (d)).

This region extends to the upper half of the NPIW connecting to the bottom half of the NPEW. Below the NPEW, this region is seen at depths between 400 and 700 db from 3°N to 10°N. The region where relatively active salt finger convection can exist ($3.7 > R_\rho > 2.7$ and $60^\circ < Tu < 70^\circ$) is found just above the core of NPIW between 15 and 30°N. This area is essentially found on isopycnal layers between $25.5\sigma_\theta$ and $26.2\sigma_\theta$ (Fig. 2 (e)).

A mean potential density-salinity curve was determined for each area (Fig. 2 (f)). A subsurface salinity maximum exists at all areas. It is lowest at Area A (34~30°N) with highest value of density ($S \sim 34.73$, $\sigma_\theta \sim 24.78$) and becomes more saltier, but less dense towards south ($S \sim 35.00$, $\sigma_\theta \sim 24.14$) at Area D (20~15°N, NPTW). It becomes less salty at Area E ($S \sim 34.92$, $\sigma_\theta \sim 24.00$, NPTW) to Area F ($S \sim 34.77$, $\sigma_\theta \sim 24.35$). At Area G, the subsurface salinity maximum (NPEW) is highest (~ 35.05) and σ_θ is lowest ($\sim 23.66\sigma_\theta$). A salinity minimum ($S \sim 34.15$) corresponding to the core of NPIW is found on $26.8\sigma_\theta$ surface at Area B and C (30~20°N). This salinity minimum becomes saltier and less dense towards Area D ($S \sim 34.25$ and $\sim 26.67\sigma_\theta$) and Area E ($S \sim 34.40$ and $\sim 26.58\sigma_\theta$). This feature is also seen in Fig. 2 (e) as a slight upward inclination of a trace of salinity minimum (a dashed line) towards south. This means that the core of NPIW gradually increases its salinity and temperature transported downward in the course of spreading to the south, suggesting the salt finger convection might have a role in this modification process. These values are summarized in Table 1 together with those for summer and winter averages. At Areas F and G, weak salinity maximums ($S \sim 34.59$) are found at $26.88\sigma_\theta$ and salinity minimums ($S \sim 34.52$) at $27.2\sigma_\theta$ surface. In a layer sandwiched by these minimums and maximums, favorable condition for the onset of salt finger convection is satisfied (Fig. 2 (d)).

3.2 Seasonal structures of currents and water masses

The appearances of currents seen in summer average and winter average (Fig. 3) are essentially same as those in summer/winter

Table 1. Changes in the salinity maximum (S_{\max}), salinity minimums (S_{\min}) and potential density (σ_{θ}) from Area A through Area G.

Summer and winter

			NPTW	NPTW	NPTW		NPEW
	Area A	Area B	Area C	Area D	Area E	Area F	Area G
S_{\max}	34.73	34.86	34.92	35.00	34.92	34.77	35.05
σ_{θ}	24.78	24.47	24.35	24.14	24.00	24.35	23.66
	NPIW	NPIW	NPIW	NPIW	NPIW		
S_{\min}	34.27	34.15	34.15	34.25	34.40	34.53	-----
σ_{θ}	26.94	26.80	26.75	26.67	26.58	26.34	-----

Summer

			NPTW	NPTW	NPTW		NPEW
	Area A	Area B	Area C	Area D	Area E	Area F	Area G
S_{\max}	34.74	34.87	34.93	34.99	34.94	34.81	35.08
σ_{θ}	24.97	24.51	24.34	24.10	24.06	24.12	24.43
	NPIW	NPIW	NPIW	NPIW	NPIW		
S_{\min}	34.28	34.16	34.15	34.25	34.40	34.53	-----
σ_{θ}	26.93	26.80	26.76	26.72	26.57	26.39	-----

Winte

			NPTW	NPTW	NPTW		NPEW
	Area A	Area B	Area C	Area D	Area E	Area F	Area G
S_{\max}	-----	-----	34.91	35.00	34.94	34.75	35.08
σ_{θ}	-----	-----	24.33	24.16	24.08	24.36	23.91
	NPIW	NPIW	NPIW	NPIW	NPIW		
S_{\min}	34.27	34.15	34.15	34.25	34.39	34.53	-----
σ_{θ}	26.93	26.81	26.78	26.68	26.59	26.38	-----

averages (Fig. 2); however, the STCC seems to be weakened in winter because the development of mixed layer seems to suppress the upheaval of the isotherms (isopycnals, Fig.3 (c) and (d)). Recently, NOH *et al.* (2007) used eddy-resolving OGCM to reproduce the inter-annual variability of STCC. They showed that the eddy kinetic energy (EKE) in general is highest in summer and lowest in fall, but the value of EKE showed a variation with latitude. Near 19°N, the EKE is highest in summer and lowest

in winter that is coincided with our results qualitatively.

Mean structures of water masses in summer is also essentially same as those in summer/-winter averages, except that a high temperature water exceeding 25°C extends farther north to the Kuroshio region (Fig. 3 (a)). In winter, as was mentioned above, the surface mixed layer develops to a depth of 180 db at 31°N and gradually shallows toward south (Fig. 3 (b)). As a consequences of the deepening

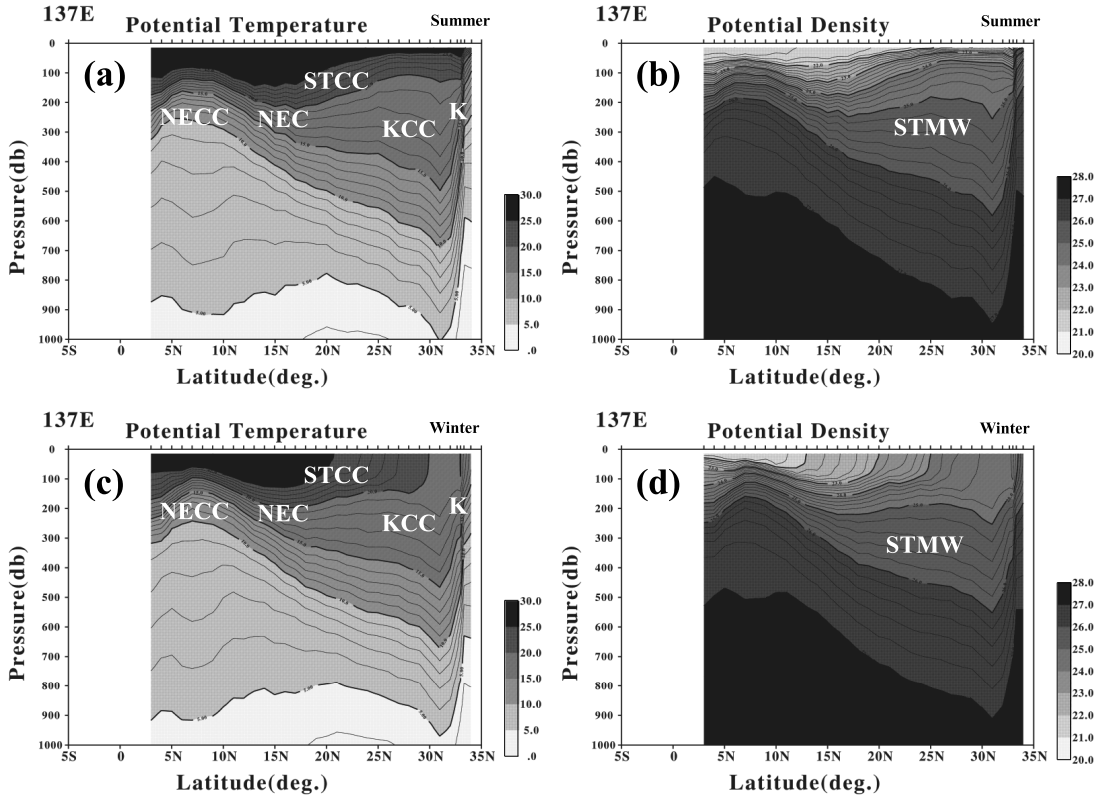


Fig. 3. Vertical cross sections of (a) potential temperature and (b) potential density in summer, and (c) potential temperature and (d) potential density in winter. Abbreviations in the figure are as same as in Fig. 2.

of the mixed layer, the gradient of potential density in the STMW area becomes large (for example, the upheaval of $25.0\sigma_\theta$ is suppressed around 25°N at a depth of 200 db), suggesting the weakening of the STMW in winter (Fig. 3 (d)). The salinities at the cores of NPTW, NPEW and NPIW do not change seasonally; however, σ_θ at these cores slightly changed especially for the salinity maximums of NPTW and NPEW (Table 1). The slight upward inclination of salinity minimum of NPIW is also seen in summer and winter, respectively (not shown here).

3.3 ENSO composite structures of currents and water masses

In the summer of El-Niño periods (1991, 1992, 1998, 2002), upheaval of isotherms intensified in the surface layer between 30 and 25°N

forming a distinct boundary between the KCC and the STCC (Fig. 4 (a)), suggesting these currents become strong during the El-Niño summer. QIU and JOYCE (1992) calculated the geostrophic transport of KCC, and showed that the KCC has a tendency of increasing its transport in summer, but strongly affected by the Kuroshio path, namely, in a meandering year, the KCC reduces its transport. However, they did not show any tendency of variability of geostrophic transport of KCC among El-Niño, La-Niña and Normal periods. Thermal structure in La-Niña and Normal summer is almost identical (Fig. 4 (c) and 4 (e)). In the winter of El-Niño periods, the area of high temperature layer ($>25^\circ\text{C}$) does not reach beyond 20°N as is so for La-Niña and Normal periods (Figs. 4 (b), 4 (d) and 4 (f)).

Salinity distributions show changes in the

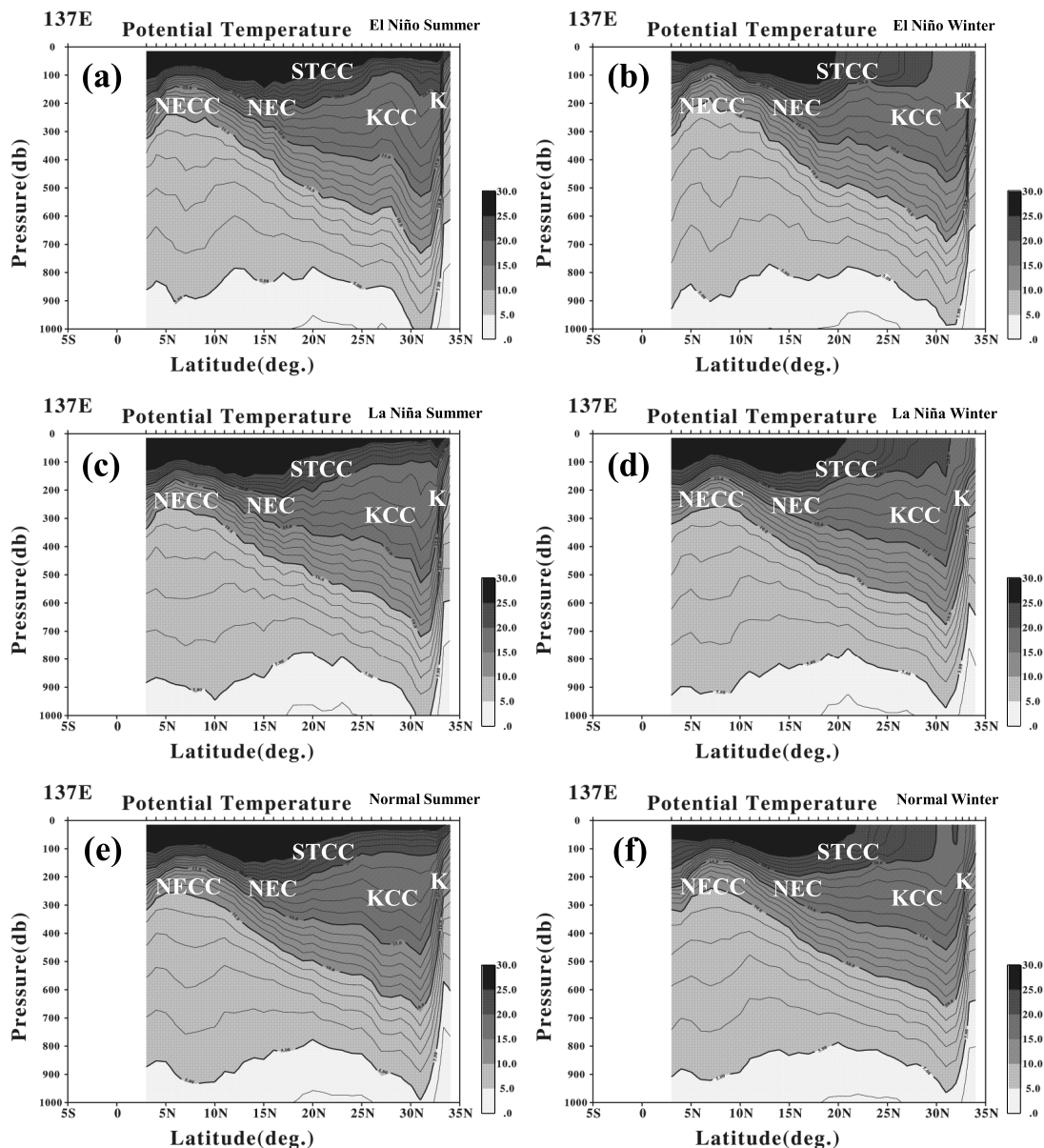


Fig. 4. Vertical cross sections of potential temperature in (a) El Niño summer and (b) El Niño winter, (c) La Niña summer, and (d) La Niña winter, (e) Normal summer and (f) Normal winter. Abbreviations in the figure are as same as in Fig. 2.

surface layer above 300 db during ENSO periods. A low salinity water (<34.00) appears at the surface between 3 and 11°N in La-Niña summer and between 7 and 11°N in La-Niña winter suggesting the excess precipitation in the equatorial area during La-Niña periods

(Fig. 5 (c) and (d)). In El-Niño periods, low salinity water patches appeared at a depth of 200 db (Figs. 5 (a) and (b)) near 5°N. This water is found at almost same density surface to that of NPIW centered on 26.5 σ_θ isopycnal surface (Figs. 6 (a) and (b)). The formation or

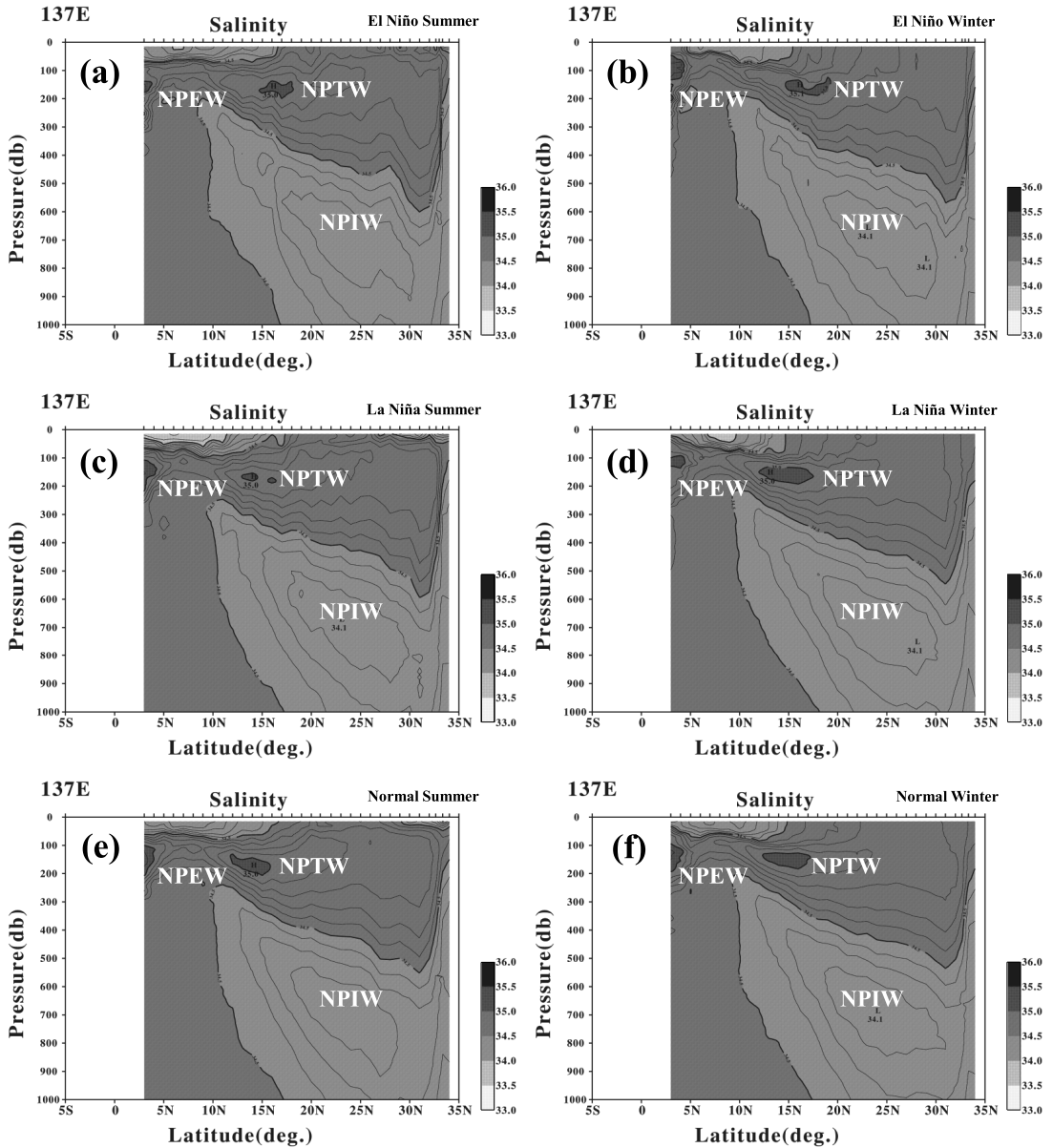


Fig. 5. Same as in Fig. 4, but for salinity.

transportation mechanism of this low salinity water in El-Niño periods is unclear at present. Salinity distributions in Normal summer and winter (Figs. 5 (e) and (f)) are almost identical to those of summer/winter average (Fig. 2 (b)).

Mean potential temperature-salinity curves

were determined for each area, and at Area G, distinct ziggy structures are found during El-Niño periods (Fig. 7 (a) and (b)). These structures are also found in La-Niña and Normal periods to the lesser extent (Fig. 7 (c), (d), (e) and (f)), indicating the high variability of equatorial region especially during El-Niño

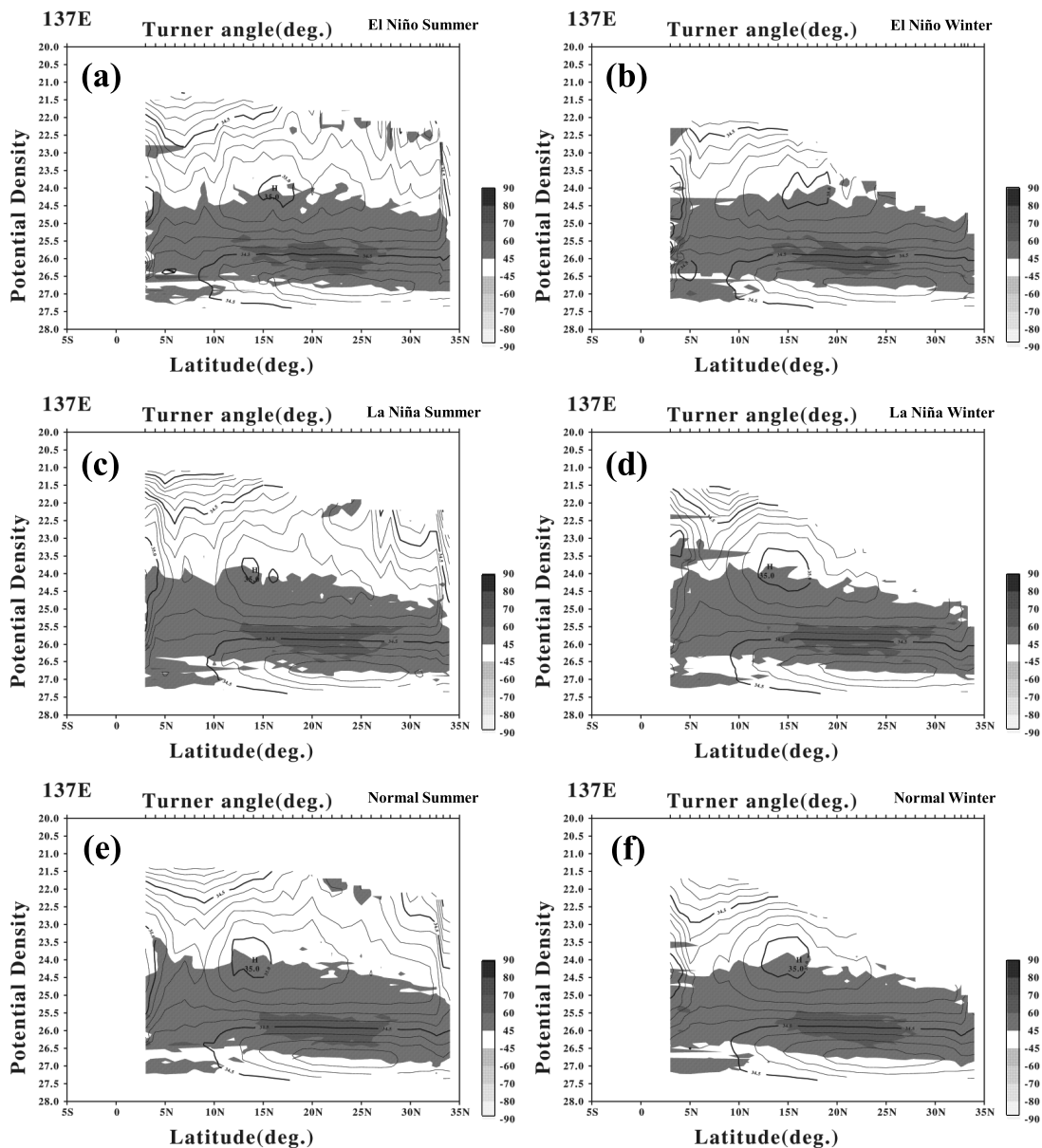


Fig. 6. Same as in Fig. 4, but for Turner angle (interval: 10 degree) overlapped on salinity distribution taking σ_θ for the vertical axis.

periods. These ziggy structures are possibly caused by the intrusion of saline or less saline water from the surrounding area. It is interesting to note that these intrusions essentially exist along isopycnal surfaces without temperature inversions as is often seen in the

frontal area where eddies or water masses having distinct contrast in temperature and salinity collide (e.g., HEBERT *et al.*, 1990; YOSHIDA, 2003). RICHARDS and BANKS (2002) showed the existence of such intrusion layers (sometimes called as “interleaving” because of the existence

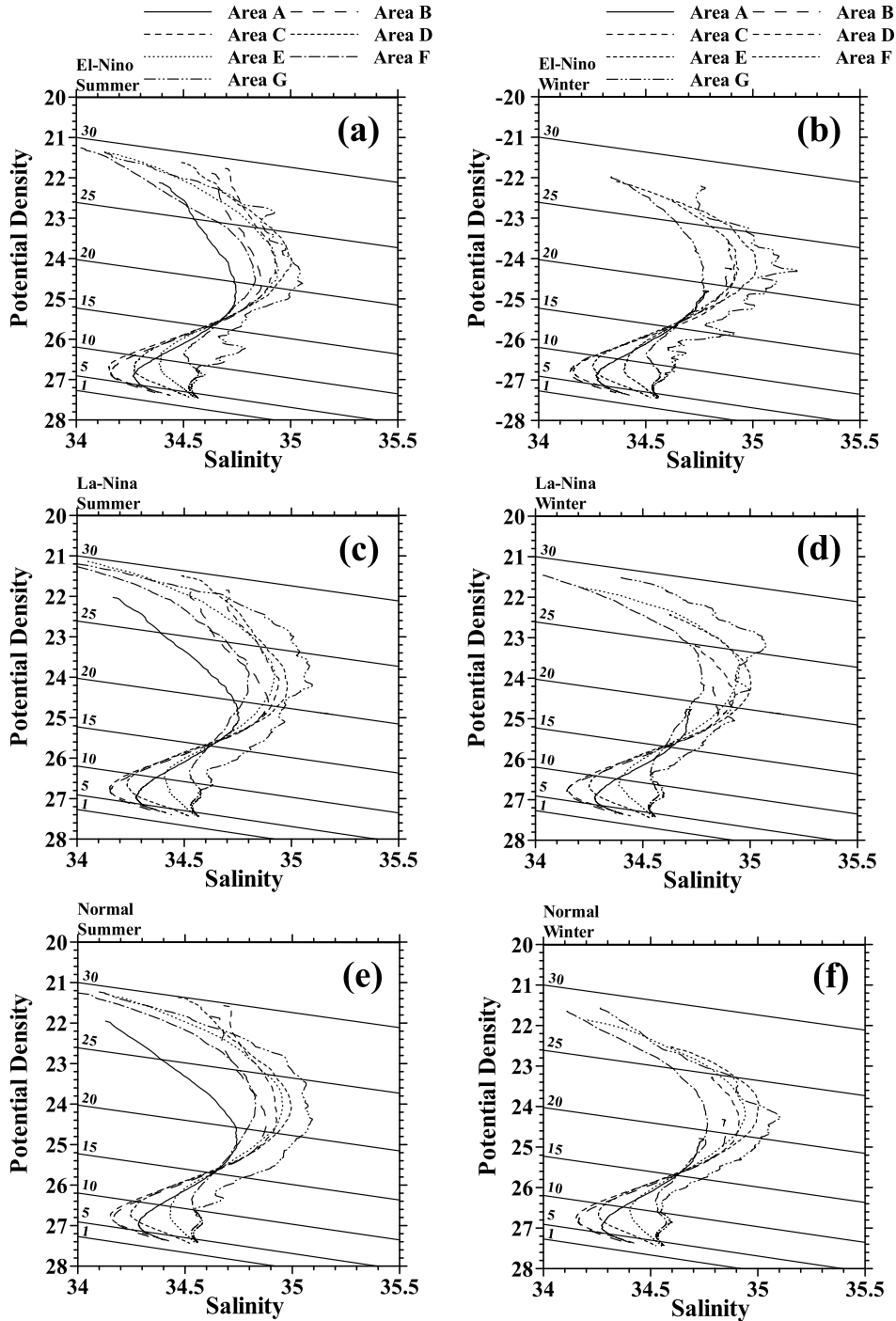


Fig. 7. Potential density-salinity relation in each area for (a) El Niño summer and (b) El Niño winter, (c) La Niña summer and (d) La Niña winter, (e) Normal summer and (f) Normal winter. Solid curves in these figures show the potential temperature.

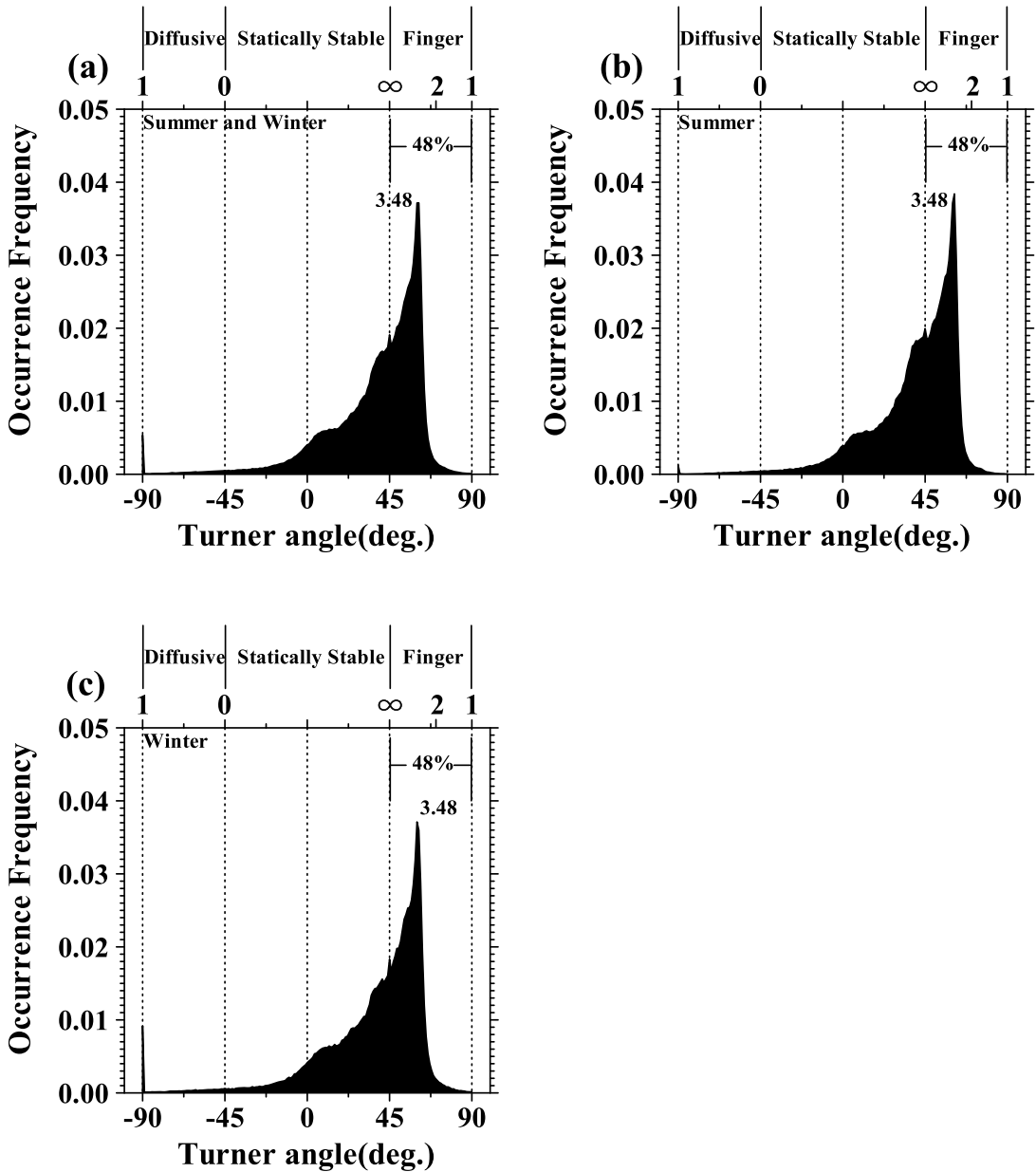


Fig. 8. Histograms of the occurrence frequency of Turner angle for (a) summer/winter, (b) summer, and (c) winter.

of warm/salty and cool/fresh layers piling up alternatively) crossing the equator from 3°S to 3°N along 165°E during La-Niña period and from 5°S to 5°N along 156°E during El-Niño period. They concluded that the observed

interleaving is the persistent feature in the equatorial Pacific, and are possibly caused by both double-diffusive instability and inertial instability. The region of salt finger favorable layer does not show remarkable change

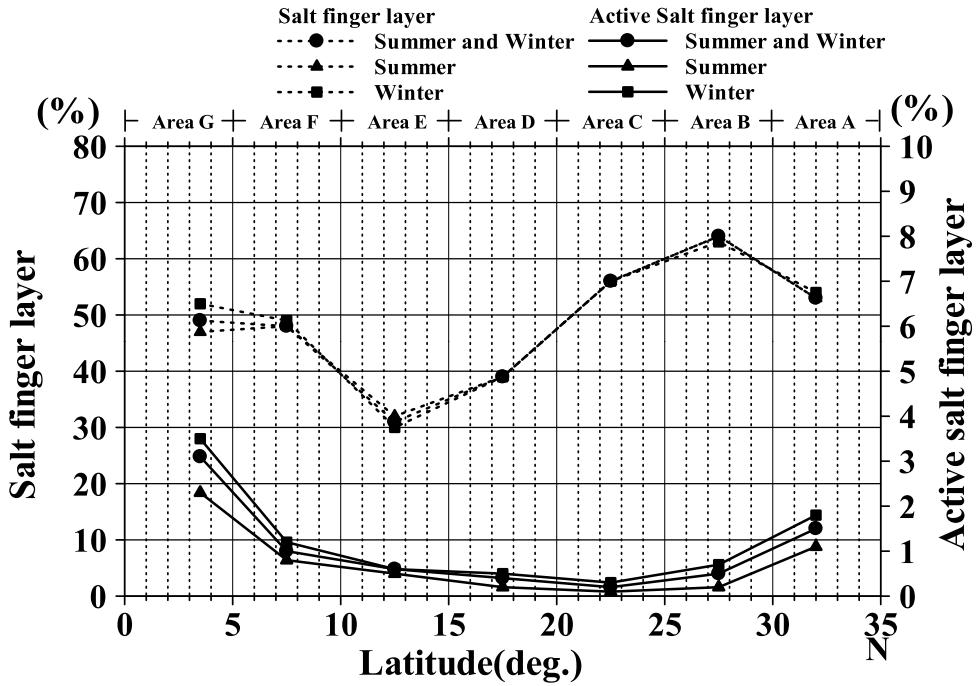


Fig. 9. Latitudinal change of the percentage of salt finger convection (● : summer and winter, ▲ : summer, ■ : winter with dotted lines) and the active salt finger convection (● : summer and winter, ▲ : summer, ■ : winter with solid lines)

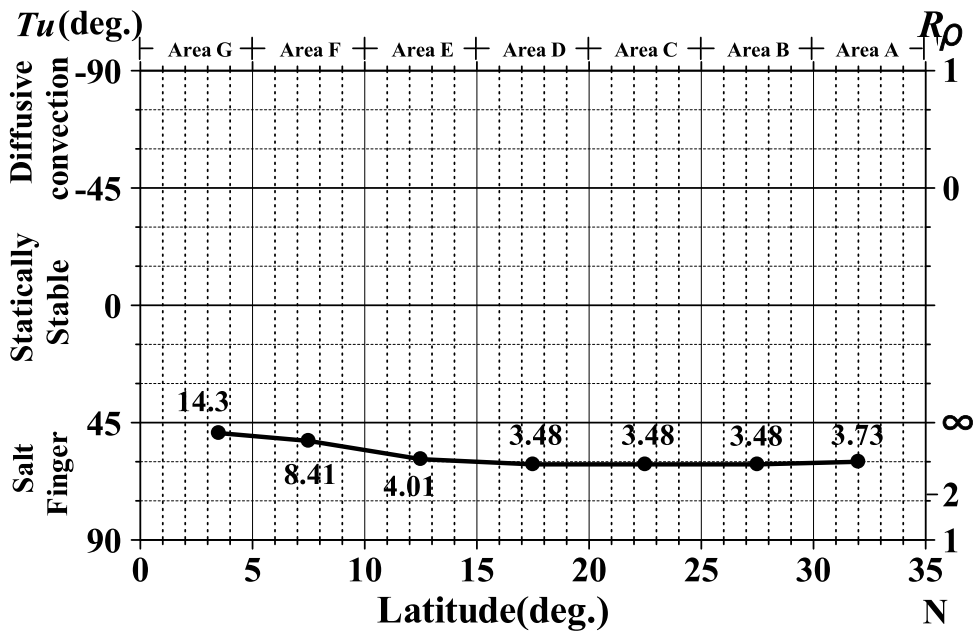


Fig. 10. Latitudinal change of Turner angle (density ratio).

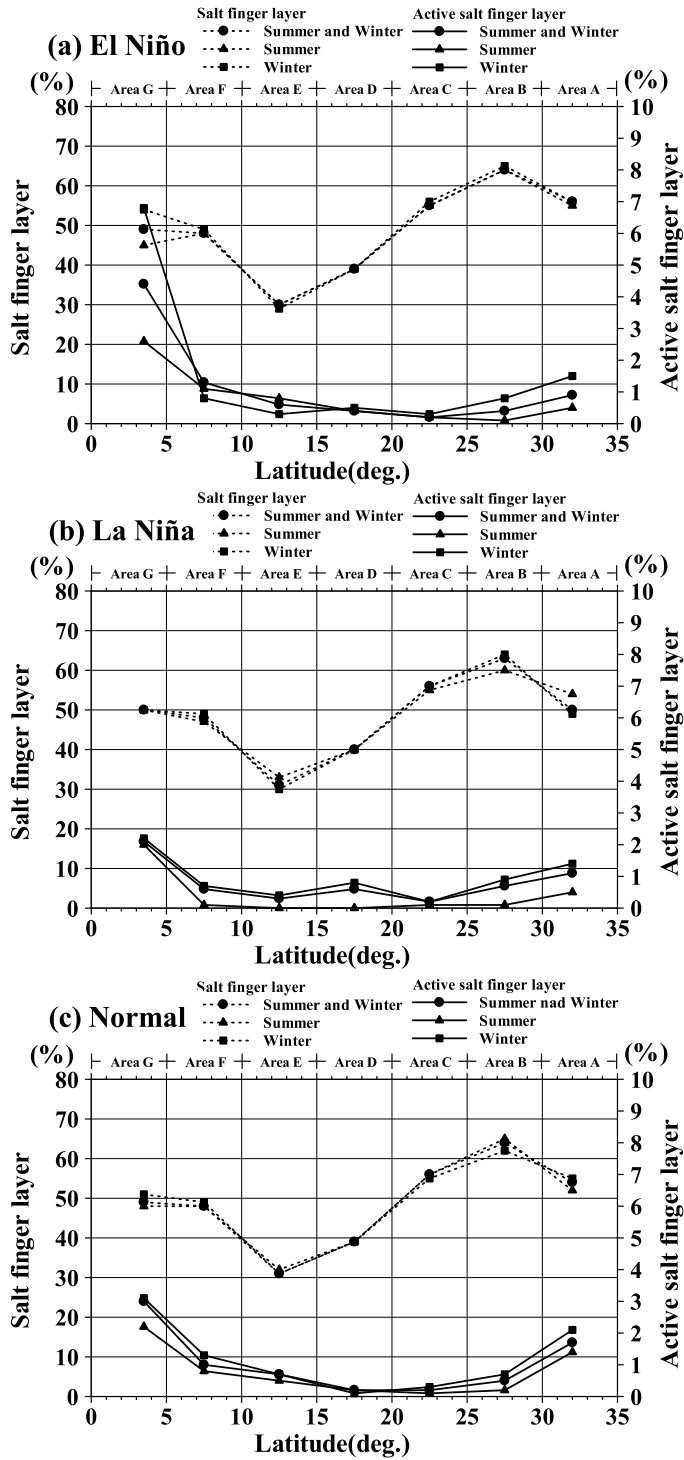


Fig. 11. Same as in Fig. 9, but for (a) El Niño, (b) La Niña and (c) Normal periods.

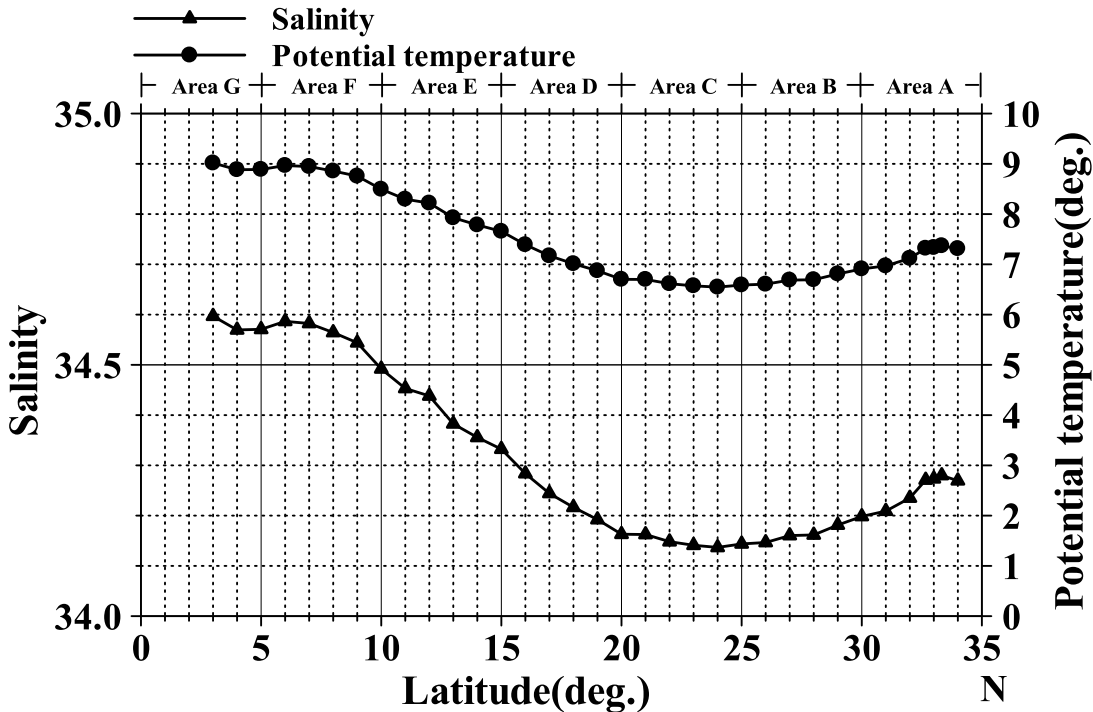


Fig. 12. Latitudinal distribution of salinity (●) and potential temperature (▲) on a $26.8\sigma_\theta$ surface.

between the ENSO and Normal periods (Fig. 6). This point will be discussed in the following section.

4. Histogram analysis of Turner Angle (Tu)

Histogram plots of Tu in (a) summer and winter, (b) summer only and (c) winter only show no remarkable seasonal variability (Fig. 8). The salt finger favourable layer occupies 48% in the total layer down to 1000 db. The mode (a peak of occurrence frequency) of Tu appears in the salt finger regime, and is 61 degree ($R_\rho \approx 3.48$), meaning that almost half of the stratification is favorable for onset of salt finger convection; however, its activity is not so high along 137°E . This value is within the range those obtained by FIGUEROA (1996) and YOU (2002) in the central Pacific Ocean.

In each area, such histogram plots of Tu were conducted to obtain area to area variability of the activity of salt finger convection and summarized in Figs. 9 and 10. The percentage of salt fingering layer in each area does not

change seasonally, which was above 50% from Area A through Area C (34°N to 20°N), being the highest in Area B (29°N to 25°N), where the core of NPIW just exists. It gradually decreases to Area E (14 to 10°N corresponding to the southern edge of NPIW), and increases to about 50% at Areas F and G (Fig. 9 (a)) because of high salinity in the upper layer in these areas. The mode value of R_ρ in each area also does not change seasonally. It gradually increases towards south (Fig. 10). The high mode values in Area F and Area G mean that the activity of salt finger convection is low in these areas. The active salt finger regime ($72^\circ < Tu < 90^\circ$, $1 < R_\rho < 2$) behaves differently. Namely, the percentage of active salt finger layer is generally small over the entire area, but is relatively high in Areas A, F and G, especially in winter (see Fig. 9). This tendency is distinct during El-Niño winter (Fig. 11). The percentage of active salt finger regime is high and is up to 7%. This higher value should be due to the development of ziggy structures in El-Niño

winter (Fig. 7 (b)). The percentage of salt finger layer and modes of do not change from seasonal average among El-Niño, La-Niña and Normal periods.

5. Summary

In the present study, we investigated in detail the variability of hydrographic structure along 137°E line using CTD data obtained from 1990 through 2007. We compared our results to those obtained by classical Nansen cast data from 1966 through 1989. In addition, we first apply density ratio analysis along 137°E line to discuss the effect of double diffusive convection. Some results are summarized as follows;

- (1) The region where the stratification is favourable for the onset of salt finger convection ($R_\rho > 3.7$ and $45^\circ < Tu < 60^\circ$) is found in the bottom half of North Pacific Equatorial Water (NPEW) and North Pacific Tropical Water (NPTW), which extends to the upper half of North Pacific Intermediate Water (NPIW). This region exists isopycnally on the surface between $24.0 \sigma_\theta$ and $26.8 \sigma_\theta$ persistently along 137°E line.
- (2) A slight upward inclination of a trace of salinity minimum along the NPIW core is detected, suggesting that salt finger convection might play a role in modification of the NPIW.
- (3) The percentage of salt finger layer occupying in the total layer down to 1000 db along 137°E line is about 48%. The mode value of Tu is 61 degree ($R_\rho \approx 3.48$). These values do not change seasonally and in ENSO periods; however, it changes regionally, as is relatively high in mid-latitude and equatorial region, and is low in the lower latitude.
- (4) The active salt finger convection is anticipated in equatorial region (3°N to 5°N) especially in El-Niño winter. The high activity of salt finger convection might be associated with the development of interleaving structure in this region.

Acknowledgements

This work is a part of Ph.D. thesis of Lamona I. Bernawis at the Tokyo University of Marine Science and Technology. This work was supported by Grant-in-Aid for Scientific

Research from the Ministry of Education, Culture, Sports, Science and Technology of Japanese Government are greatly appreciated..

References

- BINGHAM, F.M., T. SUGA and K. HANAWA (2002): Origin of waters observed along 137°E. *J. Geophys. Res.*, **107**(C12), 3073, doi : 10.1029/2000JC000722.
- FIGUEROA, H. A. (1996): World ocean density ratios. *J. Phys. Oceanogr.*, **26**, 267–275.
- HEBERT, D., B.R. RUDDICK and N.S. OAKEY (1990): Evolution of a Mediterranean salt lens: Scalar properties, *J. Phys. Oceanogr.*, **20** (9), 1468–1483.
- INOUE, R., J. YOSHIDA, Y. HIROE, K. KOMATSU, K. KAWASAKI and I. YASUDA (2003): Modification of North Pacific Intermediate Water around Mixed Water Region. *J. Oceanogr.*, **59**, 211–224.
- MASUZAWA, J. (1969): Subtropical Mode Water. *Deep-Sea Res.*, **16**, 463–472.
- NOH, Y., B. Y. YIM, S. H. YOU, J. H. YOON and B. QIU (2007): Seasonal variation of eddy kinetic energy of the North Pacific Subtropical Countercurrent simulated by an eddy-resolving OGCM. *Geophys. Res. Lett.*, **34**, L07601, doi : 10.1029/2006GL029130
- QIU, B. and T. M. JOYCE (1992): Interannual variability in the mid- and low-latitude Western North Pacific. *J. Phys. Oceanogr.*, **22**, 1092–1079.
- REID, J. L. (1965): Intermediate Waters of the Pacific Ocean. The Johns Hopkins Oceanographic Studies, No. 2, The Johns Hopkins Press, Baltimore, 85 pp.
- RICHARDS, K. J. and H. BANKS (2002): Characteristics of interleaving in the western equatorial Pacific, *J. Geophys. Res.*, **107** (C12), 3231, doi : 10.1029/2001JC000971.
- RUDDICK, B.R. (1983). A practical indicator of the stability of the water column to double-diffusive activity. *Deep-Sea Res.*, **30**, 1105–1107.
- SHUTO, K. (1996): Interannual variations of water temperature and salinity along the 137°E Meridian. *J. Oceanogr.*, **52**, 575–595.
- STEWART, R.H. (2005): Introduction to Oceanography. Department of Oceanography. Texas A&M University. 344pp.
- SUGA, T. and K. HANAWA (1994): Interannual variations of North Pacific Subtropical Mode Water in the 137°E Section. *J. Phys. Oceanogr.*, **25**, 1012–1017.
- SUGA, T., K. HANAWA and Y. TOBA (1989): Subtropical Mode Water in the 137°E section. *J. Phys. Oceanogr.*, **19**, 145–175.
- SVERDRUP, H. U., M. W. JOHNSON and R. H. FLEMING (1942): The Oceans: Their Physics, Chemistry and General Biology. Prentice-Hall, Englewood

Cliffs, New York, 1087 pp.

- TALLEY, L. D., (1993): Distribution and formation of North Pacific Intermediate Water. *J. Phys. Oceanogr.*, **23**, 517–537.
- TALLEY, L. D. and J. Y. YUN (2001): The role of cabbeling and double diffusion in setting the density of the North Pacific Intermediate Water salinity minimum. *J. Phys. Oceanogr.*, **31**, 1538–1549.
- TSUCHIYA, M., R. LUKAS, R. A. FINE, E. FIRING and E. LINDSTROM (1989): Source waters of the Pacific Equatorial Undercurrent. *Progr. Oceanogr.*, **23** (2), 101–147.
- YOSHIDA, J. (2003): The activity of double diffusive convection investigated through the density ratio distribution in the Mixed Water Region (MWR) off Joban-Kashima and Sanriku Coasts to the north-east of Honshu, Japan. *La mer*, **41**, 52–59.
- YOU, Y. (2002): A global ocean climatological atlas of the Turner angle: implications for double-diffusion and water-mass structure. *Deep-Sea Res.*, **49**, 2075–2093.

Received: November 2, 2007

Accepted: December 17, 2007

Final form: March 11, 2013

浜名湖の埋立地に建設された人工水路の魚類群集構造 —隣接した開放的な沿岸海域との比較—

瀧ヶ崎一弥^{1)*}・佐野光彦¹⁾

Fish assemblage structure in an artificial canal on reclaimed land in Lake Hamana, central Japan: comparison with an adjacent shore zone

Kazuya TAKIGASAKI* and Mitsuhiko SANÔ

Abstract : To determine whether or not fish assemblage structures differed between a concrete-walled canal, with a sandy bottom and markedly slower current velocity, on reclaimed land and the adjacent sandy shore with scattered boulders, sampling using a seine net was conducted in Lake Hamana, Shizuoka Prefecture, Japan, in March, June and September 2012. The mean total number of fish species per tow was significantly lower in the canal than along the adjacent shore throughout the study period, because of the lower number of resident benthic fish species in the canal. The mean total number of individuals, on the other hand, was greater in the canal in June due to higher juvenile abundances of the goby *Favonigobius gymnauchen* and nibbler *Girella punctata*, although not in other months. A similarity index indicated a distinct difference in species composition of the fish assemblages in the canal and along the shore. In addition, the mean standard length of all fishes collected throughout the study period was significantly less in the canal. These results suggested that the fish assemblage structures differed significantly between the canal and shore, with some juvenile fishes preferring the former environment, despite its lessened suitability for many species.

Keywords : Artificial canal, Fish assemblage, Reclaimed land, Lake Hamana

1. はじめに

沿岸域は海域と陸域との間のエコトーンに相当し、地球上で最も生産性の高い生態系のひとつを形成している。その沿岸生態系は高い生物多様性や生態系機能を有するために、保全の必要性が高い領域となっている（清野，2000）。その一方で、著しく進行する都市化や活発化する人間活動により、沿岸生態系は急激に劣化し（LOTZE *et al.*,

2006）、その問題は世界的な関心事となっている（SEAMAN, 2007）。

我が国においては、1960年代以降、高度経済成長と歩調を合わせるように、産業・住宅用地や海浜公園の造成、海岸防災の徹底などを目的とした沿岸域の埋立てが急速に進められた。その結果、沿岸浅海域の多くは陸地化し、沿岸生物の生息場は減少、あるいは場所によっては消滅してしまった（倉田，1977；堀江，1994；石川ら，1999）。このため、多くの沿岸生物が影響を受け、個体数の低下や絶滅がみられた（中条ら，2008）。

このように、埋立てによる陸地化は沿岸生物の生息場を奪うが、その一方で埋立地には今までにない新たな生息環境が造りだされることもある。例えば、自然石や消波ブロックなどを用いた石積傾斜護岸、あるいは導水や排水、親水、船舶の航行などを目的に建設される、コンクリート張りの人工水路である。石積傾斜護岸では岩礫性の生息

1) 東京大学大学院農学生命科学研究科生圏システム学専攻

〒113-8657 東京都文京区弥生 1-1-1

Department of Ecosystem Studies, Graduate School of Agricultural and Life Sciences, The University of Tokyo.

1-1-1 Yayoi, Bunkyo-ku, Tokyo, 113-8657, Japan

Tel/Fax: 03-5841-8921

* E-mail: kzy0615@gmail.com

環境が形成され、潮下帯においては大型褐藻が繁茂したり、メバル類やアイナメ類などの多様な魚類が出現したりすることが報告されている (e.g., 森ら, 1991; 日下部ら, 2005)。一方、海域と連結する人工水路も、海水が流入するため、魚類を含めた沿岸生物の生息場として機能する可能性がある。しかし、人工水路がどのような環境を形成し、どのような魚類の生息場となっているのかはほとんどわかっていない。

そこで本研究では、静岡県西部に位置する浜名湖において、埋立地に建設されたコンクリート張りの人工水路と周囲の開放的な海域とを比較することによって、人工水路の環境特性を把握し、そこにどのような魚類群集が形成され、その群集構造が周囲の海域のものとの程度異なるのかを明らかにすることを目的とした。

2. 材料と方法

2.1 調査地の概要と調査時期

本研究は、浜名湖の埋立地（浜松市弁天島）に建設された人工水路（ $34^{\circ}70'N$, $137^{\circ}60'E$ ）、およびそれに隣接する開放的な海域（以下、それぞれ水路内、水路外と呼ぶ）において、2012年の3月、6月および9月に行った (Fig. 1)。浜名湖（総面積 74 km^2 , 周囲 141 km ）は、南端の今切口で遠州灘に接続しており、潮汐周期で外洋水が流入する内湾である (松田, 1999)。

人工水路は、幅約 4 m 、全長約 420 m の小規模なもので、親水および導・排水の目的で1988年に建設された (Fig. 2a)。底面は平坦なコンクリートで、その上には中砂 (須田・早川, 2002) が厚さ 5 cm 程度で堆積していた。両側面はコンクリートあるいは積み石による垂直護岸となっている。人工水路の両端は周囲の開放的な水域と繋

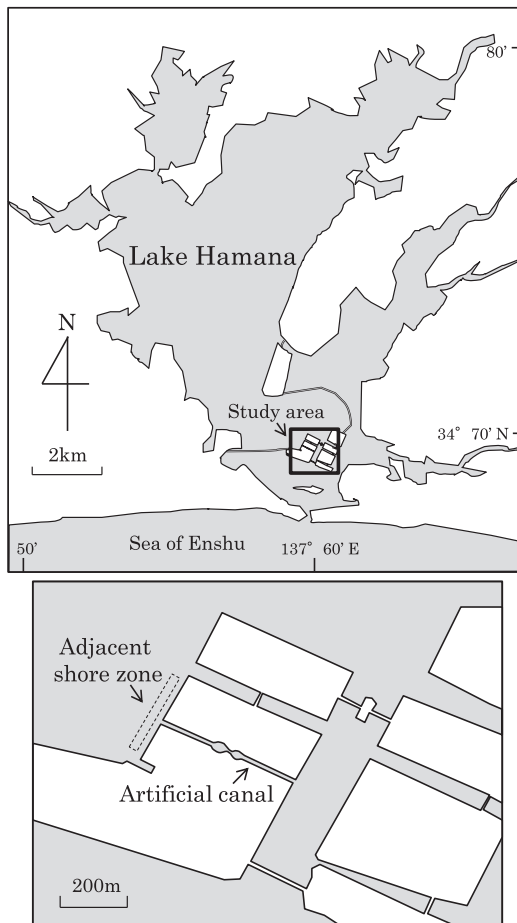


Fig. 1. Map of Lake Hamana, western Shizuoka Prefecture, central Japan, showing study sites (artificial canal and adjacent shore zone).

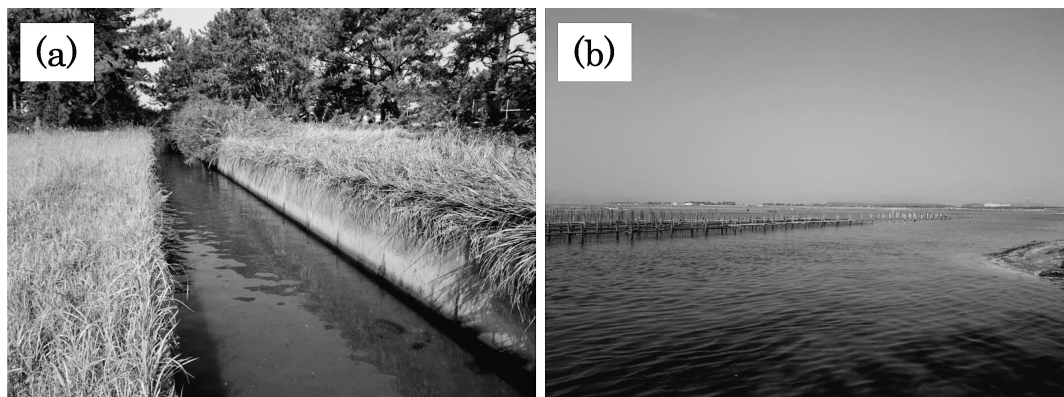


Fig. 2. Two study sites: artificial canal (a) and adjacent shore zone (b).

がっており、潮汐による海水面の上下変動に伴い、水路の両端から海水の出入りが起こる (Fig. 1)。水路内における満潮時の水深は約 80 cm であった。一方、水路外の開放的な海域は浜名湖南部においてふつうにみられる環境であり、底質は砂で大小様々な石が散在していた (Fig. 2b)。調査を実施した地点の水深は満潮時で約 90 cm であった。

2.2 物理環境調査

水路内と水路外で物理環境に違いがあるかどうかを明らかにするために、水質と流速の調査を以下の方法で行った。いずれの調査も、各月に水路内と水路外においてそれぞれ 4 回実施した。なお、調査は魚類の採集と並行して行った。

水質についてはマルチ水質計 Quonta (Hydrolab 社製) を用いて、水温 (°C)、塩分、溶存酸素量 (mg/L) および濁度 (NTU) の測定を行った。

流速の測定は、円筒形の表面浮子 (直径 6.5 cm, 高さ 12.3 cm) を用いて、満潮から 2~3 時間後の下げ潮時に行った。投下した浮子が一定区間の距離 (4 m) を流れるのにかかった時間を計測し、その値から流速 (cm/s) を算出した。

2.3 魚類調査

水路内と水路外で魚類群集の構造に違いがあるかどうかを明らかにするために、魚類の採集を行った。採集は、各月に水路内と水路外のそれぞれにおいて、大潮の満潮時に 4 回実施した。

採集には曳網 (袖網 3.8 m, 袋網 1.2 m, 高さ 0.9 m, 目合い 3 mm) を用いた。網の間口を 4 m に保ちながら 10 m 曳網し、1 回の採集面積を 40 m² とした。その際、曳網開始地点から 10 m 先の場所に目合い 3 mm の仕切り網を張り、遊泳力の大きな個体も逃さないようにして採集した。各曳網は 50 m 以上離れて行った。採集した個体は、ただちに 10% ホルマリン溶液で固定して研究室に持ち帰った。持ち帰った個体は、中坊 (2000) や KAI and NAKABO (2008) に従って種の同定を行い、種ごとに個体数を計数した。さらに、各個体について標準体長 (以下、体長) の測定を行った。

各種の生活・行動様式に基づいて、採集した魚類を底生定住魚と中層遊泳魚に分類した。前者は海底に接した生活を送り、定住性が強い種であり、後者は水柱の中層を活発に遊泳し、移動性が高い種である。

2.4 統計分析

物理環境の各項目、採集した魚類の総種数・総

個体数、底生定住魚と中層遊泳魚の種数・個体数について、調査区間 (水路内と水路外) および月間での差の有無を調べるために、一般化線形モデルを用いた。ここでは、物理環境の各項目、魚類の種数と個体数をそれぞれ目的変数に、カテゴリカル変数として調査区と月、さらにそれらの交互作用を説明変数に指定した。モデルの誤差構造は、物理環境の各項目については正規分布、種数についてはポアソン分布、個体数については負の二項分布とした。リンク関数として、正規分布においては identity を、ポアソン分布と負の二項分布においては log を指定した。各説明変数の有意性は尤度比検定によって調べた。月間で有意差がみられた場合には、多重比較法 (Holm-Bonferroni test) を用いてどの月の間で有意な差があるかを調べた。また、調査区と月の交互作用が存在した場合には、調査区を説明変数に指定したモデルにより、月ごとに調査区間での有意差の有無を調べた。さらに、魚類の体長において、調査区間で有意な差があるかどうかを Mann-Whitney U-test で検討した。

調査区間および月間での種組成の類似性を調べるために、各月、各調査区で採集した各種の個体数に基づき類似度を求め、クラスター分析を行った。類似度には Bray-Curtis 指数 (PS₂) を、クラスター連結には群平均法を用いた (小林, 1995)。

$$PS_2 = \sum \min(n_{iA}/N_A, n_{iB}/N_B) \times 100$$

ここでは、 $N_A = \sum n_{iA}$, $N_B = \sum n_{iB}$ で、 n_{iA} , n_{iB} はそれぞれある月の調査区 A, 調査区 B における種 i の個体数を示し、種組成が完全に異なる場合は $PS_2 = 0$ 、全く同じ場合には $PS_2 = 100$ となる (小林, 1995)。なお、個体数は種によって大きく異なり、類似度は個体数の多い種に影響されやすい。このため、個体数の少なかった種の貢献度を高めるために、各種の個体数は対数変換 ($\log(x+1)$) した。

以上の検定は統計ソフト R 2.14.2 を用いて行った。なお、本研究の目的は物理環境と魚類群集の構造に調査区間でどのような違いがあるのかを明らかにすることである。このため、月間の違いについては結果において詳述しなかった。

3. 結果

3.1 物理環境

各月の各調査区 (水路内と水路外) における水質と流速の結果を Fig. 3 と Table 1 に示した。

水温においては、調査区と月の間で交互作用がみられた。そこで、月ごとに調査区間の差を調べ

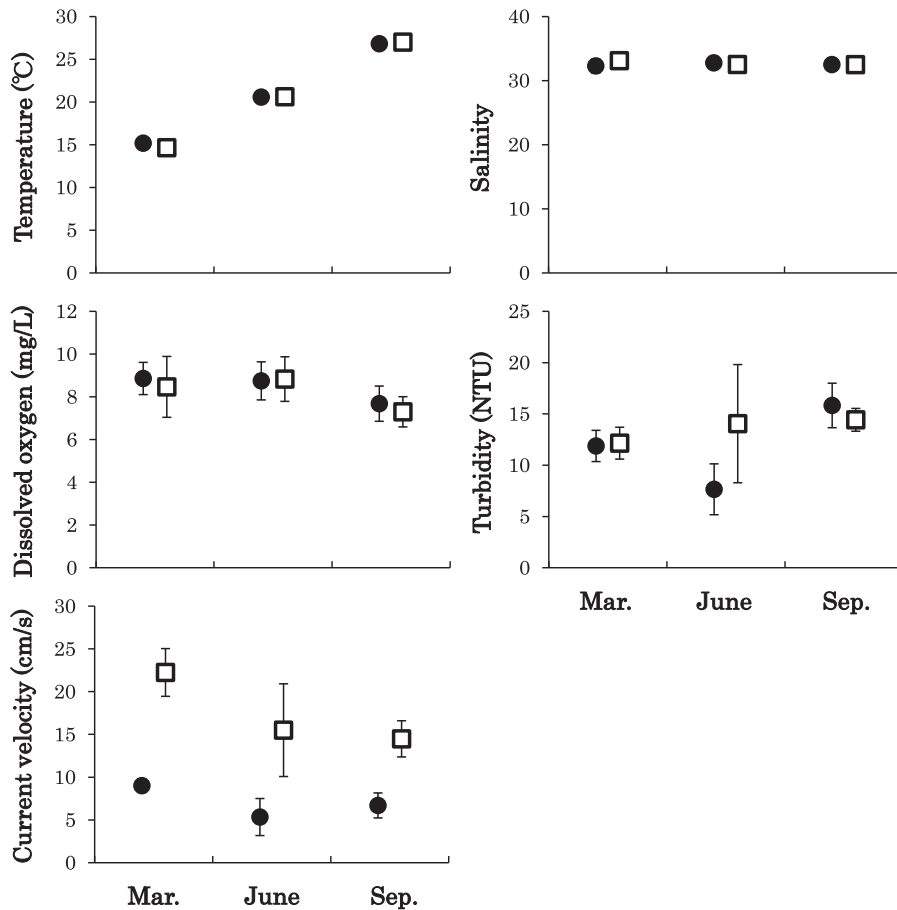


Fig. 3. Water temperature (mean \pm standard deviation, $n = 4$), salinity, dissolved oxygen, water turbidity and current velocity in the artificial canal (●) and adjacent shore zone (□) in March, June and September, 2012.

たところ、3月においては水路内で、9月においては水路外で有意に高かった。しかし、どの月においてもその差はわずかで、それぞれ 0.5°C と 0.2°C であった。塩分では、調査区間、月間のいずれにおいても差がみられなかった。溶存酸素量については月の主効果が認められたものの、調査区間には有意な差はみられなかった。濁度においては交互作用が存在した。このため、月ごとに調査区間の差を調べたが、どの月においても有意差は認められなかった。

流速においては、調査区間で有意な差がみられ、水路内で著しく遅かった（水路外の $1/2 \sim 1/3$ の速さ）。

3.2 魚類群集の構造

調査期間を通して、水路内では13科14種784個体が採集された（Table 2）。このうち個体数が多かった種としては、ヒメハゼ *Favonigobius gymnauchen* が339個体（全体の43.2%）、ボラ *Mugil cephalus cephalus* が276個体（35.2%）、メジナ *Girella punctata* が88個体（11.2%）、アイゴ *Siganus fuscescens* が63個体（8.0%）であり、これらで全体の97.7%を占めた。一方、水路外では16科18種549個体が採集された。個体数の多かった種はヒメハゼ（269個体、49.0%）、クロサギ *Gerres equulus*（98個体、17.9%）、ハオコゼ *Hypodytes rubripinnis*（94個体、17.1%）、アカオビシマハゼ *Tridentiger trigonocephalus*（35個体、6.4%）であり、これらで全体の90.3%

Table 1. Results of likelihood ratio (LR) tests examining differences in mean physical environmental factors ($n = 4$) among sites (artificial canal and adjacent shore zone) and months (March, June and September). Holm-Bonferroni test was conducted when likelihood ratio test results indicated significant month effects ($p < 0.05$).

(a) Water temperature					
Explanatory variables	df	LR χ^2	p	Holm-Bonferroni test	
Site	1	0.9	0.351		
Month	2	8647.1	<0.001		
Site×Month	2	8.6	0.013		
Results of likelihood ratio tests examining differences between sites in each month due to a significant site×month interaction in the above test.					
Month	Explanatory variable	df	LR χ^2	p	
March	Site	1	7.8	0.005	Canal>Shore zone
June	Site	1	<0.05	0.867	
September	Site	1	169.9	<0.001	Canal<Shore zone
(b) Salinity					
Explanatory variables	df	LR χ^2	p	Holm-Bonferroni test	
Site	1	0.7	0.405		
Month	2	0.6	0.749		
Site×Month	2	4.3	0.118		
(c) Dissolved oxygens					
Explanatory variables	df	LR χ^2	p	Holm-Bonferroni test	
Site	1	0.3	0.615		
Month	2	6.5	0.038	Mar.=June>Sep.	
Site×Month	2	0.2	0.888		
(d) Water turbidity					
Explanatory variables	df	LR χ^2	p	Holm-Bonferroni test	
Site	1	1.7	0.196		
Month	2	7.0	0.030		
Site×Month	2	6.1	0.048		
Results of likelihood ratio tests examining differences between sites in each month due to a significant site×month interaction in the above test.					
Month	Explanatory variable	df	LR χ^2	p	
March	Site	1	<0.05	0.827	
June	Site	1	3.1	0.077	
September	Site	1	1.0	0.320	
(e) Current velocity					
Explanatory variables	df	LR χ^2	p	Holm-Bonferroni test	
Site	1	59.4	<0.001	Canal<Shore zone	
Month	2	12.9	0.002	Mar. >June=Sep.	
Site×Month	2	2.7	0.255		

を占めた。

各月の各調査区における1曳網(40 m²)あたりの平均総種数と平均総個体数をFig. 4に、各種の1曳網あたりの平均個体数をTable 2に示した。調査区間、月間で総種数と総個体数が異なるかどうかを調べたところ、総種数では水路外で有意に多く、また月間にも差が認められた

(Table 3)。一方、総個体数については交互作用が存在した。このため、月ごとに調査区間での差を調べると、6月において水路内で有意に多かった(Table 3)。これは、この月にヒメハゼの稚魚(体長22~40 mm, 45個体/40 m²)とメジナの稚魚(体長14~34 mm, 22個体/40 m²)が水路内に多数出現したためであった。

Table 2. Mean number of individuals per haul (40 m², n = 4), size range in standard length (SL), life modes (LM) and feeding groups (FG) of fish species collected by seine net from the artificial canal and adjacent shore zone in March, June and September, 2012.

Family	Species	SL (mm)	LM	FG*	March			June			September		
					Canal	Shore zone	Shore zone	Canal	Shore zone	Shore zone	Canal	Shore zone	Shore zone
Gobiidae	<i>Favonigobius gymnauchen</i>	17–63	B	Be	19.0 (11.1)	36.5 (36.4)	63.0 (23.8)	27.5 (16.5)	2.8 (1.6)	3.3 (2.3)			
	<i>Tridentiger trigonocephalus</i>	30–67	B	Po		6.3 (4.0)		2.5 (2.6)					
	<i>Acentrogobius pflaumii</i>	38–56	B	Be			0.5 (0.9)	0.8 (1.3)				0.3 (0.4)	
Mugilidae	<i>Mugil cephalus cephalus</i>	21–37	M	Zo	67.3 (91.7)		1.8 (3.0)						
	<i>Gerres equulus</i>	22–47	M	Po								24.5 (27.5)	
Tetraogridae	<i>Hypodytes rubripinnis</i>	21–50	B	Be		1.3 (1.3)	22.0 (34.7)	0.8 (0.8)				21.5 (10.3)	
Girellidae	<i>Girella punctata</i>	14–34	M	Zo									
Siganidae	<i>Siganus fuscescens</i>	23–34	M	Pl		2.0 (2.1)					15.8 (27.3)	1.0 (1.0)	
Syngnathidae	<i>Syngnathus schlegelii</i>	90–237	M	Zo				0.5 (0.9)			0.3 (0.4)	0.8 (1.3)	
Tetraodontidae	<i>Takifugu niphobles</i>	21–42	M	Zo							0.3 (0.4)	2.0 (3.5)	
Haemulidae	<i>Plectorhinchus cinctus</i>	50–76	M	Be							0.5 (0.5)	1.3 (1.6)	
Monacanthidae	<i>Rudarius ercodes</i>	29–37	M	Be				0.3 (0.4)				0.5 (0.5)	
	<i>Stephanolepis cirrifer</i>	71, 76	M	Be								0.5 (0.9)	
Sparidae	<i>Acanthopagrus schlegelii</i>	40–55	M	Zo							1.0 (1.0)	0.3 (0.4)	
Lutjanidae	<i>Lutjanus russellii</i>	48–53	M	Be							0.3 (0.4)	0.8 (0.8)	
Microcanthidae	<i>Microcanthus strigatus</i>	17–24	M	Be			0.8 (1.3)						
Cottidae	<i>Pseudoblennius cottoides</i>	52–66	B	Be				0.5 (0.5)				0.3 (0.4)	
Callionymidae	<i>Repomucenus beniteguri</i>	51–77	B	Be								0.8 (1.3)	
Scorpaenidae	<i>Sebastes inermis</i>	40, 47	M	Be				0.3 (0.4)				0.3 (0.4)	
Teraponidae	<i>Rhyncopelates oxyrhynchus</i>	21, 29	M	Be							0.5 (0.5)		
Blenniidae	<i>Petrosirtes breviceps</i>	23	B	Be								0.3 (0.4)	
Sphyraenidae	<i>Sphyraena pinguis</i>	74	M	Be								0.3 (0.4)	
	<i>Sphyraena barracuda</i>	78	M	Be							0.3 (0.4)		
Pleuronectidae	<i>Kareius bicoloratus</i>	25	B	Be		0.3 (0.4)							

B, resident benthic fish; M, swimming mid-water fish.

*, Feeding habits determined from published dietary data (e.g. Horinouchi and Sano, 2000; Kanou *et al.*, 2004; Inoue *et al.*, 2005).

Be, benthic crustacean feeders; Pl, plant feeders; Po, polychaete feeders; Zo, zooplankton feeders.

Standard deviations shown in parentheses.

Table 3. Results of likelihood ratio (LR) tests examining differences in mean numbers of fish species (a) and individuals (b) per haul (40 m², n = 4) among sites (artificial canal and adjacent shore zone) and months (March, June and September). Holm-Bonferroni test was conducted when likelihood ratio test results indicated significant month effects ($p < 0.05$).

(a) Number of species

Explanatory variables	df	LR χ^2	p	Holm-Bonferroni test
Site	1	6.2	0.013	Canal<Shore zone
Month	2	11.5	0.003	Mar.=June<Sep.
Site×Month	2	0.9	0.623	

(b) Number of individuals

Explanatory variables	df	LR χ^2	p	Holm-Bonferroni test
Site	1	0.5	0.500	
Month	2	1.0	0.607	
Site×Month	2	6.5	0.039	

Results of likelihood ratio tests examining differences between sites in each month due to a significant site×month interaction in the above test.

Month	Explanatory variable	df	LR χ^2	p	Holm-Bonferroni test
March	Site	1	0.9	0.331	
June	Site	1	5.6	0.018	Canal>Shore zone
September	Site	1	2.4	0.120	

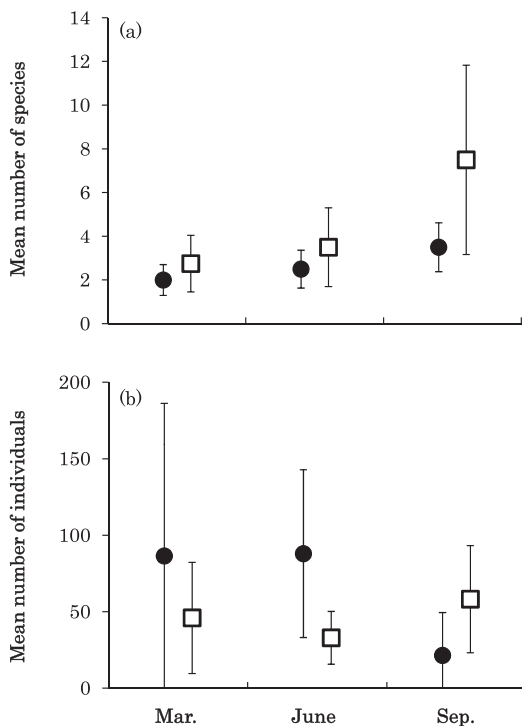


Fig. 4. Mean numbers of fish species (a) and individuals (b) per seine net haul (40 m², n = 4) from the artificial canal (●) and adjacent shore zone (□) in March, June and September, 2012. Bars indicate standard deviation.

各月、各調査区の魚類群集に対してクラスター分析を行った結果、類似度 45% で 4 つのグループに分けることができた (Fig. 5)。すなわち、3 月と 6 月の水路内 (グループ I) と水路外 (グループ II)、および 9 月の水路内 (グループ III) と水路外 (グループ IV) である。したがって、どの月においても種組成は水路内と水路外で明瞭に異なっていた。

採集した魚類を底生定住魚と中層遊泳魚に分け、1 曳網あたりの平均種数と平均個体数が調査区間および月間で異なるかどうかを調べた (Fig. 6, Table 4)。その結果、底生定住魚の種数は水路外で有意に多かったが、中層遊泳魚の種数では調査区間で有意な差が認められなかった。個体数については、底生定住魚と中層遊泳魚の双方において交互作用がみられたため、月ごとに調査区間の差を調べた (Table 4)。3 月の中層遊泳魚と 6 月の底生定住魚の個体数は水路内で有意に多く、9 月の底生定住魚は水路外で多かった。これは、中層遊泳魚のボラの稚魚と底生定住魚のヒメハゼの稚魚がそれぞれ 3 月と 6 月の水路内で、また底生定住魚のハオコゼが 9 月の水路外で主に多いためであった (Table 2)。

各調査区で採集したすべての底生定住魚と中層遊泳魚の体長を 5 mm ごとのヒストグラムで示した (Fig. 7)。体長の中央値は、底生定住魚と中層遊泳魚ともに水路外よりも水路内で有意に小さかった (Mann-Whitney U-test, 底生定住魚、

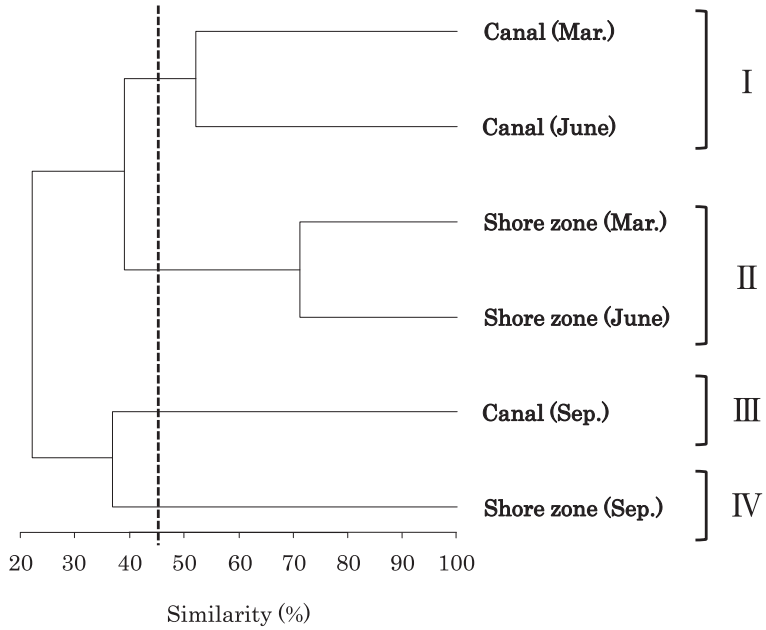


Fig. 5. Dendrogram of cluster analysis showing similarities of fish assemblages based on the number of individuals of each fish species in the artificial canal and adjacent shore zone in March, June and September, 2012. Assemblages were divided into four groups (I–IV) at 45% level of similarity.

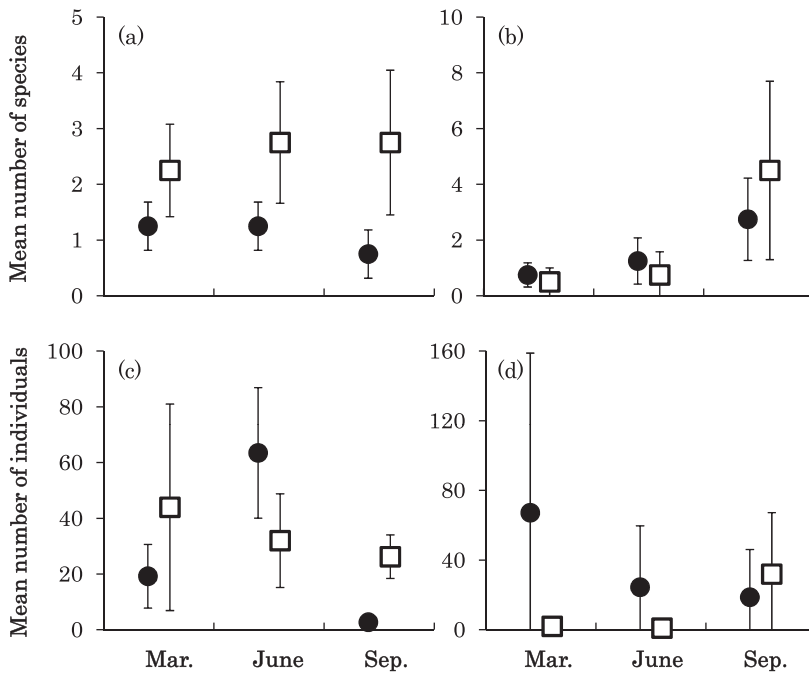


Fig. 6. Mean numbers of species and individuals per haul (40 m², n = 4) of resident benthic (a, c) and swimming mid-water (b, d) fishes caught by seine net from the artificial canal (●) and adjacent shore zone (□) in March, June and September, 2012. Bars indicate standard deviation.

Table 4. Results of likelihood ratio (LR) tests examining differences in mean numbers of species and individuals per haul (40 m², n = 4) for resident benthic (a, c) and swimming midwater fishes (b, d) among sites (artificial canal and adjacent shore zone) and months (March, June and September). Holm-Bonferroni test was conducted when likelihood ratio test results indicated significant month effects ($p < 0.05$).

(a) Number of resident benthic fish species				
Explanatory variables	df	LR χ^2	p	Holm-Bonferroni test
Site	1	7.6	0.006	Canal<Shore zone
Month	2	0.2	0.914	
Site×Month	2	0.7	0.691	

(b) Number of swimming mid-water fish species				
Explanatory variables	df	LR χ^2	p	Holm-Bonferroni test
Site	1	0.4	0.537	
Month	2	23.0	<0.001	Mar.=June<Sep.
Site×Month	2	2.0	0.362	

(c) Number of resident benthic fish individuals				
Explanatory variables	df	LR χ^2	p	Holm-Bonferroni test
Site	1	5.9	0.015	
Month	2	20.0	<0.001	
Site×Month	2	19.7	<0.001	

Results of likelihood ratio tests examining differences between sites in each month due to a significant site×month interaction in the above test.

Month	Explanatory variable	df	LR χ^2	p	Holm-Bonferroni test
March	Site	1	2.0	0.158	
June	Site	1	3.9	0.047	Canal>Shore zone
September	Site	1	57.7	<0.001	Canal<Shore zone

(d) Number of swimming mid-water fish individuals				
Explanatory variables	df	LR χ^2	p	Holm-Bonferroni test
Site	1	7.1	0.008	
Month	2	5.3	0.069	
Site×Month	2	7.7	0.021	

Results of likelihood ratio tests examining differences between sites in each month due to a significant site×month interaction in the above test.

Month	Explanatory variable	df	LR χ^2	p	Holm-Bonferroni test
March	Site	1	6.1	0.013	Canal>Shore zone
June	Site	1	<0.05	0.977	
September	Site	1	0.4	0.535	

$p = 0.001$; 中層遊泳魚, $p < 0.001$). 特に水路内では、体長 30 mm 以下の中層遊泳魚が多かった。

4. 考察

4.1 人工水路内の環境特性

水温、塩分、溶存酸素量および濁度といった水質環境については、水路内と水路外でほとんど差は認められなかった。一方、流速には違いがみられた。すなわち、水路内には流速の著しく遅い環境が形成されていた。本調査地の水路では流路が

直線的で、基質表面が平坦かつ単純化されており、起伏がほとんどないため、水の流れを阻害するものが少なかった。しかし、そのような構造にもかかわらず、流速は著しく遅かった。これは、水路において勾配がほとんどなく、両方向から水の出入りがあるためと考えられた。

4.2 人工水路内に形成される魚類群集構造

魚類の群集構造は水路内と水路外で有意に異なった。総種数と底生定住魚の種数は調査期間を通して水路内で少なく、総個体数は6月に水路内で多

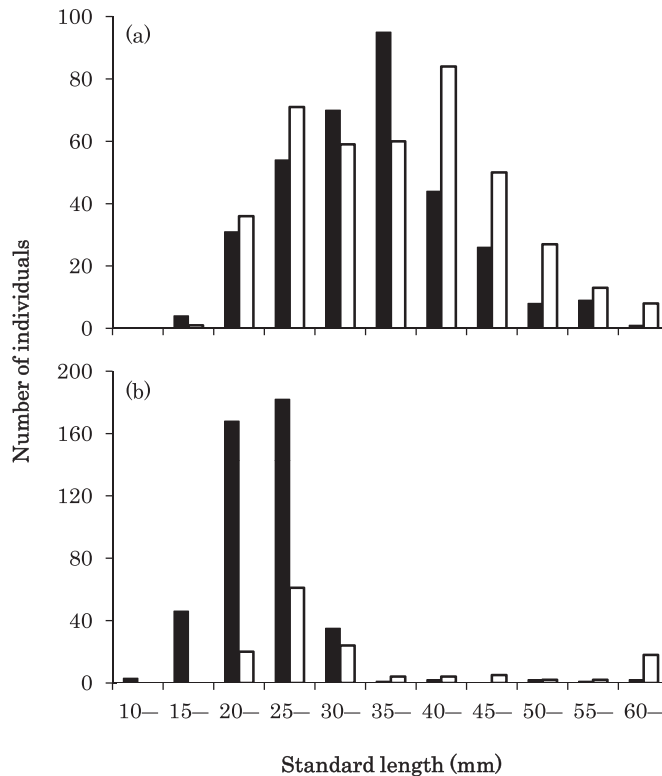


Fig. 7. Frequency distributions of standard lengths of all resident benthic (a) and swimming mid-water (b) fishes in the artificial canal (■) and adjacent shore zone (□) during the study period.

かった。また、種組成も水路内と水路外で明瞭に異なった。

総種数が水路内で少なかったのは、底生定住魚の種数が乏しかったためであると考えられる。水路内ではヒメハゼが多く分布していた以外は、底生定住魚の生息は極めて限定的であった (Table 2)。種組成が水路内と水路外で異なったのも、これが一因であろう。このように水路内で底生定住魚の種数が少なかった要因としては、基質の表面構造が単純で均質化されていることが考えられる。水路内の底面は、コンクリート基質の上に砂が一樣に堆積する単調な環境であるが、水路外の海底には大小様々な転石や起伏が多くみられ、多様な生息環境が存在する。既往研究でも、底質の物理構造が複雑であるほど魚類の種数が増加する傾向にあると報告されており (e.g., McCLANAHAN, 1994; FRIEDLANDER and PARRISH, 1998; GRATWICKE and SPEIGHT, 2005; 西田ら, 2008; WILSON *et al.*, 2012; 立松ら, 2013), 底質構造との関わりが深い底生定住

魚でその影響が顕著であったと考えられる (SANO *et al.*, 1987; LEWIS, 1997)。一方、底質構造への依存度が低い中層遊泳魚の種数には、水路内と水路外で違いがみられなかった。

総種数は調査期間を通して水路内で少なかったが、総個体数は6月に水路内で多かった。これは、底生定住魚であるヒメハゼの稚魚と中層遊泳魚のメジナの稚魚がこの月においてのみ水路内で多かったことに起因していた (Table 2)。また、中層遊泳魚の個体数も3月にのみ水路内で多かった。これは、ボラの稚魚が多数出現したためであった (Table 2)。このように、水路内で個体数が多かったのは、稚魚の季節的な出現に起因していた。

体長を水路内と水路外で比較すると、底生定住魚と中層遊泳魚ともに水路内で有意に小さかった。特に、水路内では体長 30 mm 以下の中層遊泳魚が多かった。稚魚などの小型魚は遊泳能力が低く (FISHER *et al.*, 2000), 水流の強さはそのような魚類に対して分布の制限要因になり得る (FULTON *et al.*, 2001)。水路内では流速がかなり

遅かったため、小型魚にとって水路内は、周辺海域で生じる強い水流を避ける場所（避難場所）となっていた可能性が高い。3月にボラの稚魚が、また6月にヒメハゼやメジナの稚魚が水路内で多かったのは、このためであるかもしれない。

一方、これらの稚魚は水路内を避難場所ではなく、餌が多い場所（餌場）として利用している可能性もある (KUO *et al.*, 2001)。しかし、ボラやメジナの稚魚の主要な餌である動物プランクトンの量は、水路内の海水が潮汐によって水路外から流入してくるため、水路内と水路外でほぼ同じであると考えられる。また、ヒメハゼの稚魚は底生甲殻類食であり、餌が水路内で多いならば、他の底生甲殻類食魚も水路内に多数出現するはずである。しかし、そのような結果は得られなかった (Table 2)。したがって、多くの稚魚は水路内を餌場としてよりも、避難場所として利用していると推察された。

4.3 魚類の生息場としての人工水路

本研究により、浜名湖の埋立地に建設された人工水路内には、周囲の水域と比較して種多様性の低い魚類群集が形成されていることが判明した。その一方で、遊泳能力の低い小型魚、特に稚魚が多く生息し、水路内はそれらの避難場所として機能していることもわかった。したがって、埋立地の人工水路は多くの魚類にとって適した生息場ではないものの、小型魚や稚魚などの一部の魚類に対しては重要な生息場となり得ることが示唆された。

しかし、すべての人工水路がこのような魚類の生息場となるわけではない。人工水路は、海水の出入りが少ない場合や閉鎖性が強い場合、水路内に水が停滞して有機物が堆積しやすい環境となる。特に、夏季においてこのような状況になると、底層水の貧酸素化が生じ、魚類を含めた沿岸生物の生息場としては不適になる可能性がある (柳, 2004; 大澤・檜垣, 2012)。本研究の水路では、水路外からの海水の流入によって、溶存酸素量は夏季でも高い値 (7~9 mg/L) を維持していた (Fig. 2)。このように、人工水路が魚類の生息場として機能するには、水路外との海水の交換が十分にあることが重要となるであろう。

謝辞

野外調査を行うにあたり、多大なご協力をいただいた東京大学大学院農学生命科学研究科附属水産実験所の鈴木讓教授、高見隆江氏、水野直樹氏、城夕香氏、藤田真志氏、同研究科水域保全学研究室の青木茂氏、金井貴弘氏、田中裕一氏、立松沙

織氏、また有益なご助言をいただいた同研究室の岡本研准教授、北海道大学大学院環境科学院の佐藤允昭氏、英文校閲をしていただいた Graham S. HARDY 博士に厚く御礼申しあげる。

引用文献

- FISHER, R., D. R. BELLWOOD and S. D. JOB (2000): Development of swimming abilities in reef fish larvae. *Marine Ecology Progress Series*, **202**, 163-173.
- FRIEDLANDER, A. M. and J. D. PARRISH (1998): Temporal dynamics of fish communities on an exposed shoreline in Hawaii. *Environmental Biology of Fishes*, **53**, 1-18.
- FULTON, C. J., D. R. BELLWOOD and P. C. WAINWRIGHT (2001): The relationship between swimming ability and habitat use in wrasses (Labridae). *Marine Biology*, **139**, 25-33.
- GRATWICKE, B. and M. R. SPEIGHT (2005): The relationship between fish species richness, abundance and habitat complexity in a range of shallow tropical marine habitats. *Journal of Fish Biology*, **66**, 650-667.
- 堀江毅 (1994): 沿岸の開発。海洋環境を考える一海洋環境問題の変遷と課題 (日本海洋学会編), 恒星社厚生閣, 東京, pp. 13-27.
- 石川公敏・小倉紀雄・堀江毅・細川恭史 (1999): 「開発」から「環境」への変革。明日の沿岸環境を築く一環境アセスメントへの新提言 (日本海洋学会編), 恒星社厚生閣, 東京, pp. 1-18.
- KAI, Y. and T. NAKABO (2008): Taxonomic review of the *Sebastes inermis* species complex (Scorpaeniformes: Scorpaenidae). *Ichthyological Research*, **55**, 238-259.
- 小林四郎 (1995): 生物群集の多変量解析。蒼樹書房, 東京, 194pp.
- KUO, S. R., H. J. LIN and K. T. SHAO (2001): Seasonal changes in abundance and composition of the fish assemblage in Chiku Lagoon, southwestern Taiwan. *Bulletin of Marine Science*, **68**, 85-99.
- 倉田亨 (1977): 海面埋立ての現状と将来。海面埋立てと環境変化 (川崎健・平野敏行・嶋津靖彦編), 恒星社厚生閣, 東京, pp. 1-34.
- 日下部敬之・有山啓之・大美博昭・天野玉雄 (2005): 関西国際空港島人工傾斜護岸と自然岩礁海岸におけるカサゴ成魚の摂餌生態の比較。日本水産学会誌, **71**, 594-600.
- LEWIS, A. R. (1997): Effects of experimental coral disturbance on the structure of fish communities on large patch reefs. *Marine Ecology Progress Series*, **161**, 37-50.
- LOTZE, H. K., H. S. LENIHAN, B. J. BOURQUE, R. H. BRADBURY, R. G. COOKE, M. C. KAY, S. M. KIDWELL, M. X. KIRBY, C. H. PETERSON and J. B. C. JACKSON (2006): Depletion, degradation, and

recovery potential of estuaries and coastal seas. *Science*, **312**, 1806–1809.

- 松田義弘 (1999) : 浜名湖水のふしぎ—内湾の自然と海水の動き. 静岡新聞社, 静岡, 155 pp.
- McCLANAHAN, T. R. (1994): Kenyan coral reef lagoon fish: effects of fishing, substrate complexity, and sea urchins. *Coral Reefs*, **13**, 231–241.
- 森政次・野田頭照美・新井洋一 (1991) : 人工護岸の造成とその生物的效果について. 沿岸海洋研究ノート, **29**, 37–50.
- 中坊徹次 (編) (2000) : 日本産魚類検索全種の同定. 第2版. 東海大学出版会, 東京, 1818 pp.
- 中条武司・山西良平・石田惣 (2008) : 埋め立て・土砂供給の変化による干潟の減少. 干潟を考える干潟を遊ぶ (大阪市立自然史博物館・大阪自然史センター編著), 東海大学出版会, 神奈川, pp. 97–98.
- 西田高志・乾隆帝・鬼倉徳雄・及川信 (2008) : 北部九州岩礁域における磯魚群集と環境構造の関連性. *応用生態工学*, **11**, 51–62.
- 大澤賢人・檜垣直幸 (2012) : 小樽運河における貧酸素水塊の動態. *北海道地質研究所報告*, **84**, 47–53.
- SANO, M., M. SHIMIZU and Y. NOSE (1987): Long-term effects of destruction of hermatypic corals by *Acanthaster planci* infestation on reef fish communities at Iriomote Island, Japan. *Marine Ecology Progress Series*, **37**, 191–199.
- SEAMAN, W. (2007): Artificial habitats and the restoration of degraded marine ecosystems and fisheries. *Hydrobiologia*, **580**, 143–155.
- 清野聡子 (2000) : 日本の沿岸環境保全における応用生態工学の展望—特に海岸の現状と問題点. *応用生態工学*, **3**, 1–6.
- 須田有輔・早川康博 (2002) : 砂浜海岸の生態学. 東海大学出版会, 東京, 427 pp.
- 立松沙織・南條楠土・河野裕美・佐野光彦 (2013) : マングローブ域における護岸造成が魚類群集構造に与える影響. *沖縄生物学会誌*, **51**, 27–40.
- WILSON, S. K., R. C. BABCOCK, R. FISHER, T. H. HOLMES, J. A. Y. MOORE and D. P. Thomson (2012): Relative and combined effects of habitat and fishing on reef fish communities across a limited fishing gradient at Ningaloo. *Marine Environmental Research*, **81**, 1–11.
- 柳哲雄 (2004) : 貧酸素水塊の生成・維持・変動・消滅機構と化学・生物的影響. *海の研究*, **13**, 451–460.

受付：平成 25 年 2 月 19 日

受理：平成 25 年 4 月 1 日

Distribution of the invasive hard clam, *Mercenaria mercenaria*, in the intertidal zone of Sanbanze in the inner part of Tokyo Bay

Junpei SHINJI¹*, Shinnosuke TERUYA², Kensuke ICHIDA³,
Teruki TOMIZAWA⁴, Asuka TOMINAGA⁴ and Risa ITO³

Abstract : We investigated the distribution of the invasive hard clam, *Mercenaria mercenaria*, and other shellfish in the intertidal area of the tidal flats of Sanbanze in Tokyo Bay. We found that the distribution of *M. mercenaria* was negatively correlated with silt-clay content. Almost all the shellfish collected belonged to 1 of the following 3 species: *Ruditapes philippinarum* (41.6%), *M. mercenaria* (27.7%), or *Phacosoma japonicum* (24.1%). Within the study site, few sampling plots were completely occupied. Therefore, *M. mercenaria* did not strongly out-compete other species in this study site.

Keywords : *distribution, invasive species, Mercenaria mercenaria, Tokyo Bay*

1. Introduction

Invasive marine species often have a serious influence on native ecosystems and local fisheries. The invasive marine hard clam, *Mercenaria mercenaria*, was introduced into Tokyo Bay in Japan in the 1990s (KUROZUMI and OKAMOTO, 2002; NISHIMURA, 2005; HIWATARI and KOHATA, 2005; HIWATARI *et al.*, 2006; SUGIHARA *et al.*,

2012). This species is native to the east coast of North America, where it forms a very important fishery resource. In Tokyo Bay, *M. mercenaria* is distributed in highly eutrophic coastal areas and has not yet been observed in other areas in Japan (HIWATARI *et al.*, 2006). SUGIHARA *et al.* (2012) reported that the *M. mercenaria* populations in Tokyo Bay might be native to the Florida Peninsula. Further, it has been shown that *M. mercenaria* has excellent filter-feeding ability (TENORE *et al.*, 1973) and tolerance for environmental changes, such as hypoxic and low salinity conditions (HIWATARI and KOHATA, 2005). Such advantages have probably enabled this species to survive after its introduction into Tokyo Bay. It has been assumed that this clam may compete with native species, including commercially important species such as *Ruditapes philippinarum* (HIWATARI and KOHATA, 2005). Therefore, it is necessary to clarify the impact of this invasive clam on native ecosystems.

Only limited information is available about the environmental factors that affect the distribution of *M. mercenaria* in Japan. Obtaining

1) Department of Global Agricultural Sciences, Graduate School of Agricultural and Life Sciences, The University of Tokyo, Bunkyo-ku, Tokyo 113-0032, Japan

2) Department of Earth and Planetary Sciences, Graduate School of Science, The University of Tokyo, Bunkyo-ku, Tokyo 113-0033, Japan

3) Department of Marine Biosciences, Faculty of Marine Science, Tokyo University of Marine Science and Technology, Minato-ku, Tokyo 108-8477, Japan

4) Course of Marine Life Sciences, Graduate School of Marine Science and Technology, Tokyo University of Marine Science and Technology, Minato-ku, Tokyo 108-8477, Japan

*Corresponding author: Junpei Shinji
aa097107@mail.ecc.u-tokyo.ac.jp

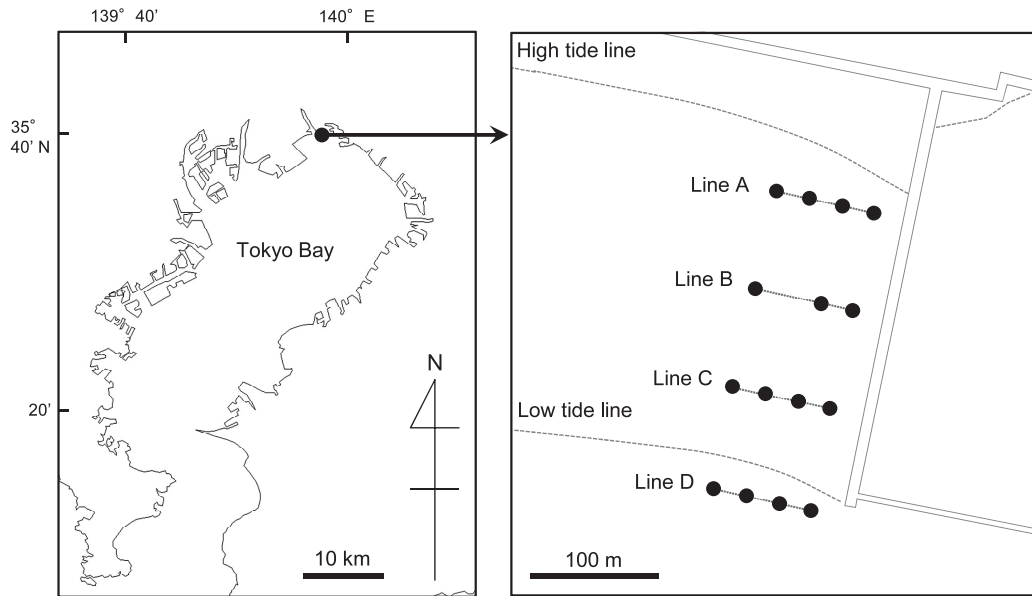


Fig. 1. The study site in Tokyo Bay and the location of the sampling plots. Sampling lines (A-D) were 80 m apart, and the sampling plots were created at 20-m intervals along the lines. The straight solid lines represent a dike.

more information about the distribution of both native and invasive clams should be the first step in evaluating the impact of the invasive clam on native ecosystems. This study was conducted to provide fundamental information for further ecological studies. We examined the tidal flats of Sanbanze in the inner part of Tokyo Bay in late summer, during which a large number of *M. mercenaria* can be found (NISHIMURA, 2005).

2. Materials and methods

Sanbanze is located in the inner part of Tokyo Bay and is one of the largest tidal flats in the bay. Most of the area has a muddy-sand bottom (ACHIARI and SAKAI, 2007). The survey was conducted at low tide, during which the 2.69-km² tidal flats were maximally exposed. (CHIBA PREFECTURE, 2012). It is difficult to access the tidal flats except via Funabashi Sanbanze Kaihin Park (35°40'N, 139°58'E). Therefore, the study site was prepared within the park boundary.

A spatial survey was conducted at low tide, between 10:00 a.m. and 1:00 p.m. on September

5, 2009, when the tidal flats were the most exposed (the lowest tide was at 11:18 a.m.). Four parallel sampling lines were set at 80-m intervals. The first line was set slightly below the high tide line, and the last line was set below the low tide line (Fig. 1). Sampling plots were created at 20-m intervals along each 80-m line by installing a 150-cm bar for determining the water depth at high tide. To analyze mollusk assemblages, sediment was collected using 30 × 30-cm quadrats at each sampling plot. Sediment collected 0–5 cm from the surface was sieved using a 2-mm mesh, and the animals obtained were fixed in 10% formalin immediately after sampling. To analyze environmental conditions, sediment samples were collected near each mollusk-sampling site by using 10 × 30-cm quadrats. Sediment temperature was measured at 3-cm depth by using a stick thermometer. A 0.8-cm-diameter corer was used to collect a 2-ml sediment core from 0–3 cm below the surface. This sediment was used to analyze water content. A 2.7-cm-diameter corer was used to collect a 100-ml sediment core from 0–3 cm below the surface. This sediment was used

Table 1. Density of animal species collected along sampling lines in Sanbanze (mean \pm standard deviation [SD]). Each sampling line contained 3–4 sampling plots.

Class	Family	Species	Density (individuals/m ²)				Number of plots where present
			Line A	Line B	Line C	Line D	
Bivalvia	Mactridae	<i>Mactra veneriformis</i>		3.7 \pm 6.4		8.3 \pm 10.6	3
	Tellinidae	<i>Macoma incongrua</i>			2.8 \pm 5.6		1
	Solenidae	<i>Solen strictus</i>				8.3 \pm 10.6	2
	Veneridae	<i>Mercenaria mercenaria</i>	2.8\pm5.6	44.4\pm50.9	41.7\pm16.7	27.8\pm11.1	11
		<i>Phacosoma japonicum</i>		3.7 \pm 6.4	11.1 \pm 15.7	77.8 \pm 76.4	7
		<i>Ruditapes philippinarum</i>		85.2 \pm 78.8	55.6 \pm 27.2	38.9 \pm 14.3	10
		<i>Cyclina sinensis</i>			2.8 \pm 5.6	1	
Polychaeta	Polychaeta sp.		47.2 \pm 38.9	44.4 \pm 50.9	2.8 \pm 5.6	13.9 \pm 16.7	8

to determine sediment characteristics.

Animals were sorted into species or taxa. They were then counted and their density was calculated. To analyze sediment water content, samples were weighed before and after drying at 105°C for 5 h, and the water content was calculated from the difference in mass. To analyze the sediment characteristics, samples were treated with 30% hydrogen peroxide to remove organic compounds and then dried at 60°C for 96 h. The composition of sediment grain sizes was determined using a series of sieves with 2-, 1-, 0.5-, 0.25-, 0.125-, and 0.063-mm meshes, and the median grain size and silt-clay content were measured.

For homogeneity of variance and normality, all numerical data were log-transformed and percent data were arcsine transformed, as per the study by ZAR (1984). Differences between the means of environmental factors along each sampling line were compared using one-way analysis of variance (ANOVA) and Bonferroni's method. Pearson's product-moment correlation coefficient was calculated between major bivalve species. The correlation coefficient was tested using a *t* test. Stepwise multiple regression analysis was performed to examine correlations between the density of *M. mercenaria* and environmental conditions. Differences were considered significant if the associated *p*-value was less than 0.05.

3. Results and discussion

Seven bivalve species were found in the study site (Table 1). A vast majority of these bivalves were 1 of 3 species of filter feeders: Of the total number of bivalves found, 41.6% were *R. philippinarum*, 27.7% were *M. mercenaria*, and 24.1% were *Phacosoma japonicum*. *M. mercenaria* was found in a greater number of sampling plots (11 sampling plots) than any of the other species. Thus, the invasive clam, *M. mercenaria*, was one of the dominant species in the study site. The distribution of *M. mercenaria* was similar to that of *R. philippinarum*, and few sampling plots were entirely occupied by *M. mercenaria*. NISHIMURA (2005) reported that, although the number of individuals varied between seasons and places, 80% of all samples acquired in 2002 from Chiba Port in Tokyo Bay were *M. mercenaria*. We observed no such extreme dominance, and there was no negative correlation between the density of *M. mercenaria* and that of the other 2 major species, namely, *R. philippinarum* ($R=0.59$; $P < 0.05$) and *P. japonicum* ($R=0.17$; $P > 0.05$). These results imply that the presence of *M. mercenaria* did not exclude other species from the study site. Therefore, there was no evidence that *M. mercenaria* strongly out-competes other species in the study site.

Sampling lines A–C in this study were placed in the intertidal zone, and line D was in

Table 2. Environmental conditions, species richness, and total density of collected animals along sampling lines in Sanbanze (mean \pm standard deviation [SD]).

	Line A	Line B	Line C	Line D
Water depth at high tide (cm)	62.5 \pm 5.0 ^a	95.0 \pm 10.0 ^b	118.8 \pm 4.8 ^c	NA*
Emersion (h)	7.1 \pm 0.3 ^a	5.3 \pm 0.6 ^b	4.2 \pm 0.3 ^c	0.0 \pm 0.0 ^d
Temperature ($^{\circ}$ C)	32.1 \pm 0.3 ^a	30.3 \pm 1.2 ^b	29.4 \pm 0.5 ^b	26.1 \pm 0.8 ^c
Water content (%)	23.0 \pm 2.0 ^a	20.5 \pm 6.2 ^a	21.1 \pm 2.6 ^a	27.4 \pm 0.9 ^a
Median grain size (μ m)	78.3 \pm 6.5 ^a	103.7 \pm 12.0 ^b	88.4 \pm 6.0 ^{ab}	82.4 \pm 4.2 ^a
Silt-clay contents (%)	7.8 \pm 4.5 ^a	0.3 \pm 0.2 ^b	0.4 \pm 0.2 ^b	0.7 \pm 0.3 ^b
Species richness	1.0 \pm 0.0 ^a	2.7 \pm 1.5 ^{ab}	3.3 \pm 1.0 ^b	4.5 \pm 0.6 ^b
Density (individuals/m ²)	50.0 \pm 34.5 ^a	136.1 \pm 107.5 ^b	116.7 \pm 32.1 ^b	175.0 \pm 80.8 ^b

Different letters within rows indicate significant differences ($n = 3-4$; $P < 0.05$).

* The water depth at high tide on line D was deeper than 150 cm, which is the length of the bar used to measure water depth in this study.

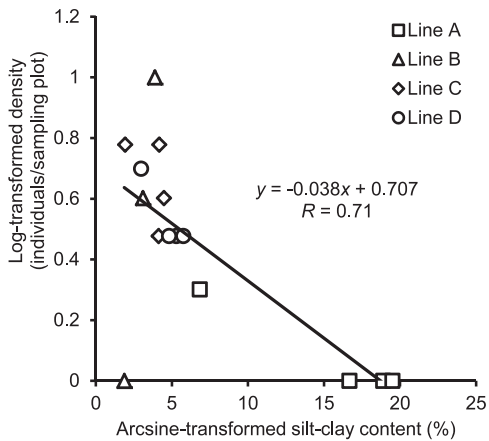


Fig. 2. Correlation between silt-clay content and the density of *M. mercenaria* in sampling plots (30 \times 30 cm²) located in Sanbanze mudflat in Tokyo Bay.

the subtidal zone. Although the water depth at high tide and emersion differed between lines B and C, the environmental conditions were similar along these 2 lines (Table 2). The following formula was obtained using stepwise multiple regression analysis:

$$y = -0.038x + 0.707 \quad (r = 0.71),$$

where y is the density of *M. mercenaria* and

x is silt-clay content. The distribution of *M. mercenaria* in this study was negatively correlated with silt-clay content (Fig. 2). No other correlations were observed between environmental conditions and the abundance of *M. mercenaria*. The negative correlation between sediment silt-clay content and density of *M. mercenaria* was conspicuous along sampling line A (Table 1, 2). It has been reported that the presence of 44 mg/L of silt in the water decreases the growth rate of *M. mercenaria* (BRICELJ *et al.*, 1984). Such changes in growth rate may depend on the efficiency of selection between nutritious substances and suspended sediments in the water (BRICELJ and MALOUF, 1984). It may be that the high silt-clay content observed in all the sediments was caused by a large quantity of suspended sediments in the water at high tide. The absence of *M. mercenaria* at line A may therefore be due to high silt-clay content of the water in that area. However, the silt-clay content of the sediments was approximately 8% or less along all sampling lines, including line A, which had the fewest individuals of this species. Contrary to the results of our study, NISHI *et al.* (2008) reported that *M. mercenaria* was found in several areas of Yokohama Port, which opens into Tokyo Bay, where the silt-clay content was more than 15.7% and the substratum had low

oxidation-reduction potential. Although our study results do not indicate the reason for this difference in silt-clay content between Sanbanze and Yokohama Port, it is assumed to be one of the reasons that the study site used by NISHI *et al.* (2008) and that used in our study were geomorphologically different. The study site used by NISHI *et al.* (2008) was located in a canal, whereas in our study, the site was an intertidal zone in a tidal flat. Sediments are well-raised from surf zone to swash zone (SHUTO, 1988), and the intertidal zone in this study was within these zones. Therefore, the study site used by NISHI *et al.* (2008) is assumed to be less affected by waves from the sea than the site used for our study. The negative correlation we observed between silt-clay content and the density of *M. mercenaria* may result from geomorphological features that cause a relatively large amount of suspended sediment in areas with high silt-clay content. In this study, we did not directly test this hypothesis. Therefore, a more detailed survey and additional experiments are necessary, even though it appeared that silt and clay were among the major factors that affected the distribution of *M. mercenaria* in the study site.

In this study, we investigated the distribution of *M. mercenaria* in a part of Sanbanze. *M. mercenaria* is abundant in Sanbanze, as it is in other places in Tokyo Bay (NISHIMURA, 2005; NISHI *et al.*, 2008). Our study data should help to clarify the distribution of *M. mercenaria* in Tokyo Bay. Furthermore, Sanbanze faces land subsidence; the area of the tidal flats has decreased by over 50% over the past 3 years, primarily because of the Great East Japan Earthquake (CHIBA PREFECTURE, 2012). Therefore, this study, which describes the biological distribution of bivalves before the Great East Japan Earthquake, can also be used as a baseline survey for tracing ecological and geographical changes after the earthquake. Further research is required to obtain more details about the distribution of the invasive species, *M. mercenaria*.

Acknowledgements

We thank Dr. K. OKAMOTO and Dr. N. M. SUGIHARA (Graduate School of Agricultural and

Life Sciences, University of Tokyo) for offering important advice about the ecological characteristics of *M. mercenaria* and the geographical characteristics of Sanbanze. Further, we express our gratitude to Dr. H. KUROKURA (Graduate School of Agricultural and Life Sciences, University of Tokyo) for providing the experimental equipment. In addition, we thank Dr. S. WATANABE (Japan International Research Center for Agricultural Sciences) and Dr. K. KON (Shimoda Marine Research Center, University of Tsukuba) for their instructions on conducting the ecological survey.

References

- ACHIARI, H. and J. SAKAI (2007): Numerical analysis of wind-wave climate change and spatial distribution of bottom sediment properties in Sanbanze Shallows of Tokyo bay. *Journal of Coastal Research*, **50**, 343–347.
- BRICELJ, V. M., R. E. MALOUF and C. DE QUILLFELDT (1984): Growth of juvenile *Mercenaria mercenaria* and the effect of resuspended bottom sediments. *Marine Biology*, **84**, 167–173.
- BRICELJ, V. M. and R. E. MALOUF (1984): Influence of algal and suspended sediment concentrations on the feeding physiology of the hard clam *Mercenaria mercenaria*. *Marine Biology*, **84**, 155–165.
- CHIBA PREFECTURE (2012): A report on investigation of the influence of earthquake (depth in Sanbanze) (in Japanese). CHIBA PREFECTURE, Chiba, 1–73 pp.
- HIWATARI, T. and K. KOHATA (2005): An exotic hard clam *Mercenaria mercenaria* introduced in Tokyo Bay (in Japanese). *Journal of Japan Society on Water Environment*, **28**, 614–617.
- HIWATARI, T., Y. SHINOTSUKA, K. KOHATA and M. WATANABE (2006): Exotic hard clam in Tokyo Bay identified as *Mercenaria mercenaria* by genetic analysis. *Fisheries Science*, **72**, 578–584.
- KUROZUMI, T. and M. OKAMOTO (2002): Some newly introduced mollusks in the southern Kanto region (in Japanese). Summary of the annual meeting of the Malacological Society of Japan. *Venus*, **61**, 111.
- NISHI, E., A. SAKAMOTO, H. MIZUO, Y. KOICHI and K. SHIMOMURA (2008): Record of an alien clam *Mercenaria mercenaria* from the Yokohama port, Tokyo Bay (in Japanese). *Natural History Report of Kanagawa*, **29**, 181–183.
- NISHIMURA, K. (2005): Distribution of the hard clam *Mercenaria mercenaria* (Veneridae) in the short-

- necked clam beds of Tokyo Bay (in Japanese). *Chiribotan*, **36**, 63–66.
- SHUTO, N (1988): Physical environment: Environmental characteristics in estuary and coastal zone. *In Ecology and Ecotechnology in Estuarine-Coastal Area*. Kurihara, Y. (ed.), Tokai University Press, Tokyo, p. 3–25.
- SUGIHARA, N. M., T. FURUTA and K. OKAMOTO (2012): Genetic structure of the exotic hard clam *Mercenaria mercenaria* in Tokyo Bay, determined using mitochondrial DNA. *Fisheries Science*, **78**, 569–575.
- TENORE, K. R., J. C. GOLDMAN and J. P. CLEARNER (1973): The food chain dynamics of the oyster, clam and mussel in an aquaculture food chain. *Journal of Experimental Marine Biology and Ecology*, **12**, 157–165.
- ZAR, J. H. (1984): Data transformations. *In Biostatistical analysis*, Prentice Hall, Englewood Cliffs, New Jersey, 236–243 pp.

Received: August 24, 2012

Accepted: August 4, 2013

Numerical simulation on sedimentation in Yangon River and its navigation channel

TOE TOE AUNG¹⁾, Takenori SHIMOZONO and Akio OKAYASU*

Abstract : A shallow area called, Inner Bar, near Yangon Port is a major obstacle for Yangon River traffic. In order to obtain basic information for the sedimentation problem, characteristics of flow, sediment transport and bed level changes were investigated for Yangon River and its navigation channel by means of numerical simulation. 3-D Princeton Ocean Model (POM) with a wetting and drying scheme was used to cope with large tidal ranges for predicting the river and tidal flows. Topographic data, upstream river discharges and tidal elevations at the river mouth were given as the input data for the models. Computed depth-averaged velocity was verified against field data of NELSON (2000). Bed shear stress was evaluated from bottom velocity calculated by the 3-D flow model. Bed level change was simulated with a 2-D sediment transport model for different seasonal and tidal conditions. Sediment diameter used in the calculation was obtained by sand sampling from material of Inner Bar. The simulation clearly showed large amount of sand deposition at Inner Bar and some other areas in the river. Estimated amount of sedimentation around Inner Bar was roughly equivalent to that of bottom material dredged by Myanmar Port Authority to maintain the depth.

Keywords : Yangon River, sedimentation, numerical calculation, tide, wetting and drying

1. Introduction

Sedimentation in rivers and estuaries is a common problem for maintenance of waterways. The river fresh water and daily or twice-daily reversing flows due to tidal action make flows in estuaries and tidal section of rivers complex. Fig. 1 shows the area of interest for the present study, the Yangon River which is on an eastern branch of Ayeyarwaddy River. The Ayeyarwaddy River is the fifth largest in the world in terms of sediment discharge, depositing more than 360 million tons of sediment annually into the continental shelf in the

1) Phone: 95-1-556375;

Email: toetoeoung@gmail.com

* Corresponding author:

Coastal Environment and Engineering Laboratory, Department of Ocean Sciences, Tokyo University of Marine Science and Technology, 4-5-7, Konan, Minato, Tokyo 108-8477, Japan
Phone: 03-5463-0473; Fax: 03-5463-0517
Email: okayasu@kaiyodai.ac.jp

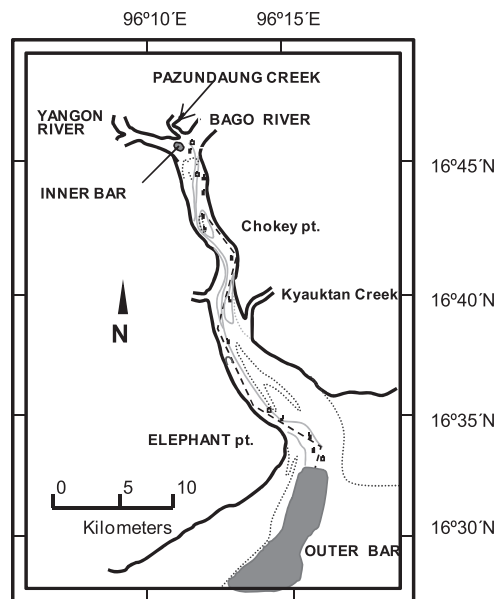


Fig. 1. Locations of Yangon River and Estuary and the two sand bars, Inner Bar and Outer Bar

northern Andaman Sea. Yangon River is the most important river to Myanmar for 90% of its international marine trades are transported through this channel. The distance between the Yangon Port and the river mouth is about 45 kilometers and the width of river in the region is from 2 kilometers to 7 kilometers. Active sediment transport due to river flows and tidal currents causes two major shallow water areas; one is called "Inner Bar" located inside the river near Yangon Port and the other is "Outer Bar" which extends out from the river mouth as shown in Fig. 1. Dredging works are required to maintain depth of the channel at these areas. Despite knowledge gathered on the Yangon River and Estuary system, little information is currently available on the behavior of sediment transport caused by the river flow and the tidal currents. Therefore it is difficult to take effective measures for sedimentation other than dredging.

There were some researches focused on the problem due to sedimentation at shallow water areas in Yangon River. SIR ALEXANDER GIBB and PARTNERS (1974) investigated physical conditions of Yangon River through an extensive field study. NELSON (2000) conducted a field study on the behavior of fine-grained sediment in Yangon River by measuring the current speed, depth, salinity and sediment concentration. CHINA TRANSPORTATION ENGINEERING (2006) made a proposal on an improvement of the conflux of the Yangon River, Pazundaung Creek and the Bago River. They proposed three types of dikes for controlling the main flow. TOE TOE AUNG *et al.* (2011) computed flows and sediment transport in Yangon River by a 2-D numerical model. In their paper, sediment transport was simulated from depth-averaged velocity given by the 2D flow model and sediment particle size (8 to 50 μm and the mean diameter is 11 μm) used in the calculation was based on the results of field study by SIR ALEXANDER GIBB and PARTNERS (1974), where actual sediment diameter at Inner Bar was much larger than that used in the calculation.

Although near-bottom velocity generally gives a dominant effect to sediment transport, most of the previous studies didn't consider three dimensionality of the flow field. Since the

tidal range in the area is very large, dry-up of the river bottom should also be considered in the calculation. In this study, 3-D Princeton Ocean Model with the wetting and drying scheme was used for flow evaluation to obtain the near bed velocity fields which are important both for bed load and suspended sediment transport. Sediment diameter of interest is another important factor for evaluation of sediment transport. Thus, a field observation was carried out to obtain the sediment diameter of which forms the shallow area at Inner Bar.

Then, 2-D sediment transport has been computed by using the calculated bottom velocity and water surface elevation resulted from the flow model and the sediment diameter obtained from the field observation described above. It was assumed in the present study that near-bottom sediment transport is dominant also for suspended sediment transport. Thus velocity calculated by the 3-D flow model for the bottom layer was used to evaluate suspended load in the 2-D sediment transport model. The deposition rate of sediment at Inner Bar was evaluated and compared with the amount of dredging conducted by Myanmar Port Authority.

2. MODEL DESCRIPTIONS

2.1 Flow model

The 3-D Princeton Ocean Model (POM) with a wetting and drying scheme was used for the investigation of flow characteristics in Yangon River. The Princeton Ocean Model (POM) is a three-dimensional, primitive equation, numerical ocean model, mainly used for solving the hydrodynamics in the coastal region and bays and estuaries (BLUMBERG and MELLOR, 1987). The POM employs a finite difference scheme to numerically solve the primitive equations. The model is calculated with external and internal modes; the external mode portion of the model has short time steps for the 2-DH flow field and the internal mode has long time steps to evaluate its vertical distribution. The horizontal finite difference grids can be rectangular (as used in this study) or curvilinear orthogonal, while the vertical grids are in sigma coordinates which are the normalized vertical coordinates with the water column depth. The

use of sigma levels gives better resolution of the boundary layers. Detailed information on the formulation and derivation of these equations including the definitions for each variable and formulas for the specific terms in these equations were included in the POM User's Guide (MELLOR, 2004).

POM08 with wetting and drying (WAD) scheme (OEY, 2005) was used in this study among versions of POM. Wetting and drying process was considered to account for the dry up areas due to high tidal ranges. For the use of WAD scheme, it is necessary to define the absolute land boundary (ALB) which must be high enough in elevation, so that water can never split into that area. In the land side of ALB, the area was always dry and the land mask FSM (time-independent land mask) and WADMASK (time-dependent mask for wet and dry condition) are set to be 0. Toward the seaward of the ALB, FSM is 1 and WADMASK was 1 or 0 depending on whether the cell is wet or dry (OEY, 2006). In Oey's WAD scheme, a minimum depth (dry depth=5 cm) is defined to determine the "dry" or "wet" state of each cell. When the total depth (D), which is the summation of water depth (H) and elevation (η), falls below the minimum depth, cells are considered as dry.

In this study, ALB were located along the river bank so that the water did not flood over the bank because the bank slope was relatively steep and the actual flood distance due to high tides were smaller than a grid size. The wet and dry process was calculated only for shoals within the river channels. Based on the Oey's scheme, the calculation was done with dry depth of 5 cm as the minimum depth to calculate velocity. 5 cm was set as the lowest limit for calculation and if the water depth was less than 5 cm, the corresponding flux was set as zero. From the results of the flow model in the study area shown in Fig. 6, it can be seen that WAD scheme is capable of calculating well for high tidal condition in the study area as illustrated in Fig.7. Without WAD scheme, computations break down at the ebb tide due to the large tidal range.

Simulations were made for two different seasons, the monsoon and the dry season, since the

seasonal variation of river discharge was significant. Moreover, the simulation was carried out on two tide conditions; spring tide with a tidal range of 5.2 m and neap tide, 1.8 m. Therefore the model was run for four cases (Table 2); spring tide at monsoon and dry season and neap tide at monsoon and dry season. Before computing the sediment transport, the Shields parameter was calculated by using the bottom velocity results from the flow model and the sediment particle sizes obtained from field study described in Chapter 3. From distributions of Shields parameter calculated for each case, possible sediment deposition areas can be estimated with a sediment transport model.

2.2 Sediment Transport Model

The velocity and water depth were interpolated from the results of the flow model for the required time step according to the courant number and used as input data for sediment transport model. The governing equation for the suspended sediment transport is the advection-diffusion equation with the entrainment and deposition terms,

$$\begin{aligned} \frac{\partial(CD)}{\partial t} + \frac{\partial(uCD)}{\partial x} + \frac{\partial(vCD)}{\partial y} = \\ \frac{\partial}{\partial x} \left(\varepsilon D \frac{\partial C}{\partial x} \right) + \frac{\partial}{\partial y} \left(\varepsilon D \frac{\partial C}{\partial y} \right) + \omega_s (E_s - \bar{C}_b) \end{aligned} \quad (1)$$

Symbol t is time, D is total water depth, ε is eddy viscosity, u and v are the velocity components in x and y direction, ω_s is settling velocity of sediment in water, C is depth-averaged sediment concentration, \bar{C}_b is near bed concentration and E_s is dimensionless rate of sediment into suspension across unit area per unit time. As described in the previous section, velocity at the bottom layer is used for evaluation of suspended load in the present study.

The eddy viscosity is calculated by LANE and KALINSKE (1941) as

$$\varepsilon = 1/D \int_0^D \varepsilon(Z) dz = u_* K D / 6 \quad (2)$$

where u_* is the shear velocity at the bed and K is the Karman constant. The entrainment of

sediment is calculated by the formula of GARCIA and PARKER (1993),

$$E_s = \frac{AZ_U^5}{1 + \frac{\alpha}{0.3}Z_U^5} \quad (3)$$

$$A = 1.37 \times 10^{-7}, Z_U = (u^*/\omega_s)^5 R_{ep}^3,$$

$$R_{ep} = \sqrt{RgD_s^3}/\nu, R = (\rho_s/\rho) - 1.$$

where R_{ep} is particle Reynolds number, ρ_s, ρ are density of sediment particle and water, ν is the kinematic viscosity of water, D_s is diameter of sediment particle. The settling velocity ω_s is calculated by the formula of CHENG (1997).

$$\frac{\omega_s D_s}{\nu} = (\sqrt{25 + 1.2d_*^2} - 5)^{1.5} \quad (4)$$

where,

$$d_* = \left(\frac{Rg}{\nu^2}\right)^{1/3} D_s \quad (5)$$

By assuming a vertical distribution of sediment concentration to be Rousean profile (ROUSE, 1937), the near bed concentration is evaluated by $C_b = \gamma_0 C$. PARKER *et al.* (1987) gave a simple fit to the profile and derived the following expression for γ_0 ,

$$\gamma_0 = 1 + 31.5 \left(\frac{u_*}{\omega_s}\right)^{-1.46} \quad (6)$$

By the combination of suspended sediment and bed load, the bed level change, Z_b is calculated by the bottom evolution equation

$$(1 - \lambda_p) \frac{\partial Z_b}{\partial t} = -\frac{\partial q_{bx}}{\partial x} - \frac{\partial q_{by}}{\partial y} + \omega_s (\bar{C}_b - E_s) \quad (7)$$

λ_p is the bed porosity. The bed load transport q_{bx}, q_{by} is evaluated by the Meyer-Peter and Muller equation (MEYER-PETER and MULLER, 1948)

$$q_b = 8\sqrt{\left(\frac{\rho_s}{\rho} - 1\right)gD_s^3} (\tau_* - \tau_{*c})^{\frac{3}{2}} \quad (8)$$

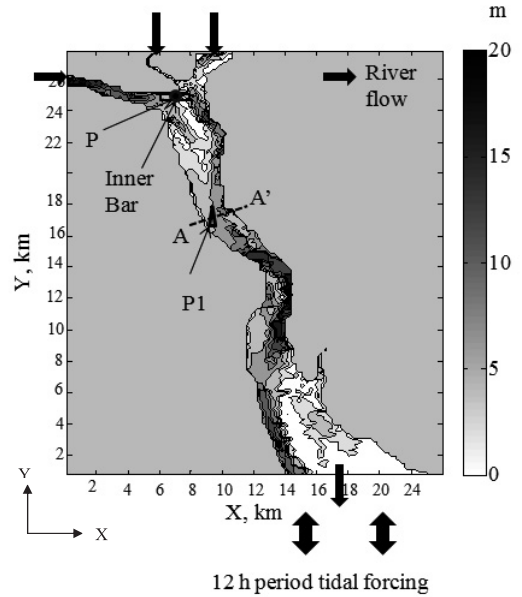


Fig. 2. Bathymetry of Yangon River and boundary elements for calculation. Section A-A' shows the location of field survey conducted by NELSON (2000). P shows one of the point in the Inner Bar and P1 indicates the location for velocity comparisons given in Fig. 5. (The datum of bathymetry is the lowest low water level.)

τ_* and τ_{*c} are the base shear stress and critical shear stress. The MacCormack Scheme is used for discretization (FENNEMA. and CHAUDHRY, 1990).

2.3 Input Data and Boundary Conditions

Bathymetry, discharge of the three rivers and the tidal elevation at the river mouth were given to the flow model as the input data. The calculating area of the Yangon River lies between $16^{\circ}30'N$ to $16^{\circ}47'N$ latitude and $96^{\circ}10'E$ to $96^{\circ}20'E$ longitude. The bathymetry data was created by digitizing the sounding chart provided by MYANMAR PORT AUTHORITY (2007) shown in Fig. 2. The grid spacing was 6 seconds for both latitude and longitude (approximately 170 meters at the site) and 6 vertical sigma levels were determined. The external time step in the flow model was 1 s and the internal time step was 4 s according to Courant-Fredrics-Levy (CFL) condition. The discharge data of

Table 1. Discharge data of three rivers in dry and monsoon (rainy) seasons

	Dry Season (m ³ /s)	Monsoon Season (m ³ /s)
Yangon River	627	6853
Pazundaung Creek	143	866
Bago River	315	1566



Fig. 3. Dredging ship and bottom material (mixture of sand and water) taken from Inner Bar (16° 45.817'N and 96°11.945'E) on 16th September 2010.

three rivers for dry and monsoon seasons were shown in Table 1. These discharge data were from the field data of SIR ALEXANDER GIBB and PARTNERS (1974). The tidal range varied between 5.2 m and 1.8 m near the city of Yangon (Myanmar Port Authority).

The present computational domain had three up-stream inflows and an outflow boundary at the river mouth as shown in Fig. 2. Estimated discharges of the upper three rivers were constantly given at the inflow boundaries while the sum of them was discharged from the outflow boundary. For the tidal current, water surface elevation and the corresponding tidal velocity were given at the outflow boundary assuming in a form of sinusoidal waves. To simplify the model, the temperature and salinity which supposed to be less important for bed level change in rivers were kept constant during the simulation.

For sediment concentration, the inlet of the

three rivers and outlet of the river were assumed to be in equilibrium state for given flow velocities. Sediment diameter was set at 0.338 mm based on the field result obtained for the Inner Bar as described below.

3. Sampling of Sedimentation Material

Particle size is one of the most important parameters for sediment transport. Since amount of sediment transport is greatly affected by sediment diameter, an appropriate sediment diameter should be chosen to evaluate sedimentation at Inner Bar. In the previous studies, sediment diameter in the Yangon River system was only given for suspended sediment (e.g. SIR ALEXANDER GIBB and PARTNERS, 1974) whose representative diameter is usually much different from that for bed materials.

In order to give an appropriate grain size of bed materials to the numerical model, field observation was conducted at the Inner Bar area in Yangon River on 16 September 2010. Sediment sample was taken from bed materials on a dredging ship (Fig. 3) being operated to dredge sediment deposited at Inner Bar.

The distribution of particle diameters was obtained by the sieve analysis for the bed material. Although it was observed that the suspended sediment sampled near river surface was composed of very fine sand, clay and silt with diameters ranging from several μm to a hundred μm , the bed material from Inner Bar had d_{75} diameter of 0.338 mm which was much larger than the suspended material. The grain size distribution curve for the bed material is shown in Fig. 4. Therefore in the present study, diameter of 0.338 mm is used as the representative sediment diameter for the bed materials in order to evaluate sand movement causing Inner Bar sedimentation.

Table 2. Four conditions of calculation in terms of tidal rage and river discharges.

	Monsoon	Dry
Spring tide (5.2 m tidal height)	Case 1	Case 2
Neap tide (1.8 m tidal height)	Case 3	Case 4

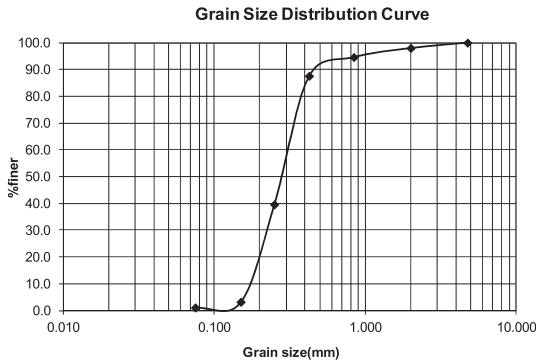


Fig. 4. Grain size distribution curve for bed material from the Inner Bar Area.

4. Results and Discussions

4.1 Calculated depth-averaged flow field and comparison with field data

Flow velocity for spring tide at monsoon season (Case 1 in Table 2) is shown in Fig. 5. Fig. 5. (a) and (b) give the depth-averaged velocity fields at the ebb and the flood tide conditions for spring tide at monsoon season, respectively. During ebb tide, the flow direction is seaward. During flood tide, the flow was directed towards the upstream of the river, since the river discharge only had a limited influence to the overall flow pattern. Comparisons of the surface and bottom flow velocity at ebb and flood tide conditions show that the bottom velocity is generally smaller than the surface velocity but the flow directions and patterns are similar.

To verify the numerical simulation, the cal-

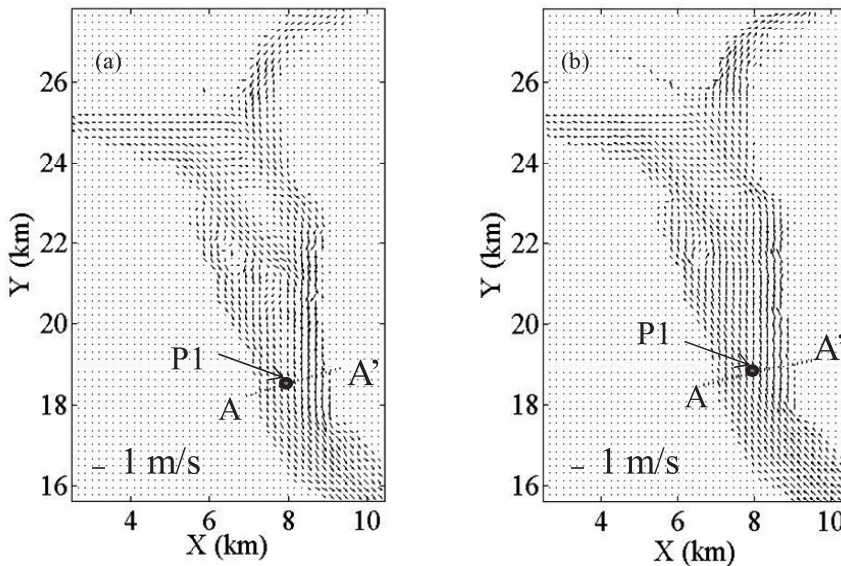


Fig. 5. The depth-averaged velocity fields for (a) ebb tide and (b) flood tide at spring tide during the monsoon season

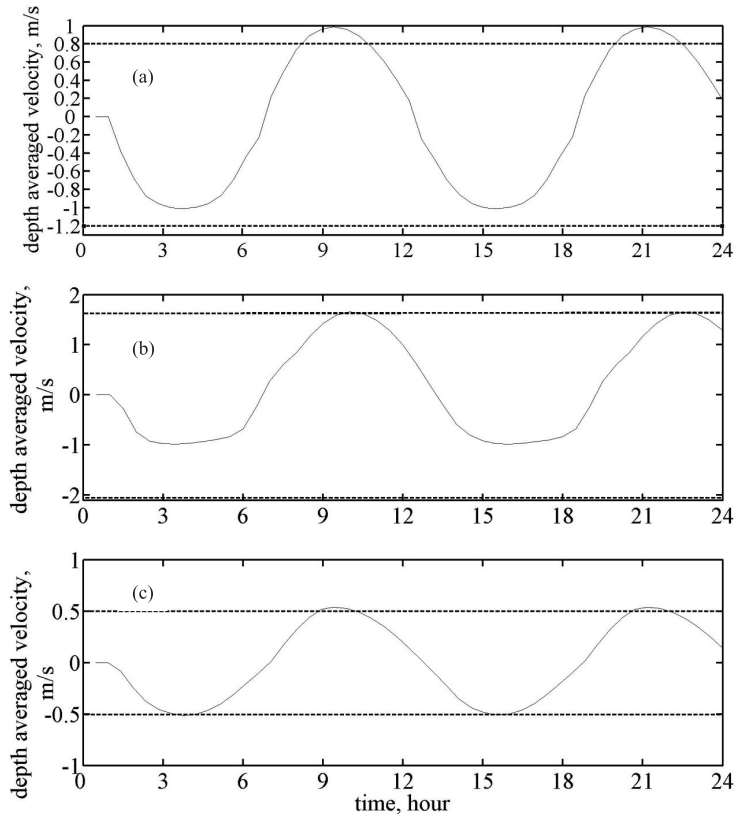


Fig. 6. The depth-average velocity for (a) spring tide in the monsoon season, (b) spring tide in the dry season and (c) neap tide in the dry season at point P1. The dotted lines show the field results of NELSON (2000). (The lines with positive values are at flood tide condition and those with negative values are at ebb tide condition.)

culated depth-averaged velocities were compared with field results obtained by NELSON (2000) at the 10 km downstream of the Yangon Port (A-A' cross section in Fig. 5). The simulation was done for three conditions; the spring tide in monsoon season, the spring tide in dry season and the neap tide in dry season according to the conditions for Nelson. The field observation of Nelson gave the maximum depth-averaged velocity for the spring tide in monsoon season and the neap tide in dry season. But for the spring tide in dry season, it gave only one value for velocity and did not mention whether it was depth-averaged velocity or maximum velocity.

Time variations of depth-averaged velocity calculated at P1 indicated in Fig.5 are shown in

Fig. 6, although information of the exact measurement location is not provided in NELSON (2000). The dotted straight lines correspond to the values of depth-averaged velocities obtained by Nelson. The model results of the spring tide in monsoon season and the neap tide in dry season are in good agreement with the field data. In the case of spring tide at dry season, the model result for flood tide velocity is nearly equivalent with the field result but the model result for ebb tide velocity is smaller than the field measurement. The discrepancy might occur due to the lack of information of the exact locations of the field study area. Since the difference is found in the ebb tide condition, another possible reason can be the river discharge which might be larger at the time of

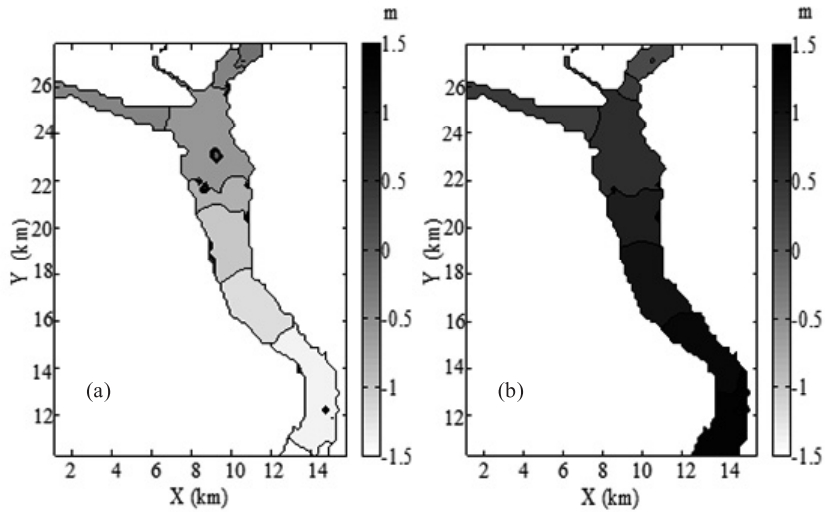


Fig. 7. The water surface elevation with respect to the mean sea level (m) for (a) ebb tide and (b) flood tide. The dried areas are shown as the water surface elevation is 0.

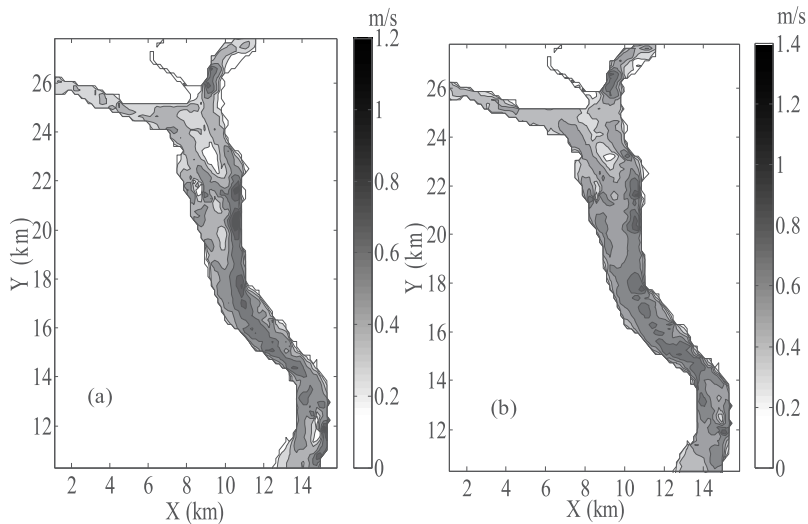


Fig. 8. The magnitude of depth-averaged velocity (m/s) for (a) ebb tide and (b) flood tide.

measurement. The river discharge used in present model was from SIR ALEXANDER GIBB and PARTNERS (1974) which were older than NELSON (2000).

4.2 Results and Discussions for flow model

The velocity fields, depth-averaged velocity and velocity for each layer of depth, water surface elevation with respect to the mean sea level

at the ebb and flood tide conditions were obtained respectively for the four cases listed in Table 2.

The results on the spring tide at monsoon season (Case 1 in Table 2) are shown in Fig. 7 and 8. Fig. 7 (a) and (b) show the water surface elevation for ebb and flood tide conditions, respectively. Some dry areas where the water surface elevation is expressed as 0 for practical

Table 3. Calculated bottom velocity and resulting Shields parameters at Inner Bar which is indicated by symbol "P" in Fig. 1.

Period	Tidal Forcing	Tidal condition	Bottom Velocity (m/s)	Shields Parameter
Monsoon	Spring	Flood	0.55	0.0091
		Ebb	0.45	0.0084
	Neap	Flood	0.24	0.0022
		Ebb	0.23	0.0017
Dry	Spring	Flood	0.44	0.0073
		Ebb	0.41	0.005
	Neap	Flood	0.082	0.0002
		Ebb	0.078	0.0002

purpose can be observed clearly in the ebb tide condition while flood water filled up the dry area. Fig.8 (a) and (b) show the magnitude of depth-averaged velocity values for ebb and flood tide conditions, respectively. The largest velocity occurred in the downstream of the Yangon River and the magnitude of the depth-averaged velocity during ebb tide and flood tide were up to 1.7 m/s. The magnitude of depth-averaged velocity takes its minimum near the junction of the three rivers as well as the places associated with the shallow water areas. This might be because flows from rivers with different directions met each other at the junction and some parts of their velocities cancelled each other out.

The model results in the monsoon and dry seasons for one of the point (indicated by P in Fig. 2) near Inner Bar area under both of the spring and neap tide conditions are shown in Table 3 together with Shields parameter calculated for sand diameter of 0.338 mm. It can be seen that the bottom velocities of flood tide were slightly larger than those of the ebb tide for all cases. The resulting values of the Shields parameter near Inner Bar area were very small and indicate that sediment deposition should occur around the area.

The results of the other three cases, Case 2, 3 and 4, are not shown in the figures but gave similar characteristic with Case 1. For water surface elevation, dry-up areas were calculated during ebb tide condition in very shallow areas.

The depth-averaged velocities for Case 2 (neap tide at monsoon season) were varying from 0.2 to 0.6 m/s. For Case 3 (spring tide at dry season), the velocities were about 0.4 to 1.5 m/s. It was found that the magnitudes of depth-averaged velocity were about 0.1 to 0.5 m/s in Case 4 (neap tide condition at dry season).

4.3 Sediment Transport and Bathymetry Change

Calculations for sediment transport were performed for the four cases given in Table 2. The ratio of the suspended load and bed load transports in the calculation around the Inner Bar area was roughly evaluated as 9 : 1. The combined results of suspended load and bed load transports are used in the calculation of bed level change and the evaluated bed level changes are shown in Figs. 9 to 12. In each figure, sub-figure (a) and (b) represent the accumulated bed level changes for one ebb tide (a half of one tidal cycle) and one flood tide and sub-figures (c) represent those for one whole tidal cycle. The zero value represents the initial river bed and negative values represent erosion and positive values are for deposition. From the results, it is found that the deposition and erosion are larger in spring tide conditions than those in neap tide conditions for both monsoon and dry seasons. Please note that the scales for sedimentation are different between the figures for spring tide conditions (Figs. 9 and 10) and those for neap tide conditions (Figs. 11 and 12).

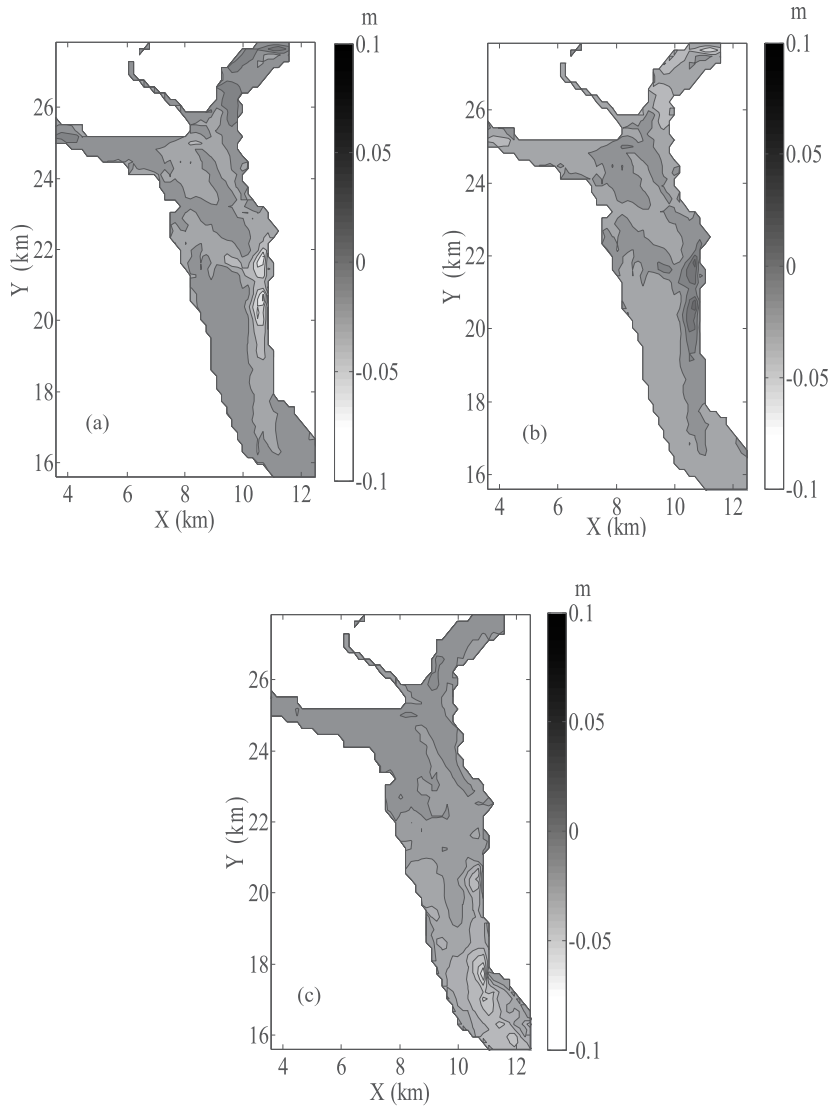


Fig. 9. Accumulated bed level change (m) for (a) ebb tide and (b) flood tide condition and (c) one tidal cycle at spring tide at monsoon season.

The results indicated that the deposition occurred around Inner Bar (indicated by the symbol P in Fig. 2) for all the cases. Remarkable deposition is seen just at Inner Bar for the case of spring tide at monsoon season (Fig. 9 (c)) in particular. In other areas, sediment deposition and erosion patterns are consistent with our preexisting knowledge such as other sand bar areas out of the navigation channel

and the downstream around the Chokey Point (see Fig. 1) area where erosion occurs in both monsoon and dry seasons.

To maintain the required depth of the navigation channel, Myanmar Port Authority (MPA) does dredging operation by a dredging ship every day. The capacity of the dredging ship is approximately 1000 m^3 and it gets sand of four to six times of its capacity per day near

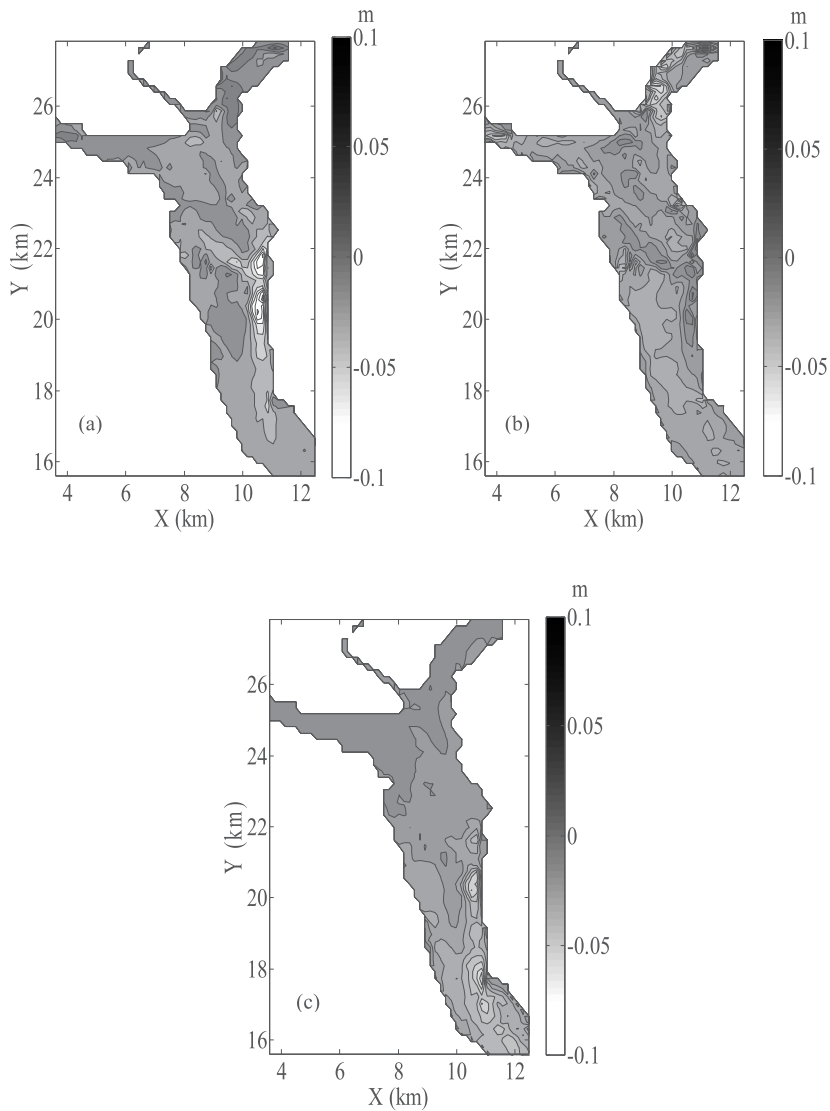


Fig. 10. Accumulated bed level change (m) for (a) ebb tide and (b) flood tide condition and (c) one tidal cycle at spring tide at dry season.

the Inner Bar area. Although it is difficult to estimate the exact volume of dredged material, the amount of it is roughly estimated as $6 \times 10^3 \text{ m}^3$ per day.

From the calculation, rate of deposition at Inner Bar is evaluated to be around 0.04 m per day. If the area of Inner Bar is assumed to be about $1.4 \times 10^5 \text{ m}^2$ (roughly estimated as 1400 m by 100 m from the dredging area and

the bathymetry), the amount of sand deposition in a day in the spring tide at monsoon season is estimated by multiplying deposition depth to the estimated Inner Bar area and it was about $6 \times 10^3 \text{ m}^3$ which is equivalent to that obtained by the dredging amount. As the calculated rate of deposition at neap tide conditions is much smaller, about $2 \times 10^3 \text{ m}^3$ per day, the overall evaluation of sedimentation should

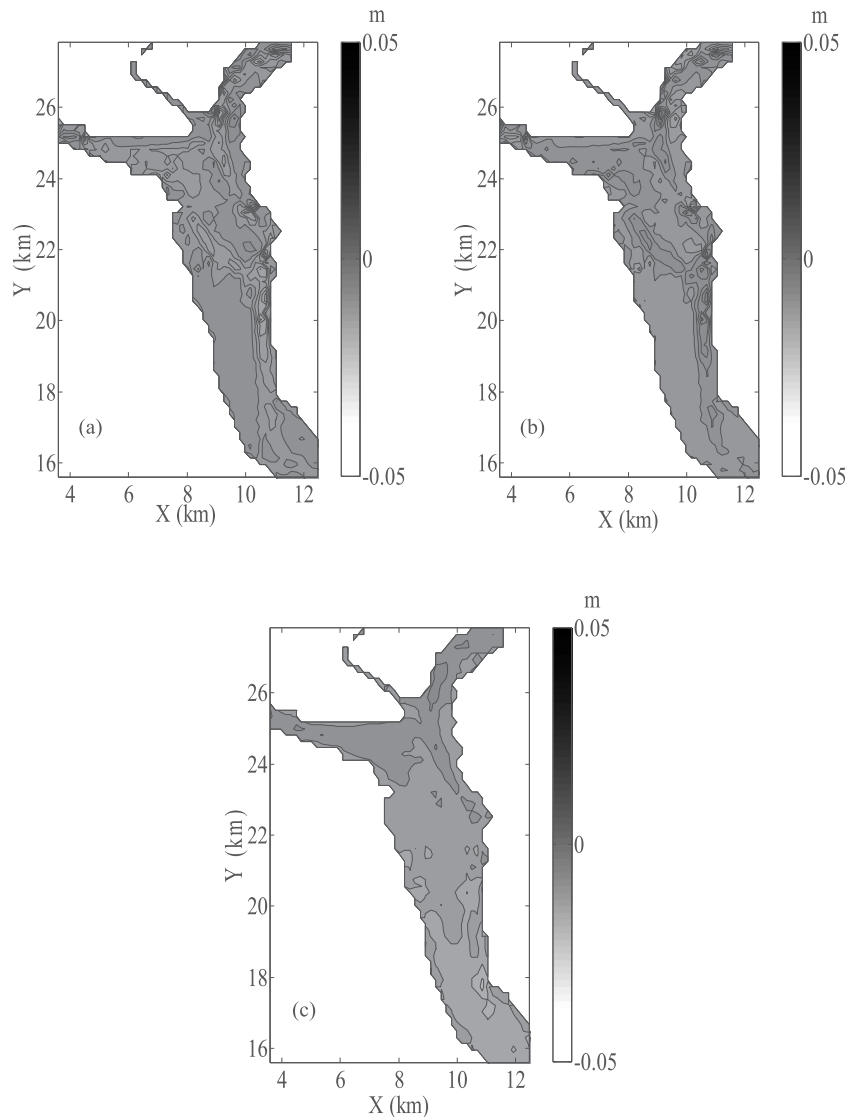


Fig. 11. Accumulated bed level change (m) for (a) ebb tide and (b) flood tide condition and (c) one tidal cycle at neap tide at monsoon season.

be much less. It can however be concluded that the model evaluation of sedimentation is fairly good.

5. Conclusion

In the present study, characteristics of flow fields and resultant sediment transport were investigated by numerical simulation for the navigation channel in Yangon River. The flow

fields were evaluated by using the 3-D Princeton Ocean Model (POM) with a wetting and drying scheme to evaluate near-bottom velocity in very shallow areas. It was found that the velocity at flood tide was generally larger than that at ebb tide. Along the navigation channel, velocity was larger at downstream of the river, however, smaller near the junction of the three rivers, Yangon River, Pazundaung Creek and

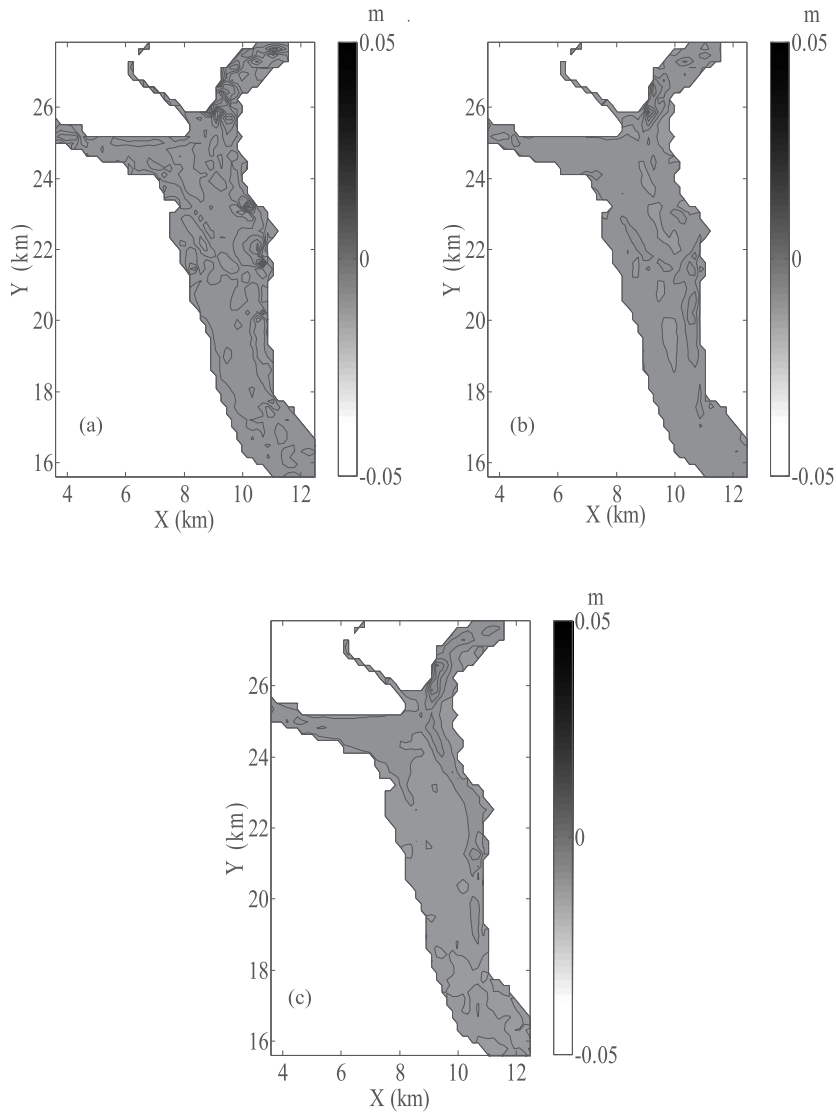


Fig. 12. Accumulated bed level change (m) for (a) ebb tide and (b) flood tide condition and (c) one tidal cycle at neap tide at dry season.

the Bago River where the Inner Bar exists. The calculated velocity showed the reasonable agreement with the field data of NELSON (2000).

Calculated near-bottom velocity was put into the sediment transport model to evaluate sediment deposition and erosion in the channel. From field observation, d_{75} sand diameter for the Inner Bar material was 0.338 mm, which

was used in the sediment transport calculation. In all tide and seasonal conditions, sand deposition is observed around the Inner Bar area. It was found that the sedimentation occurs more heavily at the spring tide condition than the neap tide condition. Thus it can be concluded that the present simulation reflects the basic mechanisms of flow and sediment transport around the navigation channel in Yangon

River and can reproduce the actual sand deposition at the Inner Bar fairly well.

The numerical model is expected to be a powerful predictive tool for considering a new measure to maintain the navigation channel and the depth around the port areas in Yangon River. In the further, more reliable field data would be however needed not only for providing accurate conditions for calculation, but also for the verification of the model results.

Acknowledgements

This research was supported by the Ministry of Education, Culture, Sports, Science and Technology (Monbukagakusho: MEXT) of Japan through a Student Research Scholarship Grant awarded to the first author.

References

- BLUMBERG, A. F. and G. L. MELLOR (1987): A description of a three-dimensional coastal ocean circulation Model. *Three-Dimensional Coastal Ocean Models*, 4, 208–223.
- CHENG, N.S. (1997): A simplified settling velocity formula for sediment particle. *J. Hydraulic Eng. ASCE*, 123, 149–152.
- CHINA TRANSPORTATION ENGINEERING (2006): Myanmar Yangon River access channel improvement project, Shanghai China.
- FENNEMA, R. J. and M. H. CHAUDHRY (1990): Explicit methods for 2-D transient free surface flows. *J. Hydraulic Eng. ASCE*, 116, 1013–1034.
- GARCIA, M. and G. PARKER (1993): Experiments on the entrainment of sediment into suspension by a dense bottom current. *J. of Geophysical Research (Oceans)*, AGU, 98, 4793–4807.
- LANE, E.W. and A.A. KALINSKE (1941): Engineering calculations of suspended sediment. *Trans. Amer., Geophy. Union*, 20, 603–607.
- MEYER-PETER, E. and R. MULLER (1948): Formulas for bed-load transport. *Proc., 2nd Meeting, IAHR*, 39–64.
- MELLOR, G. L. (2004): *User Guide to A Three-Dimensional, Primitive Equation, Numerical Ocean Model*. Princeton University Press, Princeton, 56pp.
- NELSON, B. W. (2000): Sediment dynamics in Rangoon River, Myanmar. *The Science of Total Environment*, 266, 15–21.
- OEY, L. (2005): A wetting and drying scheme for POM. *Ocean Modeling*, 9, 133–150.
- OEY, L. (2006): An OGCM with movable land-sea boundaries. *Ocean Modeling*, 13, 176–195.
- PARKER, G., M. H. GARCIA, Y. FUKUSHIMA and W. YU (1987): Experiments on turbidity currents over an erodible bed. *J. of Hydraulic Research*, 25, 123–147.
- ROUSE, H. (1937): Experiments on the Mechanics of Sediment Suspension. *Proceeding of the 5th International Congress for Applied Mechanics*, 55, 550–554.
- SIR ALEXANDER GIBB and PARTNERS (1974): Rangoon sea access channel & associated port improvement Study, United Nations Development Programme: International Bank for Reconstruction and Development: Burma Port Corporation.
- TOE TOE AUNG, T. SHIMOZONO and A. OKAYASU (2011): Numerical study of sediment transport in Yangon River and estuary. *Asian and Pacific Coasts 2011*, 1509–1516.

Received: June 14, 2013
Accepted: October 25, 2013

アラメ・カジメの幼体移植のための 着床具を用いる種苗育成法の開発

田 闊¹⁾・岡本峰雄¹⁾・鴨下真吾²⁾・岩田 至³⁾

Development of seedling cultivation methods for transplantation of young *Eisenia bicyclis* and *Ecklonia cava* plants by using settlement devices

Kuo TIAN¹⁾, Mineo OKAMOTO¹⁾, Singo KAMOSHITA²⁾, and Itaru IWATA³⁾

Abstract : We developed seedling cultivation methods for transplantation of young *Eisenia bicyclis* and *Ecklonia cava* plants using settlement devices (SDs). Experiments were conducted using four settlement devices consisting of (1) flat unglazed china, (2) unglazed china with small hollows, (3) two (06 and 07) slag-ceramic interfaces with minute (3–10 μm diameter) pores. No seaweeds grew on the flat unglazed china in a seawater circulation tank on land after release of *E. bicyclis* zoospores. Hollow china and 06 slag-ceramic SDs were deployed at depths of 0 m, 0.2 m, and 2 m in a forest of *E. bicyclis* for 6 months. The sun-illuminated sides of SDs were fully covered by small seaweeds (excluding *Eisenia*) depending on the depth (*Ulva* at a depth of 0 m, *Chondrus* at 0.2 m, and *Chondrus* and *Gelidium* at 2 m). However, attachment of *Ulva* on the two types of SDs was different. *Ulva* could be easily removed from the hollowed surface, but it could not be separated from the surface of the slag-ceramic SDs even with a knife. On the 07 slag-ceramic SDs placed in a seawater tank, *E. bicyclis* could be raised from the settled zoospores released from their mother plants. Hundred days after settlement, 17–18 sporophyte *Eisenia* (2–4 cm) grew on 1 slag-ceramic SD. It was possible for slag-ceramic SD to brush not damaging *E. bicyclis* on the SD.

Keywords : *Eisenia bicyclis*, settlement device, china, slag-ceramic

1. はじめに

日本の藻場は、沿岸域開発などで減少してきた(向井, 2008)。近年は海面水温の上昇によって、藻類と生息場をめぐって競合するサンゴが北上しており、藻場の減少の度を速めている(野島・岡

本, 2008. 岡本, 2008. 谷口, 2008.)。藻類のなかでも多年生のアラメやカジメは典型的な海中林を形成し、そこには豊かな生態系が形成されていた(谷口, 2008)。減少する藻場を再生させる試みは、藻礁の設置、投石、母藻の投入、育成した海藻の移植など、種々行なわれてきた(谷口, 1996. 荒武, 2009. 木村・山内, 2009. 桐山, 2009. 田井野, 2009)。藻場のほかに、沿岸域の重要な生態系であるサンゴ礁についても再生の取り組みが行なわれている。2002年から著者らは、セラミック製のサンゴ着床具(OKAMOTO *et al.*, 2008. 特許第3530838号)を用いて、移植後も必要に応じて追加移植を繰り返す、管理型のサンゴ再生技術を開発している。着床具は、きれいな穴や溝がないために着生適地がないミドリイシ属サンゴを対象とし、幼生の着生に適した形状であり、着生させた幼生を稚サンゴまで

1) 東京海洋大学 〒108-8477 港区港南4-5-7

2) 茨城県庁農林水産部

〒310-8555 水戸市笠松町978-6

3) 芙蓉海洋開発(株) 〒111-0051 台東区蔵前3-15-7

1) Tokyo University of Marine Science and Technology, 4-5-7 Konan Minato-ku Tokyo 108-8477, Japan. E-mail: okamotom@kaiyodai.ac.jp

2) Department of Agriculture, Forestry and Fisheries, Ibaraki Prefectural Government. 978-6 Kasamatsu-cyo Mito 310-8555, Japan

3) Fuyo Ocean Development & Engineering Co. Ltd. 3-15-7 Kuramae Taito-ku Tokyo 111-0051, Japan

Table 1. Forms of ceramic settlement devices (SDs)

Type of SD	Size of SD (mm)			Shape of settlement surface of disc	
	Disc		Spacer	Upper surface	Under surface
	Dia.	Thick	Thick		
China*	53	11	7	Flat with grooves	Flat with grooves
Hollow china*	40	9	9	Small hollows	Flat
06 Slag**	44	8	9	Flat	Flat with grooves
07 Slag**	55	9	10	Flat with grooves	Flat with grooves

* Unglazed china

** Pores (3–10 μm in diameter) unglazed ceramic

育成して移植に利用する。今まで、形状、材質、収納ケース等について、着床具の改良を行ってきた (ROEROE *et al.*, 2013)。藻場再生についても、成型が容易で安価なセラミックに多年生藻類を育成できれば、サンゴ同様に継続管理型の藻場再生が可能になると考えた。

そこで2003年から2010年にわたって、サンゴ用着床具を用いて水槽や海域で藻類の着生を試みた。その結果、水槽でアラメの着生・育成を行なうことができたが、遊走子の着生を効率的に行なううえでは、サンゴ用とは異なる形状の、海藻用の着床具の開発が必要と考えられた。

本研究では、着床具にアラメを着生させる数種の方法について検討した結果について報告する。

2. 材料および方法

2.1 着床具

実験は、素焼きの瀬戸物の2003型着床具 [Fig. 1 (a). 以下、セット, China] と、瀬戸物に不規則な窪みをつけた2005型着床具 [Fig. 1 (b). 以下、クボミ, Hollow china], 2006型スラグセラミック着床具 [Fig. 1 (c). 以下、06-スラグ, 06 slag-ceramic], 2007型スラグセラミック着床具 [Fig. 1 (d). 以下、07-スラグ, 07 slag-ceramic] の4種である (Table 1)。

セットは、石膏型で成型し、1,250度で酸化焼成した素焼きの瀬戸物である。着床板の上下面に着生面積を増やすため放射状の溝を設け、板の周囲に、重ねた着床具を釣り糸等で固縛するための溝を設けた。

クボミは、着床板上面に不規則な窪みをつけた素焼きの瀬戸物である。着床板とそれ以外の部分の2つに分けて金型プレス成型し、それらを接着して焼成した。着床板の下面に溝は無く、周囲の4ヶ所には重ねて束にするための溝を設けた。

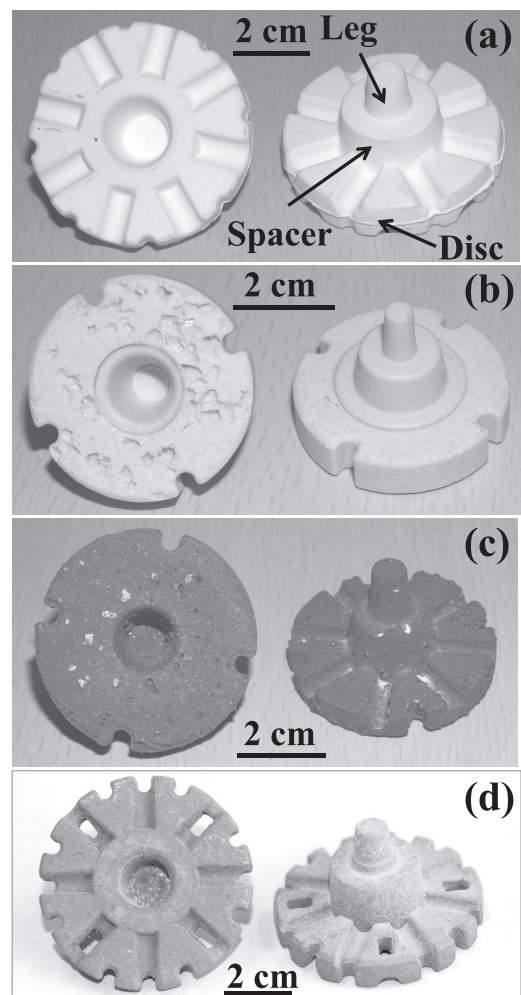


Fig. 1. Upper (left) and lower surfaces (right) of ceramic settlement devices (SDs). (a) China, (b) hollow china, (c) 06 slag-ceramic SD, (d) 07 slag-ceramic SD.

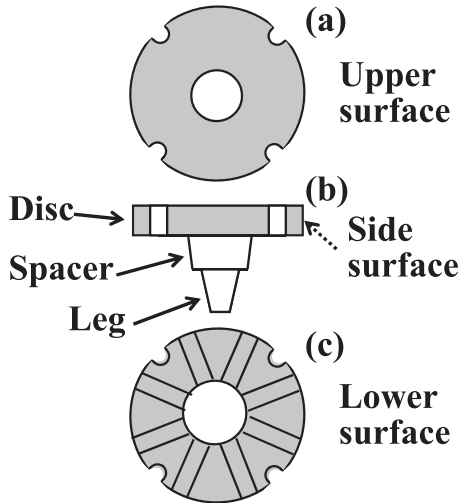


Fig. 2. Three seaweed settlement surfaces of the disc (printed area). (a) Upper surface, (b) side surface, (c) lower surface.

06-スラグは、製鋼スラグとアルミドrossを混ぜてプレス成型し、酸化焼成した。新開発の素材で、酸化鉄とアルミニウムが高温で爆発的に燃焼し（テルミット反応）、同時に不純物が気化して微細な多孔質構造（直径3~10 μ m）の強靱な陶器ができた。着床板の下面には放射状の溝を、周囲4ヶ所に組立て用溝を設けた。

07-スラグは、06-スラグをやや大型にして着床板の上下面や板側面にも溝を設けた。

4種の着床具（settlement device）の形はFig. 2 (b)に示したように共通で、上部から順に、着床板（Disc）、スペーサ（Spacer）、脚（Leg）からなる。着床板は円盤型で上面 [Upper surface, Fig. 2 (a)], 下面 [Lower surface, Fig. 2 (c)], 側面 [Side surface, Fig. 2 (b)]に藻類を着生させる。着床板上面には着床具を重ねるときに脚を差し込むための窪みがある。スペーサは重ねた着床具の着床板間の隙間を一定に保つ。脚は着床具を岩等に固定するのに用いる。4種の実験では、着床具をFig. 2 (b)のように立てて単独で固定したり、重ねた着床具を立てて着床板を水平にする場合（サンゴ着生時の使用法）と、重ねた着床具を横置きにして着床板を鉛直にする場合とがある。

2.2 実験方法

上記4種の着床具へのアラメやカジメの着生について、次の実験を行った。水槽に設置したセット

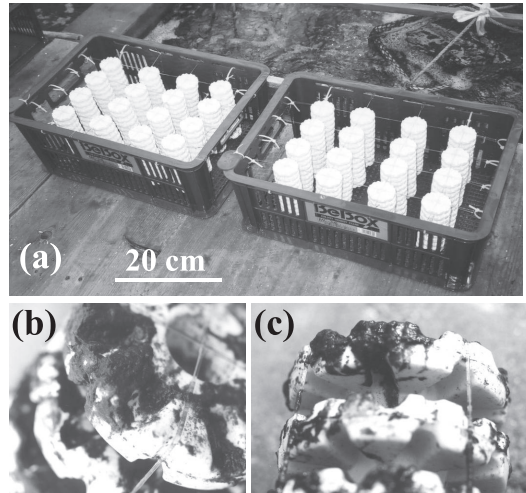


Fig. 3. Experiment 1 at Ibaraki Prefectural Fisheries Research Center. (a) Seawater tank and two containers containing 16 units of the china settlement device (SD). A unit composes of a stack of 10 SDs with a fishing line. (b) Upper side of the SD unit deployed on December 3, 2003 and sampled on October 19, 2004. Growth of diatoms indicated in black. (c) Side view of the same SD unit as in Fig. 3 (b).

にアラメ *Eicenia bicyclis* の遊走子の着生を調べる実験1、カジメ藻場に設置したクボミへのカジメ *Ecklonia cava* の着生を調べる実験2、アラメ藻場に設置したクボミと06-スラグへのアラメの着生を調べる実験3、水槽に設置した06-スラグと07-スラグへのアラメ遊走子の着生と成長を調べる実験4である。次に、それぞれの実験の内容を示す。

2.2.1 実験1

2003年と2004年に、セットを用い、茨城県水産試験場（以下、茨城水試）で実験を行った。着床具は10段に重ねて釣り糸で束にし、メッシュコンテナ [アイリスオーヤマ(株)。樹脂製 BeBox MC-34 L。約52cm \times 38cm、高さ21cm] に16束を立てて固定した [Fig. 3 (a)]。

2003年12月3日、清掃した屋内4トンコンクリート水槽（内寸：3.5m \times 1.3m、深さ0.9m）に濾過海水を満たし、コンテナ2個をその上面が水面下になるように設置した。着床具やコンテナを海水に漬けて洗浄するため、約半日、海水を掛け流しエアレーションを行なった。同日、ひたちなか市平磯漁港で成熟したアラメ15株を採取し、

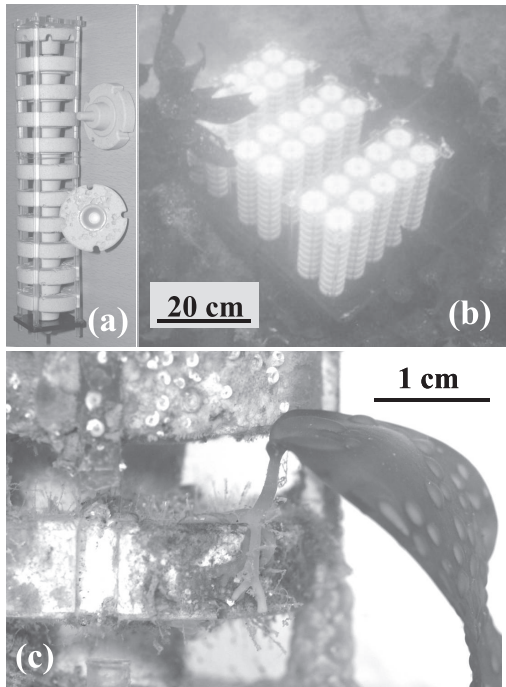


Fig. 4. Experiment 2 at Iwase, Awaji Island. (a) Unit of hollow china SDs set in a polypropylene inner case. A hollow china SD case consisted of four slender transparent rods, a black lower top, and a transparent upper top. (b) Three hollow SD cases fixed on plastic plates and deployed in an *Ecklonia cava* marine forest; each case held 10 units of hollow china SDs. A hollow china SD case was composed of a transparent upper plate, a black lower plate, and six transparent rods to bind the two plates. (c) *E. cava* growing on the disc of an SD.

遊走子を放出させるために、須藤，1948. 谷口・秋山，1982. 荒川・松生，1990. を参考に，約3時間の陰干しの後，遊走子が着生しやすいように，止水状態とした水槽に投入した。アラメは約3時間後に取り除き，濾過海水の掛け流しとしエアレーションを再開した。2004年2月26日に2束を回収し，同年10月19日には全ての着床具を回収して観察を行った。

屋内水槽の建物（約15m×30m）には，実験に用いた4トン水槽32面と6トン水槽6面が配置され，通路や資材置き場も設けられている。建物は骨組みが角材でつくられ，区画の仕切り壁はない。屋根には半透明の樹脂製波板，外壁には半透明のFRP製波板が張られ，自然採光されている。夜間作業用の蛍光灯はあるが，生物飼育専用

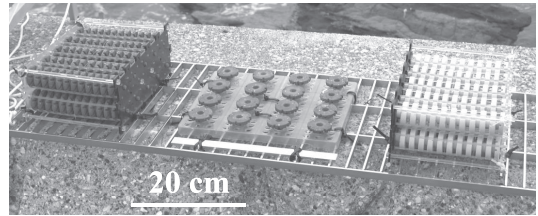


Fig. 5. Grating used for Experiment 3. Left: a 06 slag-ceramic case held 10 units of 06 slag-ceramic SDs; center: a plastic drain board to fix 16 06 slag-ceramic SDs; and right: a hollow case holding 10 units of hollow SDs. A plastic drain board was used for Experiment 4 to fix 16 07 slag-ceramic SDs for the experiment on November 9, 2009.

の照明は設置されていない。

2004年10月20日には，雑藻が生育しないように，清掃してクリーンにしたコンクリート水槽にコンテナ6個を配置し，2003年と同じ方法で実験を行った。実験を開始してから3年後の2007年12月24日に全てを回収して観察を行った。

2.2.2 実験2

2005年10月3日に，クボミを用い，兵庫県淡路島岩瀬の砂浜の海水浴場沖合約200mの小規模な転石場〔カジメが繁茂。直径約10m，水深6m（最低水面下）〕で実験を行った。

着床具は11段に重ねてポリプロピレン製の4本の棒（透明）と上蓋（透明），下蓋（黒色）で束にし〔Fig. 4 (a)〕，ポリプロピレン製ケース（12×27cm，高さ約21cm。透明な上蓋と黒色の下蓋を6本の棒で固定）に10束を固定した（束の中心間隔は5cm）。平らな樹脂架台（30cm×45cm）2枚に各3個のケースを乗せ，海底に結束バンドで固定した〔Fig. 4 (b)〕。2006年7月7日に回収してカジメの生育状況を調べた。

2.2.3 実験3

2006年に，クボミと06-スラグを用い，東京湾の2か所のアラメ藻場（神奈川県三崎市江奈湾。千葉県富津市の竹岡海岸）で実験を行った。江奈湾は1mよりも浅い水深の岩場にアラメが広く繁茂し，沖側は防波堤のような岩場があり，波浪の影響は受けにくい地形であった。竹岡海岸は，水深1~3mの岩場にアラメが生育していたが，波浪の影響を受けやすかった。

着床具としてクボミを用い，実験2と同じ方法でケースに10束を固定した。06-スラグ着床具も同様にケースに固定したが，製造のばらつき（土

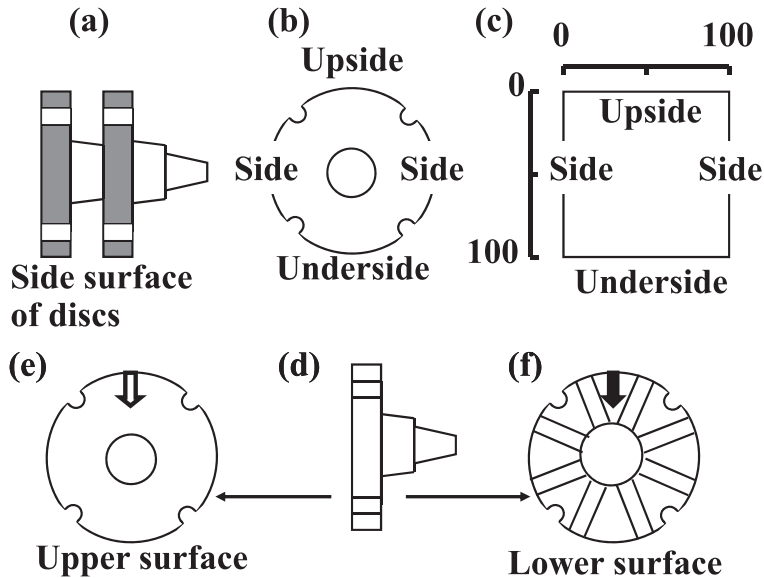


Fig. 6. Illustration of measuring seaweed cover around the four side surfaces of a disc [(a) – (c), %], and seaweed settlement depth [(d) – (f), mm] on the upper and lower surfaces of the disc. (a) Seaweed cover measurement positions (printed area) of the four side surfaces of the discs; 11–12 SDs were combined and bound as 1 unit. Ten units were fixed in a case, above and below. Cases were turned sideways and fixed on the grating as shown in Fig. 5; thus, the discs of SDs were placed vertically. (b) The four side surfaces of the discs were measured for algal cover (%). (c) Data of 10 SDs from 1 unit were averaged (%) for display. (d) Measurement of seaweed settlement depth. (e) Upper surface of the disc. Measuring maximum seaweed settlement depth (as shown in open arrow). Data of the upper five units ($n = 50$) are averaged (in mm) for each case. (f) Lower surface of the disc. Maximum seaweed settlement depth (as shown in solid arrow) is measured in the same manner as described in Fig. 6 (e).

1mm以下) により 12 段になったものもあった。

実験 1, 2 では着床板が水平になるようにケースを固定したが, 実験 3 は着床板が鉛直になるように配置した (Fig. 5, 以下, 2 層ケース)。また 06-スラグ 16 個を樹脂製スノコ (Fig. 5 中央, 30 cm×24 cm, 高さ 1 cm, 以下, スノコ板) に着床板が水平になるように固定したものも用いた。ステンレス製スノコ (100 cm×36 cm, 高さ 5 cm) に, クボミの 2 層ケース 1 個, 06-スラグの 2 層ケース 1 個, 06-スラグのスノコ板 1 枚を固定した (Fig. 5)。

江奈では, 2006 年 10 月 28 日, スノコ上面が水深 0 m と 0.2 m (最低水面下) になるよう各 1 基固定し, 2007 年 5 月 25 日に回収した。竹岡では, 2006 年 10 月 29 日に水深 2 m の海底に 1 基を固定し, 2007 年 6 月 5 日に回収した。

海水に漬けて実験室に持ち帰ったケース類は, 着床具ごとに藻類の被度, 着生位置, 湿重量, 種類を計測した。計測は着床具束の 1 段目 (最下段) から 10 段目までを対象とした。束の最上段

[11 段ないし 12 段目, Fig. 4 (a)] は着床板上部がケース上蓋と接触して藻類が生育できないため計測から除いた。

2 層ケースの着床具への藻類の生育場所は Fig. 6 に示した 2 種の方法で, 大型藻類の被度, 大型藻類の着生深度を求めた。

被度の求め方: 2 層ケースの着床具は, Fig. 4 (a) のように 4 本の透明な棒と上下蓋で固定された束を, Fig. 5 のように横向きに配置した。各束は Fig. 6 (a) の向きで, ケースに横 5 束, 上下 2 層に配置された。着床具を分解して着床板 (Disc) の上面 (Upper surface) 方向から見ると, 藻類の生育する着床板側面 [Fig. 6 (a), Side surface の塗りつぶし部] の 4 区 [Fig. 6 (b), 上部 (Upside), 下部 (Underside), また 2 側部 (Side)] が計測対象であり, 着床具ごとに 4 区の被度を 5% 刻みで求めた。計測結果は束ごと ($n=10$) の平均被度 (%) を Fig. 6 (c) のように模式化した。

着生深度の求め方: Fig. 6 (d) のように, 鉛

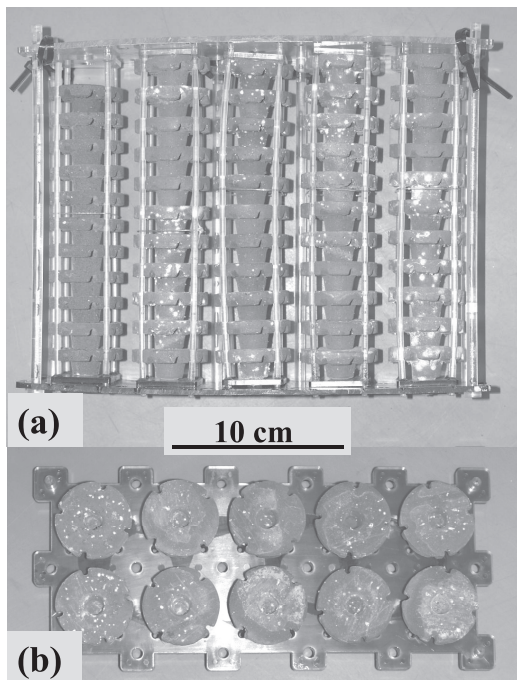


Fig. 7. 06 slag-ceramic case and plate used for Experiment 4. (a) 06 slag-ceramic case divided into halves. (b) Black lower plate of the case used to fix 10 06 slag-ceramic SDs.

直向きになった着床板 (Disc) の上面 (Upper surface) と下面 (Lower surface) に生育した藻類の最上部からの着生深度 (mm) を Fig. 6 (e, f) の矢印のように計測し ($n=50$), ケースごとの平均値を求めた。

2.2.4 実験 4

06-スラグと 07-スラグを用い, 2007 年と 2009 年に, 茨城水試の水槽で実験を行った。これらの着床具は, 実験 3 で用いたケースの上下蓋を半文にして, 束を 1 層にして固定した [Fig. 7 (a), 以下, 1 層ケース]。また 2007 年には, ケース下蓋 (黒色) に 10 個の 06-スラグを水平に固定したものを用いた [Fig. 7 (b), 以下, プレート]。2009 年には, 07-スラグ 16 個を, 実験 3 で用いた樹脂製スノコ [Fig. 5 中央, 30 cm×24 cm, 以下, スノコ板] に水平に固定して用いた。

2007 年 11 月 24 日, 屋内水槽の水深 0.2 m 層と 0.8 m 層に, それぞれ 1 層ケース 4 個とプレート 4 枚を配置した。着生は実験 1 と同じ方法で行ない, 着生の 51, 90, 112, 139, 187, 205 日後

に観察を行った。観察にあたってはケースやプレートを覆った珪藻類や浮泥は, 軽くゆすって落とすだけにとどめ, 各着床具にアラメが生育しているか否かを目視で調べた。アラメを傷める恐れがあるため, 株数や寸法の計測は行わなかった。

2009 年 11 月 9 日, 屋内水槽に 06-スラグ 1 層ケース 12 個と 07-スラグ 16 個を固定したスノコ板 3 枚を水深 0.2 m に設置し, 濾過海水掛け流しとエアレーションを行なった。翌 10 日に竹岡海岸で成熟したアラメを 15 株採取して茨城水試に運び, 3 時間の陰干しの後に 2007 年同様に遊走子を放出させる実験を行なった。実験の当日は水槽の海水中の遊走子数の計測と, 着床具への遊走子着生状況の観察を行った。その後は実験開始 167 日後まで概ね 1 週間ごとに, 着床具を覆った珪藻類を柔らかい刷毛で軽く清掃し, スノコ板の着床具 3 個を研究室に持ち帰った。持ち帰った着床具は, 初期の観察にはデジタル顕微鏡 (Keyence 製 VH-5500, ×100-1000) を用い, アラメが目視できる大きさに達した 60 日後以降は, ピンセットでアラメを採取してスケールとともに撮影し (OLYMPUS E330, 35 mm f3.5), 写真から全長を計測した。

3. 結果

3.1 実験 1

2003 年に実験を行ったセットは実験開始後断続的に目視観察を行った。着床具表面を大量の珪藻類が塊状になって覆っていたため, アラメの生育状況は確認できなかった。2004 年 2 月 26 日に着床具 2 束 (20 個) を回収したが, アラメは生育しておらず, 水槽中で着床具束を軽くゆすって珪藻類を掃除すると, 着床具の表面は実験開始時と同様に素焼きの瀬戸物が現れ, 綺麗になった。2004 年 10 月 19 日に残った 300 個を回収したが, 2004 年 2 月と同じ状況であった [Fig. 3 (b, c)]。

2004 年に実験を開始した着床具について断続的に観察を行ったが, 2003 年に実験を行なった着床具と同様に珪藻類が厚く着床具の表面を覆っていた。そのまま放置してアラメの生育を待たせたがアラメは観察できなかった。3 年後の 2007 年 12 月 24 日に 960 個の着床具を回収したが海藻は何ら生育していなかった。珪藻類の生育は, 着床具束の最上段の上面がもっとも多く [Fig. 3 (b)], 重ねた着床板の側面がそれに続き, 着床板間の横溝の中には見られなかった [Fig. 3 (c)]。

3.2 実験 2

2005 年 10 月に実験を開始した着床具 (クボミ) は, ヒドロ虫類, ウズマキゴカイ類, アオサ類,

Table 2. Wet weight of growing seaweed on horizontally fixed 06 slag-ceramic SDs deployed at three depths in Experiment 3.

Depth (m)	No. of SD	Wight of Algae (g)		Total weight composition of algae (%)			
		Range	Mean \pm SD	<i>Ulva</i>	<i>Chondrus</i>	<i>Gelidium</i>	Others
0*	16	3.2-5.26	4.02 \pm 0.72	100	0	0	0
0.2*	12	1.83-5.67	4.51 \pm 1.10	37.7	62.3	0	0
2**	16	2.76-7.7	4.04 \pm 1.22	1.4	74.6	17.0	0.94

*Ena bay, Kanagawa Prefecture. Deployed: October 28, 2006. Sampled: May 25, 2007.

**Takeoka, Chiba Prefecture. Deployed: October 29, 2006. Sampled: June 05, 2007.

浮泥などに薄く覆われていた。2006年7月7日に回収して着床具660個を観察した結果、3株のカジメ（全長5-6cm）を確認できた。仮根は着床板の側面と上面にわたって伸びていた [Fig. 4 (c)]。

3.3 実験3

実験は江奈（0m, 0.2m）と竹岡（2m）の2カ所で行なったが、水深の違いで着生した大型藻類が異なっていた。そこで計測結果は、0m, 0.2m, 2mの3水深のデータとしてまとめた。

スノコ板に水平に固定した06-スラグ (Fig. 5) は、3水深とも着床板の上面から側面がびっしりと大型藻類に覆われ、いずれも被度は100%であった [Fig. 8 (a, b)]。生育した海藻の種類や湿重量を Table 2 に示した。0m深はアオサ類、0.2m深はツノマタ類が多くアオサ類がそれに続いていた。2m深はツノマタ類が主でマクサ類が混じっていたがアラメは確認できなかった。06-スラグ1個あたりに生育していた藻類の湿重量は3層ともに平均4g以上であった (Table 2)。

2層ケースのクボミと06-スラグも (Fig. 5)、水深によって藻類が異なっていた。0.2m深と2m深では、クボミ、06-スラグともに、藻類は Fig. 9 (a) のようにケース上面を密に覆い、各着床具の境界は目視による確認はできなかった。0m深は大型藻類が少なく、着床板 (Disc) の側面 (Side surface) 上部 (Upside) を覆うのみで、着床板間の隙間にはあまり生育していなかった。Table 3 に、着床具に生育していた藻類の湿重量と構成比を示した。0m深は、クボミはアオサ類のみ、06-スラグはアオサ類が主でツノマタ類が1割ほど混じっていた。0.2m深はツノマタ類が主であった。2m深はツノマタ類が主で、マクサ類が3割弱混じっていた。アラメは、2m深に設置したクボミのケースに1株だけ確認できた。着

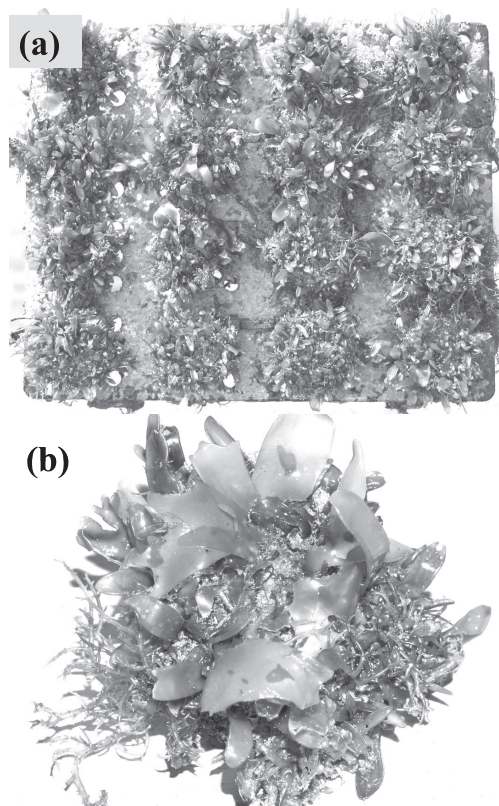


Fig. 8. Seaweed growing on 06 slag-ceramic SDs fixed on a drain board in Experiment 3. Deployed at a depth of 2 m in Takeoka between October 29, 2006 and June 05, 2007. (a) 16 06 slag-ceramic SDs covered by *Chondrus* and *Gelidium*. (b) Separated 06 slag-ceramic SD.

床具1個あたりの藻類の湿重量は、0m深は06-スラグが多かったが、0.2m深、2m深ともにクボミのほうが多かった (Table 3)。ただし、どの深度帯も着床板を水平に固定した06-スラグの生

Table 3. Wet weights of growing seaweed on upper five units (n = 50) of hollow china SD case and 06 slag-ceramic SD case deployed at three depths in Experiment 3.

Type of SD	Depth (m)	Weight of Algae (g)		Total weight composition of algae (%)			
		Range	Mean \pm (SD)	<i>Ulva</i>	<i>Chondrus</i>	<i>Gelidium</i>	Others
Hollow china	0*	0.25–1.67	0.68 (0.72)	100	0	0	0
	0.2*	0.99–4.28	2.28 (1.01)	0	99.1	0.5	0.4
	2**	2.16–5.58	3.40 (0.97)	0.1	68.5	28.7	2.7
06 slag-ceramic	0*	0.52–1.94	1.02 (0.41)	90.9	9.1	0	0
	0.2*	0.39–3.51	1.58 (0.87)	3.8	96.2	0	0
	2**	2.6–3.64	2.17 (0.63)	0.1	71.4	26.5	2

*Ena bay, Kanagawa Prefecture. Deployed: October 28, 2006. Sampled: May 25, 2007.

**Takeoka, Chiba Prefecture. Deployed: October 29, 2006. Sampled: June 05, 2007.

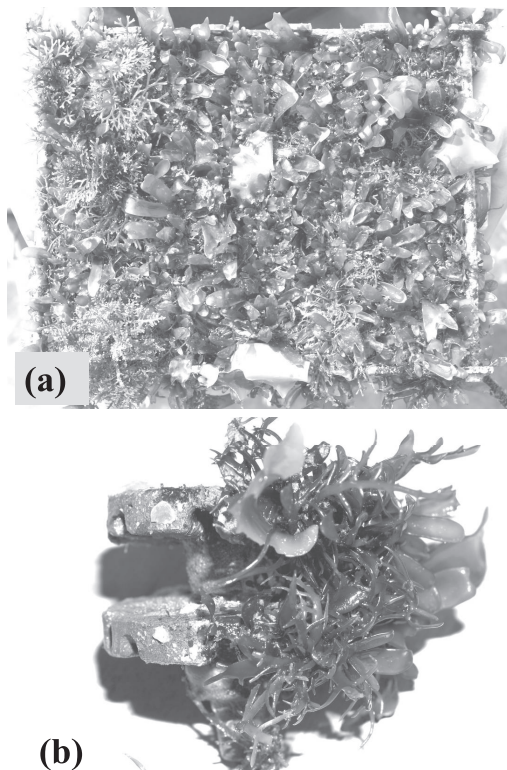


Fig. 9. Seaweed growing on a 06 slag-ceramic SD case in Experiment 3. Deployed at a depth of 2 m in Takeoka between October 29, 2006 and June 05, 2007. (a) Upper side of a 06 slag-ceramic SD case covered by *Chondrus* and *Gelidium*. (b) Seaweed was growing on the upper side of the side surfaces of the disc exposed to the sun, given that the discs of SDs were fixed vertically in the case.

育量 (Table 2) には及ばなかった。

2層ケースの着床具に生育した大型藻類は、Fig. 6に示した2種の方法で、大型藻類の被度(%), 大型藻類の着生深度(mm)を求め、Figs. 10–12に示した。

クボミ [Fig. 10 (a–c)] は、0.2 m 深、2 m 深とも上部 (Upside) の藻類被度はほぼ 100%であったが、0 m 深の被度は 37–77%と低かった。着床板側面 (Side surface) の測部 (Side) や下部 (Underside) で光が十分にあたらない場所には藻類は生育していなかった。06–スラグでは [Fig. 11 (a–c)], 0 m 深と 2 m 深の上部被度はほぼ 100%であったが、0.2 m 深では食害の影響と考えられた疎らな着床具も見られた。

各ケースの着床板 (Disc) の上面 (Upper surface)・下面 (Lower surface) での着生深度は、クボミ [Fig. 12 (a)] では上部にわずかに着生し、06–スラグ [Fig. 12 (b)] のほうがより深くまで着生していた。面の凹凸と着生部位については、クボミは、窪みのある上面よりも平らな下面のほうが深くまで着生していた。06–スラグは、平らな上面のほうが溝のある下面よりも深くまで着生していた。

その他、観察により、0 m 深における、2段ケース上段のクボミと 06–スラグへのアオサ類の着生状況には極めて大きな相違があった。クボミの場合、アオサ類は仮根の部分まで簡単に剥れて株数を計測できたが、剥した着床具表面には他の付着生物類 (ウズマキゴカイ類, サンゴモ類, コケムシ類など) が生育していた状況が観察された。06–スラグの場合、表面にアオサ類が密生して株数の計測が出来なかった。これをナイフで削っても (着床具はナイフでは削れない) 微細な葉体の一

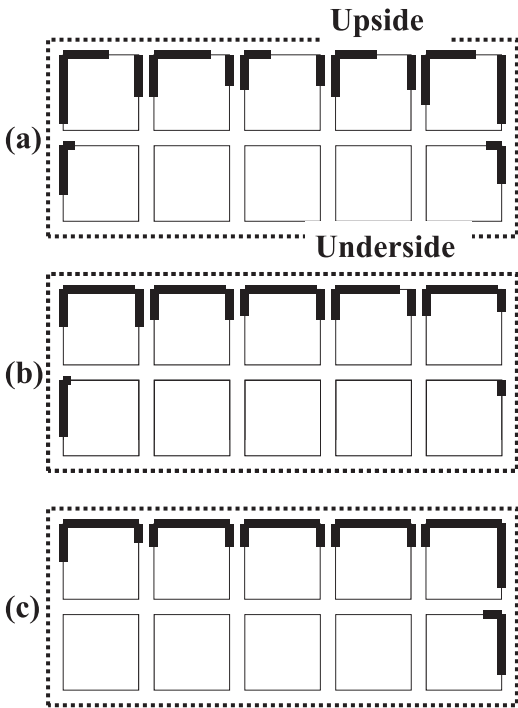


Fig. 10. Seaweed cover [average (%) of 10 SDs] on the four sides of hollow SD units in Experiment 3. (a) 0 m, (b) 0.2 m, (c) 2 m.

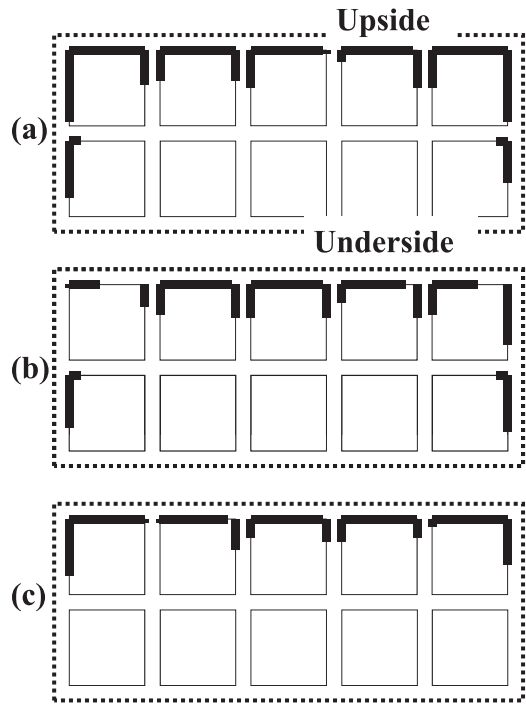


Fig. 11. Seaweed cover [average (%) of 10 SDs] on the four sides of 06 slag-ceramic SD units in Experiment 3. (a) 0 m, (b) 0.2 m, (c) 2 m.

部が着床具表面から内部に入り込んでいて、完全には削り採れなかった。

3.4 実験 4

2007年11月に開始した実験は、1層ケースとプレート水槽の0.2 m深と0.8 m深に配置した。0.2 m深では着生51日後にアラメは確認できなかったが、90日後、ケースの着床具全て（着床板は鉛直。n=220）とプレートの着床具全て（着床板は水平。n=40）に、2~5 cmに成長したアラメを確認できた。以後、112, 139, 187, 205日後に観察を行った [Fig. 12 (a, b)]。この間アラメは成長を続けたが、アラメが育った着床具の数は、Table 4に示したように、139日後は約8割に減少し、205日後にはほぼゼロとなった。0.8 m深のものは、1層ケースの着床具（n=220）に140日後にだけアラメが13個の着床具に生育していた。

2009年11月に開始した実験では、スノコ板の07-スラグにアラメが着生し、その初期成長過程を観察できた。母藻投入（朝10時の水温16.6℃）

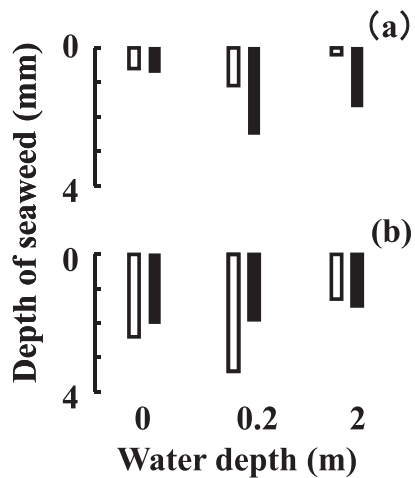


Fig. 12. Average seaweed settlement depth (mm, n = 50) of the upper (open bar) and lower surfaces (solid bar) of the disc in Experiment 3. Upper five units of an SD from each case are analyzed. (a) Average depth of a seaweed settlement on hollow china SD cases. (b) Average depth of a seaweed settlement on 06 slag-ceramic SD cases.

Table 4. Number of 06-slag-ceramic SDs with growing *Eisenia bicyclis* on Experiment 4.

Depth (m)	No. of SD and direction of disc		No. of algal growing SD (% of total SD) 90–205 days after settlement				
	No.	Direction	90	112	139	187	205
0.2	40	Horizontal	40 (100)	40 (100)	35 (87.5)	15 (37.5)	0
	220	Vertical	220 (100)	220 (100)	172 (78.2)	38 (17.3)	2 (0.9)
0.8	40	Horizontal	0	0	0	0	0
	220	Vertical	—*	—*	13 (5.9)	0	0

Settlement: November 24, 2007. *: Could not recognize by visual observation.

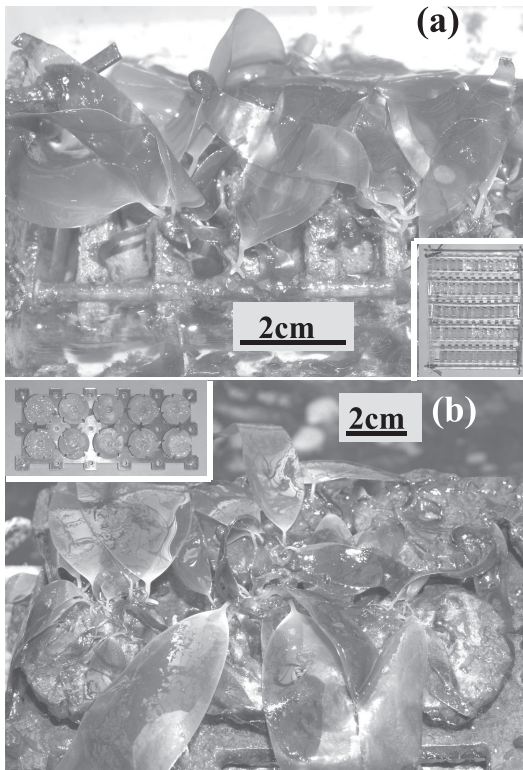


Fig. 13. *Eisenia bicyclis* growing on 06 slag-ceramic SDs in Experiment 4 112 days after settlement on November 24, 2007. (a) Side view of an SD case. (b) Bird's-eye view of SDs fixed on the plate.

から12時間後に遊走子の着生を確認し、8日後(15.3°C)に全長10~20 μ mの配偶体を確認、15日後(14.5°C)には約30 μ mの孢子体を確認した。孢子体は、28日後(15.6°C)には50~100 μ m、43日後(15.6°C)には100~500 μ mに成長した。56日後(10.1°C)には大きな孢子体

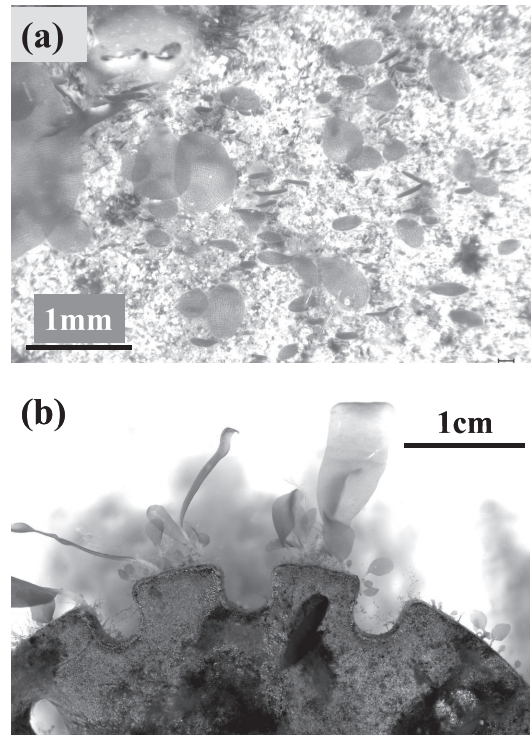


Fig. 14. *Eisenia bicyclis* growing on a 07 slag-ceramic SD in Experiment 4. Settlement: November 10, 2009. (a) 56 days after settlement. (b) 106 days after settlement.

は1mmを超えたが、肉眼では観察が困難な1mm以下の孢子体もたくさん見られた[Fig. 14 (a)]。60日(10.0°C)から167日後(9.6°C)は目視観察で株数と大きさを求めTable 5に示した。60日ころは1mm以下のものが多いため、目視で観察できた幼体の数はさほど多くなかったが、77日(9.6°C)には5mm以下

Table 5. Growth of *Eisenia bicyclis* on three 07 slag-ceramic SDs on Experiment 4. Settlement: November 10, 2009.

Days after settlement	Water Temp. at 10 AM (°C)	Growing <i>Eisenia bicyclis</i> (mm)								
		No.	Length	Mean (±SD)	Size composition in number					
					≤5	≤50	≤100	≤150	≤200	>300
60	10.0	34	0.9–11.2	4.8 (2.1)	25	8				
68	9.6	33	0.8–10.0	4.7 (2.2)	24	8				
77	9.6	65	1.2–14.8	5.1 (2.5)	49	13				
86	9.5	53	1.3–56.0	11.6 (11.6)	22	31				
98	8.5	42	2.2–34.9	10.9 (7.3)	11	41				
106	8.6	57	2.2–84.8	14.8 (12.5)	9	47	0	1		
114	9.0	39	3.4–110	19.9 (17.5)	1	37	0	1		
124	8.1	54	13.1–121	41.9 (23.5)	0	40	12	2		
140	7.8	20	4.9–180	45.7 (53.4)	1	14	2	1	2	
154	10.3	11	25–151	72.7 (45.2)	0	6	3	2	1	
167	9.6	10	54–305	106 (78)	0	0	6	1	2	1

Settlement: November 10, 2009. Three 06-slag-ceramic SDs from horizontally fixed disks were sampled and analyzed. Deployment depth: 0.2 m.

のものが着床具3個に49株育っていた。98(8.5°C)～114日後(9.0°C)には小さな株の数は急速に減り、1～5 cmのものが主になり、10 cm以上に成長した株が少数みられるようになった[Fig. 14 (b)]。124日(8.1°C)には平均約4 cmとなり、10 cm近くまで育った株が増えてきた。その後は株数が急減し167日(9.6°C)には、10 cmを超える幼体が着床具3個あたり10株生育した状態となった。

4. 考察

4種のセラミック着床具を用いて4種の実験を行い、以下の結果が得られた。(1)セトでは、水槽でアラメを着生させることができなかった。(2)クボミでは、小規模な藻場でカジメをごく少数着生できた。(3)アラメ藻場にクボミと06-スラグを設置したが、アラメは1株のみで他の藻類が密生した。(4)06-スラグと07-スラグに水槽でアラメを着生させ、167日後まで育成した。

4.1 セトとクボミへのアラメ、カジメの着生

素焼きの瀬戸物の着床具(セトとクボミ)を用いた実験1～3までのなかで、目的の海藻を着生できたのは、実験2,3の実際の海域で用いたクボミのみであった。実験2ではカジメ3株(着床具660個)が着生していたが着床具はアオサ類、付着生物や泥に薄く覆われていた。実験3(江奈

と竹岡)は比較的広いアラメ藻場で、多種の藻類が生育しており、着床具はアオサ類、ツノマタ類、マクサ類に密に覆われていた。アラメは2 m深に設置した2層ケースのクボミ(100個)に1株が育っていた。実験3では、0 m深のアオサ類の生育状況から、クボミには他の付着生物類が生育した上にアオサ類が着生した様子が同えた。アラメやカジメの遊走子放出は1ヶ月ほど続くことが知られており(須藤, 1948)、実験2,3ともに、着床具表面に他の付着生物が生育した後の残った薄い膜の上に、少数のカジメとアラメが着生したものと判断した。

4.2 スラグへのアラメの着生

2007年の実験では、実験1(2003, 2004着生)と同様に、着床具表面に繁茂する珪藻類をほとんど除去しなかったが、着生90日後には0.2 m深の全ての着床具にアラメが生育していた。以後も珪藻類の除去はほとんどせず、アラメの生育状況を観察できた。

2009年の実験では、0.2 m深のみで遊走子を着生させる実験を行った。初めての試みとして、柔らかい刷毛を用いて着床具を覆った珪藻類を除去した。アラメが目視で確認できるようになるまで(当初の2ヶ月間)は刷毛が直接着床具表面を擦るような強い除去の操作は控えた。アラメの幼体は、Table 5に示したように、着生77日～124日

後まで、着床具3個に50株ほどが生育しており、刷毛による除去作業が藻類の生育に悪影響を与えた様子はなかった。

水槽で遊走子をスラグに着生させる場合、半日ほど海水に漬けているが、特別な処理は不要である。着生後は、アラメの遊走子や若い胞子体は光を求めて珪藻類と競合するが、柔らかい刷毛で珪藻類を除去するだけで成長する。

4.3 海藻類の着生についての着床具とスラグの特徴

実験3で設置したクボミ2層ケースでは、0m深で生育したアオサ類は、着床具に他の付着生物が生育した後にできた、薄い膜のうえに生育したと判断された。一方06-スラグ2層ケースでは、アオサ類がスラグセラミック素材のなかに入り込んでいた。この着生様式の違いが、0m深のアラメの生育状況に変化をもたらした可能性が高い。クボミではアオサ類のみ生育し (Table 3), 上面被度が37~77%と低かった [図10 (a)]。それに対し、06-スラグはアオサ類のほかツノマタ類も混在し (Table 3), しかも被度がほぼ100% [Fig. 11 (a)] であった。クボミは生育したアオサ類の仮根が着床具内部に入り込める構造ではないため、アオサの固着力は弱く、時には干出する環境下で被度を減らしたと推察された。一方06スラグは、設置後速やかに着床具にアオサやツノマタの遊走子が強固に固着し、生育できたと考えた。

実験1 (茨城水試) では、セトを用い、濾過海水の室内水槽で遊走子を着生させたが、着床具表面には珪藻類が繁茂してしまった。着床具表面には微細な凹凸がほとんどないため、珪藻類を除去しようとする、アラメの配偶体や小さな胞子体も外れてしまう恐れがあり、除去できなかった。また生育したアラメを確認することはできなかった。実験4の06-スラグでは、遊走子着生実験開始28日後には胞子体の大きさは50~100 μm であった。付着珪藻の生育状況については、2011年10月26日に行なった新型スラグセラミック着床具 (4cm \times 3cm, 厚さ0.7cm) へのアラメ遊走子着生実験の際に観察を行った (田, 2012. 未発表)。実験開始12日後には1mmに満たない付着珪藻の小さな塊が各所にでき、21日後には付着珪藻が着床具全体を薄い膜のように覆い、各所に直径約1mmの塊状のものが観察された。34日後には塊状のものが直径・厚さとも3~5mmに成長して着床具表面の半分以上を覆った。仮にセトに遊走子が着生して育っていても、繁殖が早い珪藻類とは光量の面で競合し、負けた可能性が

高い。

母藻を投入して遊走子を着生させる方法では、遊走子の着生機会は僅か数時間しかない。細いシュロ縄やクレモナロープはワカメやアラメの着生に常用されているが (関山ら, 1998), それらは糸の繊維の間の隙間に遊走子が固着するため、容易に藻類を着生できる。一方、浸漬処理 (soaking) を行なっていない瀬戸物にはそうした遊走子が入り込める隙間を持つ構造はないため、遊走子が着いても海水かけ流しやエアレーションの刺激などによって、容易に滑落する可能性がある。さらに珪藻類との競合がある。濾過海水を用いた育成では、アラメ遊走子放出実験後に他の藻類の遊走子が着生する可能性は小さい。これらのことが実験1で1年経っても3年経っても大型藻類が全く生育していなかった原因であったと判断される。

4.4 大型藻類の着生位置

実験1では、セトを水槽に設置してアラメの着生を試みたが、設置した着床具の上面や側面は珪藻類で厚く覆われた。しかし、重ねた着床具間の隙間の中に珪藻は殆んど生育していなかった [Fig. 3 (b, c)]。実験2では、クボミ着床具660個を用いてカジメ3株を育成できた。当初は着床板 (Disc) の上面 (Upper surface) の凹凸の中に遊走子が着生すると予想していたが、カジメの仮根は着床板の側面 (Side surface) から上面側に伸びており、上面の凹凸の効果とは考え難かった [Fig. 4 (c)]。実験1, 2では、サンゴの場合と同様に着床具を10~11段に重ねて着床板 (Disc) を水平に配置した [Fig. 3 (a), Fig. 4 (b)]。しかし実験1, 2の結果から、水平に重ねた着床具はアラメ、カジメの着生には適さないと判断された。

実験3では、クボミと06-スラグの着床具ケースを横向きに設置して着床板が鉛直方向になるようにし、あわせて06-スラグをスノコ板に水平に配置したものも用いた (Fig. 5)。

横向き2層ケースの着床具は、0m深のクボミが06-スラグにくらべてアオサの被度 [Fig. 10 (a)] と生育重量 (Table 3) は小さかった。また0.2m深に設置した06-スラグでは海藻の被度が低い束があった [Fig. 11 (b)] が、それ以外は着床板側面 (Side surface) の上部 (Upside) を中心に密に藻類が生育していた [Fig. 11 (a, c)]。また2層ケースで光があたりにくい、上段東の下側 (Underside) や下段東の着床具には殆んど藻類が育たなかった (Figs. 10, 11)。上段東の場合も、光のあたり具合により、着床板側面 (Side surface) の光があたっていた上部 (Upside) し

か藻類は育たなかった。着床板を鉛直に設置した場合、着床板側面の全周の半分以下しか藻類の着生には機能しなかった [Figs. 9 (b), 10, 11]。

横向き2層ケースでは、着床板 (Disc) の上面 (Upper surface) と下面 (Lower surface) は、重ねた着床板間の隙間となるが、この部分の藻類の着生深度は板の最上面から最大でも4mmに達しなかった [Fig. 6 (d-f), Fig. 12]。このように、鉛直向きの着床板側面に比べ、着床板の上下面にはあまり藻類は着生しなかった。また、着床板を重ねずに着床板を水平に配置した06-スラグの上面 (Upper surface) と側面 (Side surface) は密に藻類に覆われ (Fig. 8), この配置は効果的と判断された。

2007年に行った実験4では、0.2 m 深で全ての着床具にアラメを生育させることができた (Table 4)。しかし0.8 m 深では着床板を水平に配置した着床具にアラメは着生せず、0.2 m 深に比べると生育遅れのアラメが僅かに確認できたに留まった。0.8 m 深の着床具が浮泥に覆われていたことから、浮泥の被覆 (荒川, 森永, 1994) がアラメの生育不良の原因と判断された。また0.8 m 深の1層ケースでアラメが確認されたのは、鉛直に配置した着床板の側面 (Side surface) 上部 (Upside) ではなく、着床具間の隙間になる、着床板の上面 (Upper surface) と下面 (Lower surface) の上部であった。これは浮泥堆積などの影響がある場合、その悪影響は水平面より鉛直面のほうが小さい (荒川・松生, 1990. ROEROE *et al.*, 2013) ことからである。

4.5 まとめ

以上のことから、セラミック製の海藻着床具に求められる性能をまとめてみる。素材は、スラグセラミックがセトヤクボミよりもアラメやカジメの着生には効果がある。また、スラグでは、柔らかい刷毛で珪藻を除去でき、かつ、そのような操作は、着生したアラメやカジメの遊走子の生残に影響を及ぼさない。着床具の着床板の向きは、浮泥がない場合は水平が、着床板に浮泥が堆積する場合は、着床板を鉛直方向あるいは斜めに設置する必要がある。着床板の上面、下面には溝などの着生面積を増やすための加工は不要で、平板のままでも良い。

今回は、アラメが育った着床具を藻礁や岩盤に固定する実験は行っていない。開発する海藻着床具を容易かつ確実に固定することも重要な課題である。それにより、海藻着床具を設置し、海藻が死んだ場合には、新しい着床具を追加固定する、継続管理型の藻場再生が可能となる。

謝辞

本研究を行なうにあたり、長期間の実験にご支援・ご協力を賜った茨城県水産試験場の皆様、千葉県竹岡天羽漁協の石井登参事、また東京海洋大学修士課程の院生及び卒業生の石本大樹、松本雄二、滝沢孝介、阿部知佳子、今井彩乃氏ほか多くの方々、またアラメ遊走子の着生方法やアラメの育成方法について、東京海洋大学大学院教授荒川久幸博士にご指導を賜った。これら多くの方々へ深謝する。

引用文献

- 荒川久幸, 松生治 (1990): 褐藻類カジメ・ワカメの遊走子の沈降速度および基質着生に及ぼす海中中濁粒子の影響. *Nippon Suisan Gakkai*. **56**, 1741-1748.
- 荒川久幸, 森永勤 (1994): 褐藻類ワカメ・カジメ遊走子の着生率と基質傾斜の関係. *Nippon Suisan Gakkai*. **60**, 461-464.
- 荒武久道 (2009): クロメの分布と藻場造成-宮崎県沿岸. カジメ属の生態学と藻場造成 (能登谷正浩編). 恒星社厚生閣. 東京. 116-140.
- 木村創, 山内信 (2009): 藻場造成の現状と問題点-和歌山県沿岸. カジメ属の生態学と藻場造成 (能登谷正浩編). 恒星社厚生閣. 東京. 53-71.
- 岡本峰雄 (2008): さんご礁. 消える日本の自然 (鷺谷いづみ編). 恒星社厚生閣. 東京. 88-97, 194-205.
- OKAMOTO, M. S. NOJIMA, S. FUJIWARA and Y. FURUSHIMA (2008): Development of ceramic settlement devices for coral reef restoration using in situ sexual reproduction of corals. *Fish Sci*, **74**, 1245-1253.
- 桐山隆哉 (2009): カジメ類の分布変化-長崎県沿岸. カジメ属の生態学と藻場造成 (能登谷正浩編). 恒星社厚生閣. 東京. 93-115.
- 須藤俊造 (1948): 昆布科植物の遊走子の放出, 運動並びに着生 (海藻胞子附けの研究 第一報). *日本水産学会誌*, **13**, 123-128.
- 関山重信, 松本正喜, 川嶋之雄, 栗原智明, 西尾四良, 澤田貴義 (1998): 藻類. **46**, 1-9.
- 田井野清也 (2009): カジメ・クロメの藻場造成-高知県沿岸. カジメ属の生態学と藻場造成 (能登谷正浩編). 恒星社厚生閣. 東京. 72-92.
- 谷口和也 (2008): 海中林. 消える日本の自然 (鷺谷いづみ編). 恒星社厚生閣. 東京. 98-104, 210-218.
- 谷口和也 (1996): 海中林造成の基礎と実践. *藻類*. **44**, 103-108.
- 谷口和也, 秋山和夫 (1982): アラメ配偶体の成長及び成熟に対する水温と光条件. *東北水研研究報告*. **45**, 55-59.
- 野島哲, 岡本峰雄 (2008): 造礁サンゴの北上と白化. *日本水産学会誌*, **74**, 884-888.
- 向井宏 (2008): 海岸. 消える日本の自然 (鷺谷いづみ

編). 恒星社厚生閣. 東京. 68-75, 170-181.

ROEROE K.A. M. YAP and M. OKAMOTO (2013): Development of new assessment methods for *Acropora* coral recruitment using coral settlement devices and holes of marine block. Fish Sci. 79, 617-627. DOI 10.1007/s12562-013-0632-7.

受付：平成 25 年 8 月 26 日

受理：平成 25 年 10 月 28 日

Spatial distribution of phytopigments and organic matter in surface sediments in Lake Saroma (Hokkaido, Japan)

Emi TERASAKI^{1),*}, Kou MORITA²⁾, Masaomi YASUDA³⁾,
Kimihiko MAEKAWA⁴⁾ and Shigeru MONTANI¹⁾

Abstract : In Lake Saroma, scallops have been adversely affected by hypoxic events, which are caused by long-term scallop culture in summer. In this study, we were conducive to the spatial distribution of Chl *a*, phaeopigment, total organic carbon (TOC) and total nitrogen on a grid of 54 stations in surface sediments. The temporal changes in the TOC content of the surface sediments since the initiation of scallop culture in Lake Saroma were also studied. The average Chl *a* /total pigments was 0.7 ± 0.2 in the organic poor area (PA), which was higher than 0.4 ± 0.2 in the organic rich area (RA). Benthic environments were suited for growing microphytobenthos in the PA. In contrast, the RA has become increasingly eutrophic because of the average TOC was $23 \pm 5 \text{ mg g}^{-1}$, which was higher than $6 \pm 3 \text{ mg g}^{-1}$ in the PA. During the past 40 years, after the TOC content had decreased in surface sediment owing to the excavation work, it has increased in the RA owing to the concentrated scallop culture facilities. This study concludes that benthic environments in Lake Saroma are directly and indirectly affected by human activities, particularly in the RA.

Keywords : *Sediments, Scallop culture, Phytopigment, Organic matter*

1. Introduction

Coastal lagoons are rich in nitrogen and phosphorus compounds and provide highly productive habitats for aquatic life such as fish and shellfish. Coastal lagoons are often used

for aquaculture activities, which may have direct or indirect environmental impacts, primarily because of the excessive inputs of nutrients and organic matter. Riverine inflows and the transport of allochthonous particles and organic matter also affect the physicochemical environments of lagoons, which widely fluctuate at the interface between freshwater and seawater (MEADE, 1972; ALLEN *et al.*, 1980). The large supply of organic matter derived from aquaculture and riverine inputs into coastal lagoons often cause hypoxic or anoxic events that lead to fish and benthic mortalities (GOWEN *et al.*, 1991; PEARSON and BLACK, 2001), thereby affecting aquacultural activities. Therefore, investigating the depositional environment to assess the characteristics of benthic environments could facilitate better management practices.

The organic matter in surface sediments is an important source of food for benthic fauna. However, overabundance may lead to benthic

1) Graduate school of Environmental Science, Hokkaido University, N10W5 Kita-ku, Sapporo, Hokkaido 060-0810, Japan

2) Hokkaido Aquaculture Promotion Corporation, 1-3-3 Yonesato 4 jo, Siroishi-ku, Sapporo, Hokkaido 003-0874, Japan

3) Tohoku Electric Power Company, Incorporated, 1-7-1 Hon-chou, aoba-ku, Sendai, Miyagi 980-8550, Japan

4) Aquaculture Fishery Cooperative of Saroma Lake, Sakaaura, Tokoro, Kitami, Hokkaido 093-0216, Japan

*Corresponding author: Address: Graduate school of Environmental Science, Hokkaido University, N10W5 Kita-ku, Sapporo, Hokkaido 060-0810, Japan. Tel.: +81 11 706 2322.
E-mail: hamulin@ees.hokudai.ac.jp (E. Terasaki)

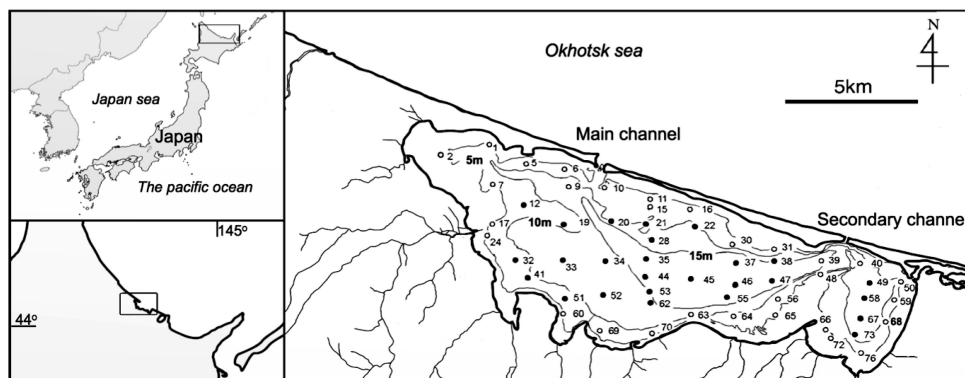


Fig. 1. The study area and sampling stations in Lake Saroma, Hokkaido, Japan. ●: In the scallop culture facility.

impairment due to oxygen depletion and build-up of toxic byproducts, associated with the breakdown of these materials (HYLAND *et al.*, 2005; MAGNI *et al.*, 2009). The negative effects of excessive loads of organics are known to be related to the hydrodynamic features of lagoons (TAGLIAPIETRA *et al.*, 2012). In the Lake Saroma, the scallop culture has an area of 80 km² or 53% of the total area and has been conducted since 1960ies, achieving a maximum production of 9000 tons in 1979. However, water quality problems such as red tide occurred, affecting scallop production that decreased to 3700 tons in 1985. Thus, a fisherman's association tried to be rebounded scallop production from the impact of water pollution by interim downturn amount of scallop culture. Additionally, it was prompted the digging of a secondary channel to improve water flow. Then, scallop production rebounded to 6,700 tons in the 1990ies and was an advantage of 6,000 tons per year at present. However, in the summer of 1987 dissolved oxygen concentration decreased to 30% in the lake below a depth of 15 m (SAMPEI *et al.*, 1997). Recently, hypoxic events are caused by the excessive input of organic matters from rivers and long-term scallop culture facilities. Several benthic environmental studies have been conducted in Lake Saroma (SATAKE, 1967; KIKUCHI *et al.*, 1984; NISHIHAMA and HOSHIKAWA, 1992; KASHIMA, 1996; SAMPEI *et al.*, 1997; SONODA *et al.*, 2002; KATSUKI *et al.*, 2009). These studies suggested that benthic

environments are influenced by scallop culture and that surface sediments are partly eutrophic. However, no statistical studies have been conducted to analyze sediment eutrophication and temporal changes in the TOC content of sediments since the initiation of scallop culture in Lake Saroma. Additionally, no study reported phytopigments contents as basic biochemical parameter in surface sediment. Phytopigments were important information because these gave an indicative of primary producer and a source of feed for filter feeder. Spatial distributions of phytopigments were necessary data to assess the impact of scallops to surface sediment because biodeposition of scallops included phytopigments. In this study, the primary goals were (i) to understand spatial distribution of phytopigments and organic matter and to assess these levels and statistically the eutrophic sediments area of Lake Saroma; and (ii) to see if there is any relationship between temporal changes in the TOC content of sediment to human activities since the initiation of scallop culture in Lake Saroma.

2. Materials and Methods

Study site

Lake Saroma is located in the subarctic zone of Japan and it is connected with the Sea of Okhotsk by a westward main channel and an eastward secondary channel (Fig. 1). It is the largest coastal lagoon in Japan with an area of 150 km², an average depth of 9 m, and a

maximum depth of about 20 m (KIKUCHI *et al.*, 1984; NISHIHAMA and HOSHIKAWA, 1992; KATSUKI *et al.*, 2009). Furthermore, ring current at high tide currents mainly toward south from the main channel and partly circulated at west end and Kimuanepu cape in Lake Saroma (SATAKE, 1967). Other ring current at high tide currents plume-form from the secondary channel after that linearly current, in contrast ring currents at low tide were reverse (HAGINO, 1985). Flow volume at the mainly and the secondary channels were able to calculate from tidal range between the open seawater. Order of flow volume at the mainly and the secondary channels were 10^8 m^3 and 10^7 m^3 per one-tide, respectively and the ratio was about 9 : 1 (TAKEUCHI *et al.*, 1990).

Field surveys

Sampling was conducted using a grid at 56 stations on September 26, 2005 (Fig. 1). Surface (0–1 cm) sediment samples were collected at each station using Ekman-Birge type bottom sampler (15 cm \times 15 cm). The samples were packed in zipper bags and stored in a refrigerator. After returning to the laboratory, the samples were stored at -20°C until analysis after removing the pore water by centrifugation (3,000 rpm for 10 min).

The present study was conducted following a hypoxic event in September 2005. During this year, Lake Saroma was characterized by high biological productivity and high biodeposition (KURATA *et al.*, 1991). In our survey, we also found that the chlorophyll-*a* (Chl *a*) concentration and primary production in the water column were as high as $3.2 \mu\text{g l}^{-1}$ and $1 \text{ g C m}^{-2} \text{ day}^{-1}$, respectively (unpublished data).

Sediment analysis

To determine the Chl *a* and phaeopigment contents of the sediments, about 0.1 g of the sediment sample was added to a test tube and Chl *a* and phaeopigment were extracted using 90% acetone. The test tube was then placed in a freezer in dark conditions at -20°C for one day. After ultrasonication for five minutes, the concentration of Chl *a* in the supernatant of the test tube was determined using a fluorophotometer (Turner 10-AU-5, Turner Designs),

according to LORENZEN's (1967) method as described by PARSONS *et al.* (1984).

To determine the organic carbon and nitrogen content in the sediments, samples were freeze-dried and ground to a powder using a mortar. Prior to the analysis, the samples were treated with 1N HCl to remove any traces of inorganic carbon, rinsed with deionized and distilled water to remove the acid, and freeze-dried. The total organic carbon (TOC) and total nitrogen (TN) content were determined using a CHN analyzer (NA-1500, Fusion Designs).

Data analysis

Cluster analysis and multidimensional scaling (MDS) were conducted to understand the sedimentary environment in Lake Saroma depending on the sources of the organic matter. Cluster analysis (Ward's method) was conducted using a Euclidean distance technique for the TOC, TN, and Chl *a*/total (Chl *a* + phaeopigment) pigments (Chl *a*/total) ratio content to categorize the sediments. The MDS ordination analysis was performed using a Euclidean distance technique with the same data to produce a two-dimensional (2D) plot of the categorized sediments.

3. Results

Sediment characteristics

The average Chl *a* and phaeopigment contents for all analyzed stations were $73 \pm 86 \mu\text{g g}^{-1}$ and $94 \pm 142 \mu\text{g g}^{-1}$, respectively. The Chl *a* content exhibited a distribution similar to that of the phaeopigment content, except at Stn. 68, where the Chl *a* content ($155 \mu\text{g g}^{-1}$) differed from the phaeopigment content ($25 \mu\text{g g}^{-1}$) [Figs. 2 (a) and (b)]. The Chl *a* content was greater than $200 \mu\text{g g}^{-1}$ at westernmost side in Stns. 1, 2, and 72, while it was about $10 \mu\text{g g}^{-1}$ at mainly seaside in Stns. 9, 11, 15, 22, 30, 63, and 70, with a minimum value of $1.4 \mu\text{g g}^{-1}$ at Stn.10 [Fig. 2 (a)]. The phaeopigment content was greater than $200 \mu\text{g g}^{-1}$ at westernmost side, where the Chl *a* content was high [Fig. 2 (a) and (b)]. In contrast, the phaeopigment content was lesser than $10 \mu\text{g g}^{-1}$ at seaside, with a minimum value at and easternmost side in Stns. 48, 59, and 68 [Fig. 2 (b)].

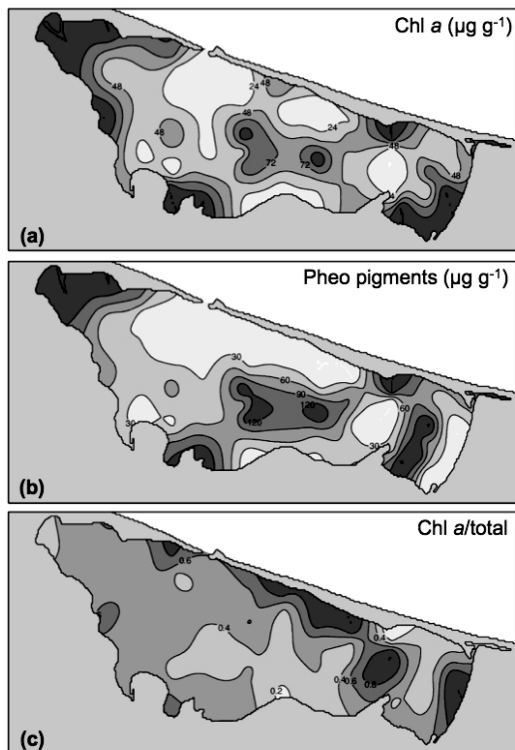


Fig. 2. (a) Spatial distributions of chlorophyll-*a* (Chl *a*) content, (b) special distribution of phaeopigment content, and (c) special distribution Chl *a*/total pigments (Chl *a*/total) ratio in the surface (0–1 cm) sediments of Lake Saroma.

The distribution of Chl *a*/total pigments exhibited a better agreement with bathymetry than those of Chl *a* and phaeopigment contents (Fig. 2). The average Chl *a*/total ratio was 0.50 ± 0.18 ; a high Chl *a*/total ratio was recorded at seaside and easternmost side, with a maximum value of 0.96. In contrast, a low Chl *a*/total ratio was recorded at Stns. 39, 63, and 67, with a minimum value of 0.17 [Fig. 2 (c)].

The TOC and TN distributions exhibited a better agreement with the phaeopigment content than with Chl *a* (Fig. 3). The average TOC and TN contents were $18 \pm 12 \text{ mg g}^{-1}$ and $2.0 \pm 1.3 \text{ mg g}^{-1}$, respectively. A high TOC content of greater than 30 mg g^{-1} was observed at Stns. 66 and 73, with a maximum value of 38 mg g^{-1} at Stn. 24 [Fig. 3 (a)]. In contrast, a low TOC content was recorded at Stns. 31 and 48, with a

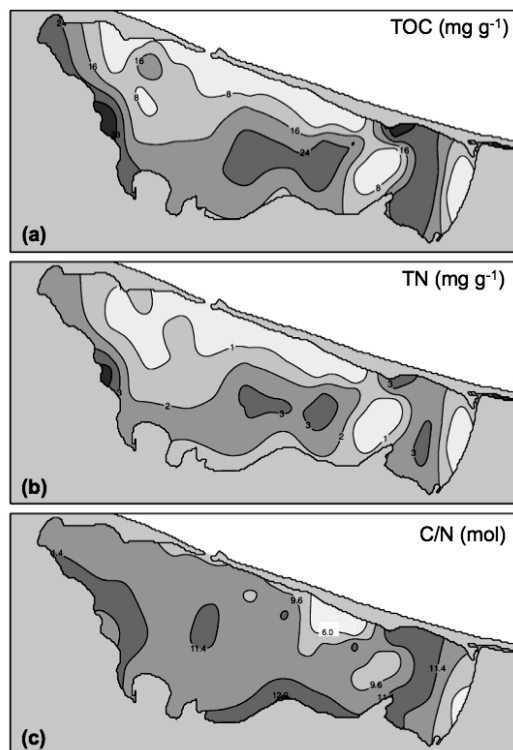


Fig. 3. (a) Spatial distribution of the total organic carbon (TOC) content, (b) special distribution total nitrogen (TN) content, and (c) carbon to nitrogen (molar; C/N) ratio in the surface (0–1 cm) sediments of Lake Saroma.

minimum value of 1.8 mg g^{-1} at Stn. 10 [Fig. 3 (a)]. A high TN content of greater than 3 mg g^{-1} was observed at depth $>10 \text{ m}$ in east basin and $>15 \text{ m}$ in west basin, with a maximum value of 4.1 mg g^{-1} at Stn. 24 [Fig. 3 (b)]. In contrast, a low TN content of lesser than 0.5 mg g^{-1} was observed at seaside and easternmost side [Fig. 3 (b)]. The C/N (mol) ratio had an average value of 10 ± 1 , whereas it was about 12 near river mouth and the secondary channel [Fig. 3 (c)]. In contrast, a low C/N ratio of 6–8 was observed at seaside and easternmost side, which agreed with the high Chl *a*/total content [Fig. 3 (c)].

Spatial patterns

Using the TOC, TN, and the Chl *a*/total data, the sediment samples were categorized into two

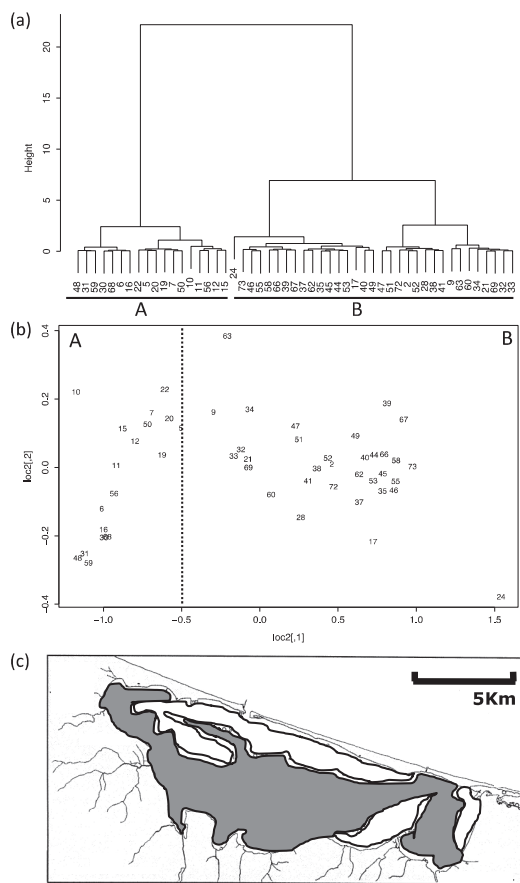


Fig. 4. (a) Dendrogram produced using Ward's clustering method and (b) multidimensional scaling (MDS) ordination plots for total organic carbon (TOC) and total nitrogen (TN) contents and chlorophyll-*a* to total pigments (Chl *a*/total) ratio data of surface sediments from Lake Saroma. Group A: the organic poor area; Group B: the organic rich area. (c) Classification map derived from (a) and (b). □: the organic poor area; ■: the organic rich area.

main groups ($n=51/58$). Group A was the organic poor area (PA) that included Stns. 5–7, 10–16, 19–22, 30, 31, 48, 50, 56, 59, 65, and 68 (Fig. 4). Group B was the organic rich area (RA) that included Stns. 1, 2, 9, 17, 21, 24–47, 49, 51–55, 58, 60–64, 66, 67, and 69–76 (Fig. 4). Spatial patterns of PA and RA agreed with the bathymetry and ring currents. The grain size composition for PA was sand and silty sand to clay for RA (NISHIHAMA & HOSHIKAWA, 1992;

SAMPEI *et al.*, 1997). The average depths in RA and PA were 13 ± 5 m and 7 ± 3 m, respectively. The scallop culture facilities were located in RA, which were at depth of greater than 10 m. The average Chl *a* and phaeopigment contents were 37 ± 36 $\mu\text{g g}^{-1}$ and 19 ± 20 $\mu\text{g g}^{-1}$, respectively, in PA, and 91 ± 102 $\mu\text{g g}^{-1}$ and 122 ± 156 $\mu\text{g g}^{-1}$, respectively, in RA. The average Chl *a*/total ratio was 0.7 ± 0.2 in PA and 0.4 ± 0.2 in RA. The average TOC and TN contents were 6.3 ± 3.1 mg g^{-1} and 0.7 ± 0.3 mg g^{-1} in PA and 23.4 ± 5.4 mg g^{-1} and 2.5 ± 0.6 mg g^{-1} in RA, respectively. The average C/N ratio was 9.6 ± 1.4 in PA and 11.1 ± 0.9 in RA.

4. Discussion

Characteristics of phytopigments and organic matter on surface sediment in Lake Saroma

The average Chl *a* and phaeopigment biomass in Lake Saroma were 299 ± 220 mg m^{-2} and 325 ± 259 mg m^{-2} , respectively. In contrast, in the Gulf of Fos in France where mussels were cultured, the average Chl *a* and phaeopigment biomass were 30 ± 5 mg m^{-2} and 215 ± 58 mg m^{-2} , respectively (PLANTE-CUNY *et al.*, 1993). In the Tasman Bay in New Zealand where mussels were cultured, the average Chl *a* and phaeopigment biomass were 24 ± 18 mg m^{-2} and 67 ± 15 mg m^{-2} , respectively (CHRISTENSEN *et al.*, 2003). However, the average Chl *a* and phaeopigment biomass were 330 mg m^{-2} and 220 mg m^{-2} , respectively, at Skagerrak in Sweden (which is located in the subarctic region) where mussels were cultured (SUNDBÄCK *et al.*, 1996). In Hichiripuu lagoon, which is located in the same prefecture as Lake Saroma and where oyster and clam were cultured, the Chl *a* biomass was 226 mg m^{-2} (KAJIHARA *et al.*, 2010). We suggested that the Chl *a* and phaeopigment contents tend to be higher in the subarctic region. The Chl *a*/total ratio in this study indicated that the Chl *a* activity was low, i.e., 0.4, in RA [Fig. 2 (c)], which was greater than the levels of 0.01–0.3 detected in Tasman Bay (CHRISTENSEN *et al.*, 2003). In contrast, the Chl *a*/total ratio was high, i.e., 0.8 in PA [Fig. 2 (c)], which were similar to the levels of 0.7–0.8 at Skagerrak at a depth of 0.5 m (SUNDBÄCK *et al.*, 1996). Therefore, the average

relative light intensity at depth of 7 m and 13 m, which were average depth at PA and RA, were $25 \pm 17\%$ and $9 \pm 6\%$ as 100% in surface layer, respectively in the summer of 2010 (in preparation). The Chl *a* content were high despite the low pheopigment, TOC, and TN at PA. Thus, at PA, organic matter was low due to sandy and light, which was enough to grow microphytobenthos reached to surface sediments. The contributions rate of Chl *a* to TOC were calculated with C/Chl *a* as 50 (ANTIA *et al.*, 1963) and was $36 \pm 28\%$ at PA as against was $17 \pm 15\%$ at RA in surface sediments. We suggested that microphytobenthos play a role on bioproduction environment at PA. TERASAKI *et al.* (in preparation) reported that deeper station had characterized by easy to be deposited OM derived from detritus and contribution rate of biodeposition was 50% on surface sediments under the scallop culture facility.

At the Marano and Grado lagoons, connected to the Adriatic Sea, and the Firth of Thames, New Zealand, where mussels were cultured, the TOC content varied from 5 to 15 mg g⁻¹ (VITTOR *et al.*, 2012) and from 16 to 19 mg g⁻¹ (GILES and PILDITCH, 2006), respectively. At Prince Edward Island, Canada, and Thau lagoon, France, where mussels were cultured, the TOC content varied from 12 to 43 mg g⁻¹ (WALKER and GRANT, 2009) and from 42 to 68 mg g⁻¹ (ANSCHUTZ *et al.*, 2007), respectively. MAGNI *et al.*, (2009) detected very high TOC levels in two Mediterranean lagoons (the Orbetello and the Venice lagoons) where bivalves were cultured, with values up to 60 and 100 mg g⁻¹, respectively. TOC and TN contents of the surface sediments from Lake Saroma where scallops were cultured is similar to or lower than those observed in coastal areas or lagoons where bivalves were cultured. Therefore, it can be deduced that Lake Saroma does not have an extreme organic load, which was also reported by SONODA *et al.* (2002). The sediments are becoming increasingly eutrophic in RA as reported by KATSUKI *et al.* (2009). The C/N ratio of phytoplankton and microphytobenthos were 4–10, whereas the C/N ratio of seagrass and terrestrial plant was greater than 12 (BORDOVSKI, 1965; HEDGES *et al.*, 1986; MEYERS, 1997). This suggests that TOC and

TN are derived from phytoplankton and microphytobenthos in PA, while they are derived from seagrass and terrestrial plant in RA. SAMPEY *et al.* (1997) reported that organic matter mainly derived from phytoplankton was found in center of this lake and organic matter derived from terrestrial material increased near the edge of lake, which was not consistent with this current study. However, the reported organic matter by stable carbon and nitrogen isotopes showed that the contributions of seagrass and terrestrial plant were high in RA, which was consistent with the study by TERASAKI *et al.* (in preparation).

Variation of TOC content of the surface sediments over the past 40 years in Lake Saroma

Aquaculture activities are generally viewed as having major negative impacts on coastal environments (DANOVARO, 2003). The impact of intensive fish farming on the benthic environment is expected to be higher than that of bivalve farming (MAZZOLA *et al.*, 1999; INGLIS *et al.*, 2000). However, mussel biodeposition in mussel farms located in the Mediterranean has adversely affected farm sediments (DANOVARO *et al.*, 2004). In Lake Saroma, previous investigations suggested that high amounts of organic matter were loaded into the sediment by scallop culture (SONODA 2002; KATSUKI *et al.*, 2009). Thus, the TOC content since 1965 during the period of scallop culture (Table 1) was evaluated and related to human activities in the surface sediment. The scallop production was 200 tons in 1965 and increased to 9,000 tons in 1980 (NISHIHAMA and HOSHIKAWA, 1992). In 1965, the spatial distribution of the TOC content was high at around 10–20 mg g⁻¹ and greater than 25 mg g⁻¹ at both depth > 10 m in east basin and depth > 15 m in west basin (deeper station), where every hypoxia occurred (Table 1). This showed that the benthic environment was highly eutrophic in 1965 and was comparable to 2005, which has a similar level. It was prompted the digging of secondary channel to improve water flow because repeated hypoxia events occurred in 1978. However, fishermen also halted scallop culture, because scallop catches were damaged by a red tide event in the 1980s. Thus, the spatial distribution of the

Table 1. Change of the spatial distribution of total organic carbon (TOC) content in surface sediments over past 40 years. Unit: % (percentage of total area); ton/year (scallop catches).

unit	total area				scallop catches	digging channel
	%				ton/year	
year	rank1	rank2	rank3	rank4		
1929	—	—	—	—	—	the main channel
1965	14	52	16	18	200	
1978	—	—	—	—	7000	the secondary channel
1988	39	56	3	2	5000	
1995	36	27	20	16	6700	
2005	33	19	15	33	6000	

*The rank 1 indicated that TOC content was $<10 \text{ mg g}^{-1}$; the rank 2 indicated that TOC content was $10\text{--}20 \text{ mg g}^{-1}$; the rank 3 indicated that TOC content was $20\text{--}25 \text{ mg g}^{-1}$; the rank 4 indicated that TOC content was $>25 \text{ mg g}^{-1}$. The percentages of total area of 1965 and 1988 were taken from NISHIHAMA and HOSHIKAWA (1992); the percentages of total area of 1995 were taken from SAMPEI *et al.* (1997). Cultured scallop catches were running mean values for five years, provided that the scallop catch of 1965 used data of 1966.

TOC content decreased between 10 and 20 mg g^{-1} at deep stations in 1988 and it decreased as compared to that in 1965 (Table 1). The benthic environments were improved by the reduction of scallop biodeposition in the sediment and water flowing through the secondary channel (NISHIHAMA and HOSHIKAWA, 1992). After the fishermen resumed scallop culture at the end of the 1980s, the scallop catches rebounded to 7,000 tons in 1990 (NISHIHAMA and HOSHIKAWA, 1992) and it remained between 6,000 and 7,000 tons in 2005 (AQUACULTURE FISHERY COOPERATIVE OF SAROMA LAKE, 2005). The spatial distribution of the TOC content increased at around $10\text{--}20 \text{ mg g}^{-1}$, and the average TOC content was $24 \pm 2 \text{ mg g}^{-1}$ at deep stations in 1995 (Table 1). After that, the spatial distribution of the TOC content increased to greater than 25 mg g^{-1} , and the average TOC content was $27 \pm 2 \text{ mg g}^{-1}$ at deep stations in 2005 (Table 1). According to the distributions of the TOC content in 1988 (NISHIHAMA and HOSHIKAWA, 1992), 1995 (SAMPEI *et al.*, 1997), and this current study, the TOC content decreased in PA and increased in RA. The TOC accumulated in the deep stations, and its extent expanded in RA. The TOC content has increased to at least 7 mg g^{-1} at deep stations

since 1988, when scallop culture was healthy (Table 1). This suggests that the benthic environments are directly or indirectly affected by human activities such as scallop culture in Lake Saroma, particularly in RA.

Biodeposition was also responsible for a significant accumulation of biopolymeric carbon, which induced significant changes in microbial and meiofaunal assemblages (MIRTO *et al.*, 2000). In Lake Saroma, the polychaete community changed between 1975 and 1995. The total population density and species diversity has decreased, and the dominant species composition has changed (SONODA, 2002). The relative abundance of *Cyclotella caspia*, an indicator species of eutrophication, was higher in 2005 as compared to 1995; it increased in the scallop culture area since 2005 (KATSUKI *et al.*, 2009).

The biogeochemical environment is seriously affected by human activities in Lake Saroma due to the interaction among the TOC content, the scallop culture, and the digging. Furthermore, previous reports state that hypoxic events and eutrophication in benthic environments have been degraded yearly by long-term scallops grazing, which has led to benthic community changes (SONODA, 2002; KATSUKI *et al.*, 2009). It is predicted that if benthic

environments are left undisturbed, and if the TOC content continues to increase in the future, this would affect the scallop culture. Nishihama *et al.* (1992) reported that benthic environment was favorable in 1988 and TOC content was $<20 \text{ mg g}^{-1}$ at depth $>15 \text{ m}$ on surface sediments. In contrast, TOC content was at least $24 \pm 1 \text{ mg g}^{-1}$ of 1995 while hypoxic events had occurred. Thus, we suggested that TOC content should be $<20 \text{ mg g}^{-1}$ to keep favorable benthic environment. In the future, it is important to focus on the TOC content and show voluntary restraint during scallop culture and be proactive in digging the secondary channels to improve benthic environments.

5. Conclusion

Lake Saroma does not have extreme organic contamination, although the sediments are becoming increasingly eutrophic in the organic rich area owing to the concentration of scallop culture facilities. TOC content has continued to increase, and hypoxic events have occurred at deep stations that are in the RA since the early 1990s. The TOC content respond to human activities such as scallop culture and digging in Lake Saroma. We suggested that effective action needed to be taken to improve benthic environments as soon as possible because the average TOC content is 27 mg g^{-1} at deep stations in 2005.

Acknowledgements

Sincere thanks to the AQUACULTURE FISHERY COOPERATIVE OF SAROMA LAKE for their cooperation in sampling and for providing scallop samples. Sincere thanks to Dr. Paolo MAGNI and anonymous reviewers for providing the valuable comments on previous versions of the manuscript.

References

- ALLEN, G. P., J. C. SALOMON, P. BASSOULLET, Y. D. PENHOAT and C. de GRANDPRÉ (1980): Effects of tide on mixing and suspended sediment transport in macrotidal estuaries. *Sedimentary Geology*, **26**, 69–90.
- ANSCHUTZ, P., G. CHAILLOU and P. LECROART (2007): Phosphorus diagenesis in sediment of the Thau Lagoon. *Estuarine, Coastal and Shelf Science*, **72**, 447–456.
- ANTIA, N. J., C. D. MCALLISTER, T. R. PARSONS, K. STEPHENS and J. D. H. STRICKLAND (1963): Further measurements of primary production using a large-volume plastic sphere. *Limnology Oceanography*, **8**, 166–183.
- AQUACULTURE FISHERY COOPERATIVE OF SAROMA LAKE (2005): Annual Report of the aquaculture fishery cooperative of Saroma Lake. Aquaculture Fishery Cooperative of Saroma Lake Press, Hokkaido, p. 16 (In Japanese).
- BORDOVSKI, O.K. (1965): Accumulation of organic matter in bottom sediments. *Marine Geology*, **3**, 33–82.
- CHRISTENSEN, P.B., R.N. GLUD, T. DALSGAARD and P. GILLESPIE (2003): Impacts of longline mussel farming on oxygen and nitrogen dynamics and biological communities of coastal sediments. *Aquaculture*, **218**, 567–588.
- DANOVARO, R. (2003): Pollution threats in the Mediterranean Sea: An overview. *Chemistry and Ecology*, **19**, 15–32.
- DANOVARO, R., C. GAMBI, G.M. LUNA and S. MIRTO (2004): Sustainable impact of mussel farming in the Adriatic Sea (Mediterranean Sea): evidence from biochemical, microbial and meiofaunal indicators. *Marine Pollution Bulletin*, **49**, 325–333.
- GILES, H. and C. A. PILDITCH (2006): Effects of mussel (*Perna canaliculus*) biodeposit decomposition on benthic respiration and nutrient fluxes. *Marine Biology*, **150**, 261–271.
- GOWEN, R. J., D. P. WESTON and A. ERVIK (1991): Aquaculture and the benthic environment: a review. *In* Nutritional Strategies and Aquaculture Waste. COWEY, C.B. and C.Y. CHO (eds.), Proceedings of the First International Symposium on Nutritional Strategies in Management of Aquaculture Waste, University of Guelph, Ontario, Canada. Fish Nutrition Research Laboratory, University of Guelph, p.187–205.
- HAGINO, S. (1985): Study on sea water exchange characteristics in Lake Saroma. Scientific Reports of National Research Institute of Fisheries Engineering, **6**, 1–15 (In Japanese with English abstract).
- HEDGES, J. I., W. A. CLARK, P. D. QUAY, J. E. RICHEY, A. H. DEVOL and U. M. SANTOS (1986): Compositions and fluxes of particulate organic material in the Amazon River. *Limnology and Oceanography*, **31**, 717–738.
- HYLAND, J., L. BALTHIS, I. KARAKASSIS, P. MAGNI, A. PETROV, J. SHINE, O. VESTERGAARD and R. WARWICK (2005): Organic carbon content of sediments as an indicator of stress in the marine benthos. *Marine Ecology Progress Series*, **295**, 91–103.

- INGLIS, G. J., B. J. HAYDEN and A. H. ROSS (2000): An overview of factors affecting the carrying capacity of coastal embayment for mussel culture. NIWA client Report: CHC00/69, Project No.: MFE00505, National Institute of Water & Atmospheric Research Ltd., Christchurch, New Zealand, 31 pp.
- KAJIHARA, R., T. KOMORITA, A. HAMADA, S. SHIBANUMA, T. YAMADA and S. MONTANI (2010): Possibility of direct utilization of seagrass and algae as main food resources by small gastropod, *Lacuna decorata*, in a subarctic lagoon, Hichirippu, eastern Hokkaido, Japan with stable isotope evidences of carbon and nitrogen. *Plankton and Benthos Research*, **5**, 90–97.
- KASHIMA, K. (1996): Diatom assemblages from lake sediments of Lake Abashiri and Lake Saroma, Hokkaido, northern part of Japan. *Laguna*, **3**, 33–39 (In Japanese with English abstract).
- KATSUKI, K., K. SETO, R. NOMURA, K. MAEKAWA and B. K. KHIM (2009): Effect of human activity on Lake Saroma (Japan) during the past 150 years: evidence by variation of diatom assemblages. *Estuarine, Coastal and Shelf Science*, **81**, 215–224.
- KIKUCHI, K., Y. NOZAWA and E. MATSUMOTO (1984): Environmental changes of Lake Saroma recorded in sediment cores. *Scientific Reports of Hokkaido Fisheries Experimental Station*, **26**, 11–24 (In Japanese).
- KURATA, M., H. HOSHIKAWA and Y. NISHIHAMA (1991): Feeding rate of the Japanese scallop *Patinopecten yessoensis* in suspended cages in Lagoon Saroma-ko. *Scientific Reports of Hokkaido Fishery Experimental Station*, **37**, 37–53 (In Japanese with English abstract).
- LORENZEN, C. J. (1967): Determination of chlorophyll and pheo-pigments: Spectrophotometric equations. *Limnology and Oceanography*, **12**, 343–346.
- MAGNI, P., D. TAGLIAPIETRA, C. LARDICCI, L. BALTHIS, A. CASTELLI and S. COMO, G. FRAGIPANE, G. GIORDANI, J. HYLAND, F. MALTAGLIATI, G. PESSA, A. RISMONDO, M. TATARANNI, P. TOMASSETTI and P. VIAROLI (2009): Animal-sediment relationships: Evaluating the 'Pearson-Rosenberg paradigm' in Mediterranean coastal lagoons. *Marine Pollution Bulletin*, **58**, 478–486.
- MAZZOLA, A. S. MIRTO and R. DANOVARO (1999): Initial fish-farm impact on meiofaunal assemblages in coastal sediments of the western Mediterranean. *Marine Pollution Bulletin*, **38**, 1126–1133.
- MEADE, R. H. (1972): Transport and deposition of sediments in estuaries. *In Environmental Framework of Coastal-plain Estuaries*. Nelson, B. W. (ed), Geological Society of America Memoirs, **133**, p.91–120.
- MEYERS, P. A. (1997): Organic geochemical proxies of paleoceanographic, paleolimnologic, and paleoclimatic processes. *Organic Geochemistry*, **27**, 213–250.
- MIRTO, S., T. LA ROSA, R. DANOVARO and A. MAZZOLA (2000): Microbial and meiofaunal response to intensive mussel-farm biodeposition in coastal sediments of the Western Mediterranean. *Marine Pollution Bulletin*, **40**, 244–252.
- NISHIHAMA, Y. (1994): *Scallop Aquaculture in Okhotsk*. Hokkaido University Press, p.112. (in Japanese).
- NISHIHAMA, Y. and H. HOSHIKAWA (1992): Distribution of grain-size composition and organic carbon content of bottom deposits in Lake Saroma, Hokkaido. *Scientific Reports of Hokkaido Fisheries Experimental Station*, **39**, 1–9 (In Japanese with English abstract).
- PEARSON, T. H. and K. D. BLACK (2001): The environmental impacts of marine fish cage culture. *In Environmental Impacts of Aquaculture*. BLACK, K.D. (ed.), Sheffield Academic Press, p.1–31.
- PARSONS, T. R., M. MAITA and C. M. LALLI (1984): *A manual Chemical and biological methods for seawater analysis*. Pergamon Press, Oxford, p.173.
- PLANTE-CUNY, M. R., C. BARRANGUEST, D. BONIN and C. GRENZ (1993): Does chlorophyllide *a* reduce reliability of chlorophyll *a* measurements in marine coastal sediments? *Aquaculture Sciences*, **55**, 19–30.
- SAMPEI, Y., Y. KURAKADO, M. SHIMIZU, K. TAKAYASU and H. ISHIDA (1997): Distribution of organic carbon, nitrogen and sulfur in surface sediments of Lake Saroma and Lake Abashiri, Hokkaido, Japan. *Researches in Organic Geochemistry*, **12**, 51–60 (In Japanese with English abstract).
- SATAKE, T. (1967): Mechanical compositions of bottom deposits of Lake Saroma. *Journal of Geological Society of Japan*, **73**, 420–440 (In Japanese).
- SONODA, T., S. NAKAO and K. TAKAYASU (2002): Polychaete community structure and temporal change through last 20 years in the intensive scallop culture area, Saroma Lagoon, northern Japan. *Laguna*, **9**, 19–30 (In Japanese with English abstract).
- SUNDBÄCK, K., P. NILSSON, C. NILSSON and B. JÖNSSON (1996): Balance between autotrophic and heterotrophic components and processes in microbenthic communities of sandy sediments: A field study. *Estuarine, Coastal and Shelf Science*, **43**, 689–706.
- TAGLIAPIETRA, D., M. SIGOVINI and P. MAGNI (2012): A unified view of benthic succession models for coastal lagoons. *Hydrobiologia*, **686**, 15–28.
- TAKEUCHI, T., T. SAKATA and Y. HAYASE (1990): A study on the environmental conservation in

lagoons of cold regions. Research and Development of Public Works Research Institute, 92 (In Japanese with English abstract).

- VITTOR, C. D., J. FAGANELI, A. EMILI, S. COVELLI, S. PREDONZANI and A. ACQUAVITA (2012): Benthic fluxes of oxygen, carbon and nutrients in the Marano and Grado Lagoon (northern Adriatic Sea, Italy). *Estuarine, Coastal Shelf Science*, **113**, 57–70.
- WALKER, T. R. and J. GRANT (2009): Quantifying erosion rates and stability of bottom sediments at mussel aquaculture sites in Prince Edward Island, Canada. *Journal of Marine Systems*, **75**, 46–55.

Received: August 23, 2013
Accepted: November 14, 2013

資 料

第 51 卷第 3・4 号掲載欧文論文の和文要旨

Lamona I. BERNAWIS^{1,2)}・根本雅生¹⁾・吉田次郎¹⁾ : 1990 年から 2007 年にかけての西部北太平洋 137 度線に沿った海洋構造

1990 年から 2007 年にかけて、CTD を用いた観測から西部北太平洋 137 度線に沿って、北緯 3 度から 34 度までの海洋構造を調べた。一般的な構造は過去のナンセン採水器を用いた結果と一致した。二重拡散対流の活発度を密度比 (R_ρ) とターナーアングル (Tu) のヒストグラムを作図することにより調べたところ、ソルトフィンガー型対流が起きる可能性がある成層構造 ($R_\rho > 3.7$, $45^\circ < Tu < 60^\circ$) は北太平洋赤道水 (NPEW) と北太平洋熱帯水 (NPTW) の下部並びに、北太平洋中層水 (NPIW) 上部に見いだされた。この領域はポテンシャル密度 $24.0\sigma_\theta$ と $26.8\sigma_\theta$ 間に恒常的に存在した。密度比 R_ρ のモード値は 3.48 であり、ソルトフィンガーの活発度は高くはないことがわかった。

(1 東京海洋大学大学院 海洋科学技術研究科 〒108-8477 東京都港区港南 4-5-7, 2 現 Bandung Institute of Technology, Gedung Labtek XI lt.1, Jl. Ganesha 10, Bandung 40132, Jawa Barat - Indonesia)

進士淳平¹⁾・照屋清之介・市田健介・富澤輝樹・富永明日翔・伊藤理紗 : 三番瀬干潟の潮間帯にみられた外来性二枚貝ホンビノスガイ *Mercenaria mercenaria* に関する情報

東京湾湾奥部に位置する三番瀬干潟の潮間帯において、外来性二枚貝ホンビノスガイ *Mercenaria mercenaria* を含む貝類の調査を行った。本調査地において、ホンビノスガイの生息密度は泥分率と負の相関を示した。採集された貝類は、アサリ *Ruditapes philippinarum* (41.6%)、ホンビノスガイ (27.7%) およびカガミガイ *Phacosoma japonicum* (24.1%) の 3 種がほとんどを占めていた。ホンビノスガイの個体密度は、アサリおよびカガミガイと負の相関を示さなかった。このことから、本調査地においてホンビノスガイの分布は排他的ではなく、他の在来性貝類 2 種と競争関係にあると考えられなかった。

(1 〒113-8657 東京都文京区弥生 1-1-1 東京大学弥生キャンパス 7 号館 B 棟 534 号室 Tel. 03-5841-8115 Fax. 03-5841-5018 e-mail aa097107@mail.ecc.u-tokyo.ac.jp)

TOE TOE AUNG・下園武範・岡安章夫* : ヤンゴン河航路周辺における堆砂の数値シミュレーション

ミャンマー、ヤンゴン港南の Inner Bar と呼ばれる浅瀬はヤンゴン河航路上の大きな障害となっている。本研究は、浅海域での 3 次元流況計算と平面 2 次元の地形変化予測モデルにより、ヤンゴン河での堆砂状況、流れの特性、それによる底質移動と河床変化メカニズムを明らかにすることを目的としたものである。流況計算にはヤンゴン河の潮位変化が非常に大きいため、 σ 座標を用い、浅瀬の干出・水没の扱える Princeton Ocean Model (POM) を用いた。河床地形と河川流入および河口潮位変動を入力条件として与え、モンスーン時期 (雨期) と乾期の大潮、小潮についてそれぞれ計算を行った。このうち 3 ケースについては Nelson (2000) による観測結果との比較を行い、精度検証を行った。地形変化計算には底質の掃流移動と浮遊移動の双方を考慮できる独自開発の平面 2 次元地形変化モデルを用い、異なる季節において計算を行った。底質粒径については、現地 Inner Bar 付近における底質サンプリングにより得た。地形変化計算においては、Inner Bar 付近を含むヤンゴン河の航路付近の地形変化について概ね再現ができることが分った。また、Inner Bar での推算堆積量は、ミャンマー港湾局が航路維持のために行っている浚渫量と概ね同じであった。

(*東京海洋大学海洋科学系海洋環境学部門沿岸域工学研究室 東京都港区港南 4-5-7 e-mail : okayasu@kaiyodai.ac.jp)

寺崎恵末*・森田 康・安田優臣・前川公彦・門谷 茂 : サロマ湖表層堆積物におけるクロロフィル *a* と有機物の空間分布

サロマ湖 (北海道) ではホタテガイ養殖が盛んに行われているが、近年夏季に貧酸素水塊が発生しホタテガイ養殖に影響している。本研究では、湖内全域に 56 地点の調査地点を設け、表層堆積物を採取し Chl *a*、フェオ色素、全有機炭素 (TOC)、全窒素を測定し、統計的に富栄養化が進行している地点を明らかにした。また、ホタテガイ養殖が開始してからの TOC の経年変化を評価した。MDS とクラスター分析から堆積物表層を海側域と陸側域に 2 分し、海側域では Chl *a*/total pigment (Chl *a*+pheopigment) 比は平均 0.7 ± 0.2 であった。一方、陸側域では 0.4 ± 0.2 であり、海側域は陸側域に比べて底生藻類の増殖に適した環境であることがわかった。TOC は陸側域で平均

23±5 mg g⁻¹であるのに対して、海側域では平均6±3 mg g⁻¹であった。陸側域では海側域に比べて富栄養化が進行していることが明らかとなった。また、ホタテガイ養殖が急激に成長した1970年頃のTOC量は現在と同程度であったが、1980年頃の第2湖口掘削後にTOCは激減した。しかし、その後順調なホタテガイ養殖とともに特に陸側域でTOCが増加し続けている。このことから、サロマ湖の底質環境は直接的もしくは間接的に人為活動の影響を受けていることが明らかである。

(*北海道大学大学院環境科学院 〒060-0810 北海道札幌市北区北十条西5丁目 TEL 011(706)2322 Email hamulin@ees.hokudai.ac.jp(寺崎))

訃報：松生 治 名誉会員

日仏海洋学会名誉会員・松生 治先生は平成 25 年 5 月 9 日に逝去されました。享年 80 歳。ここに、松生 治先生のご冥福を学会員一同と共に衷心よりお祈り申し上げます。



松生 治先生 略歴

昭和 30 年 3 月 東京水産大学水産学部漁業学科 卒業
 昭和 31 年 5 月 同大学 専攻科漁船運用学専攻 修了
 昭和 31 年 8 月 極洋捕鯨株式会社
 昭和 36 年 5 月 東京水産大学文部技官 練習船航海士
 昭和 39 年 3 月 文部教官 助手
 昭和 48 年 8 月 助教授
 昭和 54 年 4 月 教授
 平成 5 年 4 月 農林水産省水産大学校 校長
 平成 9 年 3 月 退官

以上、松生 治先生は極洋捕鯨株式会社で約 5 年間、捕鯨船（キャッチャー・ボート）の航海士として捕鯨事業に従事した。その後、東京水産大学で約 32 年間、また水産大学校で 4 年間、合計 36 年間の長きにわたり水産学の教育・研究、大学の管理運営・行政に携わった。

東京水産大学在職中、教育面においては優れた学識と卓越した経験を基に、講義・実験・実習を担当し、学生や院生の論文指導に力を注いだ。その上、彼らの就職や進学を積極的に支援し、将来の水産・海洋産業を担う人材および有能な教育・研究者を多数育成した。現在、彼らは全国の水産試験場・水産総合センター・大学・民間の海洋調査会社などで重要な仕事・役割を担っている。同時に、学生部参与、海洋環境学科主任、公開講座委員長、臨海実習主任および海洋生産学専攻主任などの要職を歴任、多大な貢献を果たした。

一方、研究面では国際海洋観測調査に参加し、太平洋黒潮流域からインド洋さらに南極海にわたる広大な大洋において、海中の光学観測や気象観測を実施して膨大な資料を得た。この資料を基盤として、学位論文「A study on optical nature in oceanic waters」を纏めた (La mer 11 (1), 1973)。この研究の特徴は、太陽エネルギー分布について、天空から海中まで一貫して考察していること、およびほぼ地球全体規模でのグローバルな視点で取り扱っていることである。斯界の高い評価を得て、昭和 48 年 1 月に京都大学から理学博士の学位を授与された。昭和 49 年には海洋光学分野の発展に寄与した功績により、日仏海洋学会賞を授与された (La mer 12 (3), 1974)。昭和 51 年に文部省在外研究員として

米国・カルフォルニア大学スクリップス海洋研究所に留学し、世界的に著名な海洋光学者 John E. Tyler 博士と交流を深めて、新たな研究分野「濁り」を打ち出した。

濁った水中における魚の視認は、懸濁粒子の餌や釣り糸などを覆うマスク現象で妨げられるので、魚の物標への反応実験を繰り返し行い、濁りの増大は魚の視認距離を減少させることを解明した。また、懸濁粒子が海中で藻類の遊走子などに吸着して生存活力を低下させるばかりでなく、海底に堆積して着底能力へ悪影響をおよぼす閾値なども明らかにし、懸濁粒子の増加は藻場枯渇の一因になることを実証して磯資源の回復に向けて多くの成果を上げた。一方、短い時間で断続や明るさの変化を繰り返す光は、海中動物に定常光とは異なる強い刺激となることを行動学実験で解明して、断続光の光束を並べて照射する「光の網」を提案した。以上、松生先生の研究は、一貫してご自身の創造力に富んだ独特な視点から編み出されており、特に海洋光学分野で偉大な業績を上げた。

学会活動では、日仏海洋学会、日本海洋学会、日本水産学会、日本航海学会の各会員で、特記として、本学会事務局の掌握や評議員と常任幹事を永く務め、日仏海洋学会の学術研究発表会や日本とフランスによる日仏海洋学シンポジウムなどの国際会議の運営に関与し、重責を果たした。

水産大学校長に就任してからは、大学校の実学を重視する教育を精力的に推進した。主な成果として、大学院水産学研究科の開設・改組による新たな水産教育体制の確立、学外交流として韓国・釜慶大学校との学術・教育交流協定の締結、および JICA の外国人研修生の教育・技術指導の実施などである。また、山口県や下関市に請われて、審議会や委員会における指導的な役割を果たし、地域社会の発展に寄与した。

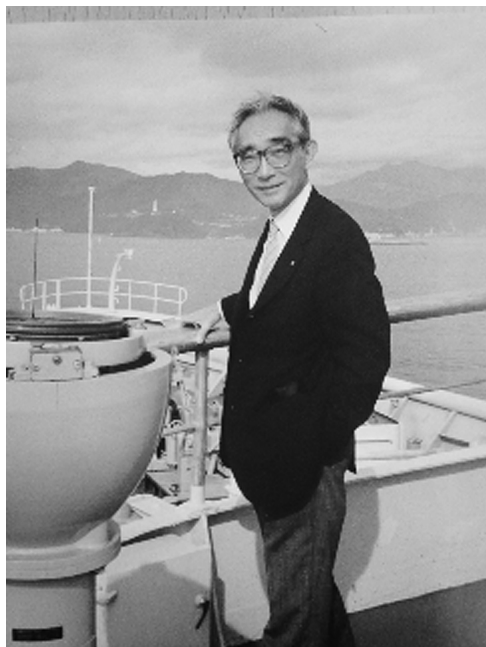
これら教育・研究活動と並行して、日中海洋水産科学技術交流協会（後に韓国を含めた日中韓の三国の協会に改称）の設立に参画し、その要として幹事長を永く務め、中国の学会および産業界において、科学者の交流、共同海洋調査、中国からの留学生および練習船の受け入れなどに尽力した。1985 年より約 25 年間、会長として職責を果たした。

これらの功績により、平成 5 年に東京水産大学（現東京海洋大学）名誉教授、平成 9 年に水産大学校名誉教授および青島海洋大学（現中国海洋大学）名誉教授を授与され、その後、平成 15 年に瑞宝中綬章受章の栄に浴した。

追記：下関の地における先生の終焉は、父・義勝博士（東京水産大学長から水産大学校長へ転出）の辿った道程と同じで、不思議な運命と思う。

森永 勤（日仏海洋学会 副会長）

東北大学名誉教授野村正氏が教育功労章を受賞



東北大学名誉教授野村正氏が2013年3月、フランス大使館より教育功労章オフィシエに叙されました。野村氏は教育者、研究者として素晴らしい業績を残してきました。今回の叙勲は長年にわたり、専門分野を超えて、日仏交流の推進に努め、大きな成果をあげた野村氏を称えるためのものです。養殖、軟体動物生物学、海洋生物化学をはじめとする海洋科学技術分野での活動を通し、野村氏は日仏交流に参加、支援するようになりました。フランス語を学んでいた野村氏は、フランス政府給費留学生試験に合格しフランスに留学。フランス国立自然史博物館のモリス・フォンテーヌ教授のもとで魚類のエストロゲンホルモンの研究をし、続いてパリ大学医学部のセダール教授のもとでも研究をしました。その後ブルターニュ大学の客員助教授としてブルターニュ地方に滞在しました。

フランスと日本の両日仏海洋学会が開催する日仏シンポジウムのほとんどに参加しましたが、単なる参加者ではなく、主催者の一人でもありました。このような科学的催しには野村氏のフランス語の知識が大いに役立ちました。新しい道を切り開きつつ、海産動物の生物化学を革新した野村氏は、一時代を画した著書「海洋生物の生理活性物質」を物にしますが、この中で取り上げられたテーマの多くは現在でも通ずるものです。牡蠣が大量死滅の危機にあった時、日仏の牡蠣個体群の交換に尽力しました。また大学の研究所やフランス海洋開発研究所（IFREMER）のラボラトリーと連携し3種のフランス牡蠣の研究に力を入れました。来日したフランスの若手研究者の多くが、公私にわたり野村氏のお世話になり、その優しく魅力的な人柄は多くの人が認めるところです。また沿岸整備にも関心を持ち、フランス滞在中にタラソセラピーを知り、その技術を日本に広めたパイオニアとなりました。

（在日フランス大使館ホームページより抜粋）

第15回日仏海洋学シンポジウム報告

小松 輝久

第15回日仏海洋学シンポジウムが、“Marine Productivity: perturbations and resilience of socio-ecosystems”というテーマで、2013年10月17-18日のBoulogne-sur-Merおよび10月21-22日のMarseilleの2都市を会場として開催され、いずれも多数の講演と参加（日本側：23名、フランス側：約60名）、活発な質疑があり、大成功を収めた。Marseilleにおけるシンポジウムは、IMPAC3（International Marine Protected Area Congress 第3回大会）のサイドイベントとして企画された。以下に2会場でのシンポジウムの概要を報告する。

(1) Boulogne-sur-Mer

Boulogne-sur-Merは、フランス第1位の水産物の水揚げを誇る漁港の都市であり、英仏海峡と北海を対象とするIFREMERの漁業研究所がある。IFREMERの世話によりBoulogne-sur-Merの商工会議所を会場に、テーマに沿った具体的例を取り上げる、19題の口頭発表と18題のポスター発表が行われた（文末のプログラム参照）。1日目（17日）午前Session 1：Process Studiesで6題、午後Session 2：Ecosystem Modellingをテーマに6題の口頭発表があった。最後に、今回の口頭発表のまとめを行った。夕刻からは会場近くの水族館Nausicaá内で歓迎レセプションが行なわれた。

2日目（18日）は、早朝に水産食品加工場を見学後、Session 3：Integrated Managementをテーマに7題の口頭発表が行なわれ、その後、水族館Nausicaá内にあるIFREMERの造波水槽施設の見学を行った。ポスターセッションは、各セッションの間のコーヒブレイクと昼食時を利用して行われた。

(2) Marseille

テーマについて普遍化するための理論的、思想的な発表を集め、4つのセッションで合計17の口頭発表が行われた。1日目（21日）には、Aix-Marseille Université本部の会議場においてSession 4：Status and Evolution of MPAsで3題、Session 5：Natural Perturbations and Impactsで5題、Session 6：Anthropogenic perturbations, adaptation and impactsで5題、2日目（22日）には、Hotel Novotel Vieux Port Marseilleの会議室においてSession 7：Integrated management and mitigation toolsで4題の講演が行われた。1日目のシンポジウム後に、海上レストランで歓迎の夕食会が開かれ、駐マルセイユ日本領事館領事夫妻ご臨席のもと、日本人参加者が全員招待された。2日目のシンポジウムでは、岡山県日生市の里海の取り組みについての発表とY. Honoques氏の関連した発表が特別に追加され、NHKパリ支局から取材班が派遣され、これらの発表を記録した。2014年1月に里海についての特集番組として放送されるとのことであった。最後に、Round Tableで総括の議論を行った。昼食をロビーにおいてとり、散会となった。

今回のシンポジウムを総括すると、日本人の発表が多く、また、活発な質疑を通して、お互いに新たな情報を得ることができ、大変有意義なシンポジウムであったと感じた。

シンポジウムプログラム

Session 1: Process Studies

- 1: Diffusion processes of radioactive materials in ecosystems of coastal areas off Fukushima. H. Arakawa, T. Tokai, Y. Miyamoto, K. Uchida, S. Akiyama, A. Matsumoto, Y. Agatsuma, S. Katayama, M. Aoki, I. Matsumoto and N. Hirakawa
- 2: Antibiotics and antibiotic-resistant fecal bacteria in water from the contamination source to the estuary: impact and / or resilience? F. Petit, T. Berthe, K. Oberlé, E. Denamur, O. Clermont, R. Leclercq, V. Cattoir and H. Budzinski
- 3: Fate and effects of long-term exposures to PCB and PBDE mixtures on fish physiology under experimental conditions and in the wild. ML Bégout, C Munsch, X. Cousin, F. Akcha, V. Buchet, M. Cannas, T. Daouk, M. Eichinger, F. Hénaff, N. Imbert, C. Lefrançois, S. Péan, O. Lepape, D Mazurais, J. Morin, S. Rochette, C. Tixier, H. Thomas Guyon, N. Wessel, J. Zambonino and V. Loizeau
- 4: Harmful shell borers, *Polydora* species (Polychaeta: Spionidae) from East Asia morphology, molecular sequence analysis, and shell infestation condition. W. Sato-Okoshi, H. Abe, K. Okoshi, W. Teramoto, B. -S. Koh, Y. -H. Kim, J. -S. Hong, J. -Y. Li
- 5: On the effects of hydrocarbon contamination on zooplankton behaviour: a French-Japanese approach. L. Seuront
- 6: Impact of repeating massive earthquakes on intertidal mollusks. K. Okoshi

Session 2: Ecosystem Modelling

- 7: Physical and biological perturbations linked to marine aggregate extraction in the eastern Channel. D. Michel and L. Robert
- 8: Use of bio-fluorescent characteristics for ecosystem monitoring on hydrothermal deposits. M. Sasano, Y. Nakajima, J. Yamamoto and Y. Furushima
- 9: Indicators for ecosystem based management: methods and applications. V. Trenkel, P. Lorance, S. Mahevas and M. -J. Rochet
- 10: Impacts of the huge tsunami on 11 March 2011 to a nearshore ecosystem in Sanriku Coast. T. Komatsu, T. Ohtaki, S. Sawayama, M. Hamana, S. Sakamoto, S. Sasa, G. Terauchi and R. Tsujimoto
- 11: Development of end-to-end models to describe the dynamics of exploited marine ecosystems in the Eastern Channel. P. Marchal, R. Girardin and M. Travers-Trolet
- 12: Rising to the challenge of reconstructing the coastal fisheries environment following the massive tsunami in Japan: the national 10-year “Tohoku Ecosystem-Associated Marine Sciences (TEAMS)” project. T. Nakano

Session 3: Integrated Management

- 13: The continuum Estuary-Bay of Seine: the need to an ecosystem-based management. J. -C. Dauvin
- 14: Degradation of fishery work population in Japan and the possibility of its recovery in the ergonomic perspective. H. Takahashi

- 15: The Channel Arena: An integrated study for a better understanding and management of the English Channel Ecosystem. A. Carpentier and P. Marchal
- 16: Reviving the Seto Inland Sea, Japan: Applying the principles of Satoumi for marine ranching projects in Okayama. T. Tanaka
- 17: From Global to Local: a comparative ocean and coastal Management approach in Western Europe, France, and East Asia, Japan. Y. Henocque
- 18: Today's aquaculture and capture fisheries in Japan. T. Yamane
- 19: A participatory integrated assessment of sea grass meadows ecosystem services in the Gulf of Morbihan. D. Bailly

Session 4: Status and Evolution of MPAs

- 20: Regulation and management of marine protected areas in Japan. N. Amako
- 21: Limits of the concept of Marine Protected Area: Adaptation of the populations and their professions in the different types of MPAs. H. Ceccaldi
- 22: A Consideration of MPA management from the perspective of Japan's experiences and lessons learned. S. Seino

Session 5: Natural Perturbations and Impacts

- 23: *Oithona davisae*, the most dominant copepod in Tokyo Bay, a highly eutrophicated embayment: Why are they so dominant? Y. Tanaka and T. Akiba
- 24: Ecosystem services of mangrove forests with reference to the transportation of organic materials to coral reefs: A case study in Palau for the MPA management. M. Tsuchiya, I. Mimura, Y. Yano, N. W. Oldiais, Y. Glibuu, Y. Fujita and K. Miyakuni
- 25: Health and degradation of coral reefs: Time scale - Natural and anthropogenic perturbations at global, regional and local scales. B. Salvat
- 26: Impacts of the 2011 mega-earthquake and tsunami on Ezo abalone *Haliotis discus hannai* at Iwaisaki, Miyagi, Japan. H. Takami and H. Nakaie
- 27: The influence of the March 11, 2011 tsunami on the environment and the phytoplankton community in Matsushima Bay. Y. Okumura, H. Ota, Y. Masuda and N. Suzuki

Session 6: Anthropogenic Perturbations, Adaptations and Impacts

- 28: Changes, adaptations and resilience: the case of French oyster farming. C. Mariojouis and J. Prou
- 29: Oyster farming in Tohoku: post-tsunami restoration and technical adaptation of culture systems. Y. Koike
- 30: Marine Litter along European coasts: sources, distribution, impacts and European policy. F. Galgani
- 31: Mapping the state of the marine ecosystem after the Great East Japan Earthquake 2011. T. Yamakita, H. Yamamoto, Y. Yokoyama, I. Sakamoto, Y. Fujiwara, S. Tsuchida, M. Kawato, D. Lindsay, T. Kasaya and H. Kitazato
- 32: A Subject of the Chlorine Management at a Thermal Power Plant on the Northwest Pacific Ocean in Japan. T. Iibuchi, S. Kobayashi, S. Nanjou, K. Satou, T. Hara and M. Kiyono

Session 7: Integration Management and mitigations tools

- 33 : Application of advanced technology to integrated coastal management – Assessment of fish habitat use by through bio-logging. H. Tanoue, T. Komatsu, S. Gonzalvo, A. Hamano and N. Miyazaki
- 34: Recent topical studies about artificial fish reef utilizations in Japan. H. Takahashi and Y. Ito
- 35: How to size “fair” compensatory mitigation for fisheries resources: HEA scoring method applied in off shore wind mill project. S. Pioch, J. Hay, A. Bas, H. Levrel, A. -C. Vayssiere and C. Kermagoret
- 36: *Sato-umi*, a new approach of marine protected area cooperated with local people. T. Komatsu and T. Yanagi

Poster presentation list

- 1. A scientific cluster: SIEGMA (Monitoring of impacts of marine aggregate extraction): a tool for regional governance in the Eastern Channel. JP. Delpech, B. Ernande and P. Marchal
- 2. Toward a dynamical approach for systematic conservation planning of Eastern English Channel fisheries. Y. Reecht, S. Vaz, S. Mahevas and P. Marchal
- 3. Modelling the relative impacts of traditional harvesting and habitat degradation on the population dynamics of Dugongs (*Dugong dugon*) in the Moreton Bay (Australia). M. Savina and P. Bayliss
- 4. A spatially-explicit MSE framework for the assessment of management measures from the new Common Fisheries Policy: an application to the Eastern Channel mixed fisheries. S. Lehuta, P. Marchal and Y. Vermard
- 5. The protection and management of offshore sea-hill fishing ground: the Hachirigase hill case study. A. Hamano, H. Tanoue, S. Shinagawa, T. Komatsu, T. Nakamura, N. Murase and T. Fujiwara
- 6. Measurements of bedload transport in the English Channel using DySPI system. M. Durafour, A. Jarno, S. Le Bot, O. Blanpain, R. Lafite and F. Marin
- 7. Morphosedimentary mobility in sandy habitats on inner macrotidal continental shelf (Eastern English Channel). Y. Ferret, P. -A Duclos, S. Le Bot, M. Desprez and R. Lafite
- 8. Offshore/coastline sedimentary transfers in a macrotidal area (Eastern English Channel). Case of the Baie de Somme. M. Charlotte, S. Le Bot, R. Lafite and S. Costa
- 9. Contamination of seabed sediments and organisms by radioactive cesium in the coastal area of southern Fukushima. H. Myouse, A. Matsumoto, N. Hirakawa and H. Arakawa
- 10. Coral observation by the boat-based fluorescence imaging lidar. M. Sasano, M. Imasato, H. Yamano and H. Oguma
- 11. Development of an analysis system for matter contributing to turbidity using a three wavelength in situ beam transmissometer. M. Narita, T. Itagaki, Y. Yoshie-Stark and H. Arakawa
- 12. Three-dimensional monitoring of Pacific blue fin tuna cultured in an offshore net cage using a digital stereo camera system. S. Torisawa, M. Morimoto, K. Komeyama, T. Takagi and

T. Yamane

13. Satellite tagging of blue sharks (*Prionace glauca*) in the Gulf of Lions: depth behaviour, temperature experience and movements: Preliminary results. F. Poisson, T. Mitsunaga, T. Kojima, B. Séret, Demarcp, S. Torisawa, A. Banègue and J. M. Groul
14. Effect of moderate or severe acute stressor on expressions of growth-related genes in cultured fish. T. Nakano, T. Yamaguchi, M. Sato and R. H. Devlin
15. Embryological development of *Pinna nobilis* Linnaeus 1758 in controlled conditions. S. Trigos, N. Vicente, J. R. García-March, J. Torres and J. Tena
16. Environmental impacts of fish farming in floating cages in coastal seawaters and coral reef lagoons. B. Thomassin
17. Ecosystem-versus species-based approach of the human impact on the Mediterranean seagrass *Posidonia oceanica*. C. F. Boudouresque, S. Personnic, P. Astruch, E. Ballesteros, D. Bellan-Santini, P. Bonhomme, D. Botha, E. Feunteun, M. Harmelin-Vivien, G. Pergent, C. Pergent-Martini, J. Pastor, J. -C. Poggiale, F. Renaud, T. Thibaut and S. Ruitton
18. La Pôle Mer Méditerranée. G. Herrouin

学 会 記 事

1. 6月22日(土)日仏会館(東京都恵比寿)において2013年度総会を開催した。

2013年度(第54回)日仏海洋学会総会 議事録

日 時: 2013年6月22日(土)15時00分~15時40分

場 所: 公益財団法人 日仏会館 会議室501号室

議事に先立ち評議員会の資格確認を行った。出席73名(出席23名,委任状による出席50名)により,本評議員会の成立(会員数136名の1/6の出席)を確認した。

議 長: 小松会長

第1号議案 2012年度事業報告

1) 庶務関係報告(荒川庶務幹事)

会員移動状況として,2012年度の会員数は+7名増加した。

2) 活動状況報告(荒川庶務幹事)

①評議員会1回(2012/6/10日仏会館),幹事会4回(2012/4/17日仏会館,2012/5/25東京海洋大学,2012/9/6東京海洋大学,2012/12/14東京海洋大学),総会1回(2012/6/10日仏会館),学術研究発表会1回(2012/6/10日仏会館)の開催。

②「三陸の沿岸漁業の復興を目指す日仏シンポジウム 特に震災からのカキ養殖の復興に向けて」(2012/10/4東北区水産研究所),東北マリンサイエンスとの懇談会,東北大学農学研究科長との懇談会(2012/10/5東北大学),講演会「日仏カキ文化:三陸の復興を目指して」(2012/10/6日仏会館)の開催。

③論文賞2件の授与

④学会賞委員半数改選

⑤編集関係報告(吉田編集委員長)

学会誌「La mer」の編集状況と50(1-4)発行した。各報告と質疑ののち,第1号議案は承認された。

第2号議案 2012年度収支決算報告および監査報告

①会計(代理荒川)より資料1に従って,2012年度収支決算が報告された。

②監査報告(代理荒川)が行なわれ,会計が適正であることが報告された。

質疑ののち,第2号議案は承認された。

第3号議案 2013年度事業案(荒川庶務幹事)

①総 会1回,学術研究発表会1回,評議員会1回,幹事会3回の開催

②学会賞,論文賞の候補者の推薦と授与

③会長選挙,評議員選挙,学会賞委員選挙(半数改選)

④学会誌「La mer」51巻1-4号 発刊予定であること,今年度学会誌「La mer」51巻1-2号が発刊済みであることが報告された。(吉田編集委員長)

⑤第15回日仏海洋学シンポジウム共催。

各項目の説明と質疑ののち,第3号議案は承認された。第4号議案 2013年度予算案(荒川庶務幹事)

2013年予算案が資料2に従って説明された。審議ののち,第4号議案は承認された。

第5号議案 2012年度-2013年度役員,評議員,学会賞推薦委員(荒川庶務幹事)

2013年度は学会賞選考委員の半数改選(2013年度-2014年度賞委員(5名))のみ行われた。

一部誤字修正ののち,第5号議案は承認された。

第6号議案 投稿規定の改訂について(荒川庶務幹事)

投稿規定9条の削除に伴う改訂を行う提案がなされた。(資料4)

①現行第9条で,1編あたり5万円の論文掲載料を定めているが,掲載料を徴収しないこととする。(第9項全文削除)

②新第9条では印刷ページチャージを3000円/頁とする。

③新第10条では,別刷り50部の無料提供を取りやめる。(すべて有料とする。)

上の三件が提案され,カラーページの料金,PDFの著者への配布,その公開規定を今後執行部で検討することとして,三案を承認した。6月22日から施行する。

第7号議案 学会ロゴの文字について(小松会長)

①フランス(日仏海洋学会)より,日仏海洋学会のロゴに文字を入れ,シンポジウムで使用したい旨の要請に対し,現学会ロゴのデザインを変えずに名称を加筆することとした。詳細案は執行部で検討することを承認した。

報告事項

①第15回日仏海洋学シンポジウム開催(2013/10/18-23,フランスにて)

会員メーリングリストでサイト告知,水産学会や海洋学会にも告知。

発表者はサイト参照,要旨は2013年7月末締切。

日仏海洋学会ホームページに英語版と仏語版のリンクを貼る。(内田広報幹事へ依頼)

②野村正名誉会員(東北大学名誉教授)がフランスパルム・アカデミック賞(教育功労章)ご受賞(中野俊樹会員より報告)仏大使館ホームページの詳細内容を学会誌「La mer」に転載予定。事務局で転載許可を得る。

2. 6月22日(土)日仏会館(東京都恵比寿)において2013年度学術研究発表会を開催した。

日 時：2013年6月22日(土) 10時00分～15時00分

場 所：日仏会館 501 会議室

プログラムは以下の通り。

10:00～10:45 座長 飯淵敏夫(海生研)

①福島県いわき市沿岸における海底堆積粒子の放射性セシウム濃度

○明瀬太志¹, 松本陽¹, 平川直人², 荒川久幸³
(1: 海洋大, 2: 福島県水試)

②東日本大震災後の気仙沼湾海底泥の油分

○中村真由子¹, 中村宏¹, 荒川久幸¹, 山川紘¹
(1: 海洋大)

③震災が仙台湾の植物プランクトン多様性に及ぼした影響

○奥村裕¹, 増田義男², 太田裕達², 鈴木矩晃³, 太田尚志⁴, 一見和彦⁵

(1: 水研セ東北水研, 2: 宮城水技セ, 3: 宮城県水産漁港部, 4: 石巻専修大, 5: 香川大)

10:45～11:30 座長 北出裕二郎(海洋大)

④高精度ポータブル溶存酸素センサーの開発

○内田裕¹, 長澤泰宏², 高井真一², 光田均³, 村田昌彦¹
(1: JAMSTEC・RIGC, 2: JFE アドバンテック, 3: 環境総合テクノス)

⑤三陸沖における乱流微細構造の観測

○梶浦俊樹¹, 中野知香¹, 嶋田啓資¹, 根本雅生¹, 吉田次郎¹
(1: 海洋大)

⑥Study on the mixing processes in the western North Pacific Ocean

○Haruka Nakano, Keishi Shimada and Jiro Yoshida (TUMSAT)

13:30～14:15 座長 中野俊樹(東北大)

⑦熱帯浅海域における底生微細藻類の重要性

○下田 徹(国際農林水産業研究センター)

⑧アイゴ稚魚の海藻と動物性餌料に対する摂食選択性

○柴田玲奈¹, 片山知史²・荒川久幸³・齊藤 肇¹
(1: (独)水研セ, 2: 東北大, 3: 海洋大)

⑨オウギガニヤドリムシが宿主に与える影響

○渡邊隆司¹, 浜崎活幸¹, 横田賢史¹, Carlos A. Strüssmann¹, 渡邊精一¹(海洋大)

14:15～15:00 座長 小松輝久(東大大海研)

⑩Escape behavior of *Oithona davisae* against pulsed suction flow

○Shujuan Xia¹, Tatsuro Akiba², Yuji Tanaka¹
(1: TUMSAT, 2: National Institute of AIST)

⑪*Oithona davisae* の捕食遊泳行動の定量化に関する研究

○程婉婷¹, 秋葉龍郎², 田中祐志¹

(1: 東京海洋大学, 2: 産総研/東京海洋大学)

⑫Behavioral adaption of *Oithona davisae* to a

constant suction flow

○B.B. Liu¹, T. Akiba², Y. Tanaka¹

(1: TUMSAT, 2: National Institute of AIST)

15:00～15:45 総会

15:45～15:50 2013年度日仏海洋学会賞・論文賞授与式

≪学会賞受賞≫ 神田穰太会員(東京海洋大学)

「海洋における生物地球化学循環に関する研究」

≪論文賞受賞≫ 中野俊樹会員(東北大学)

「Daily expression patterns of growth-related genes in growth hormone transgenic coho salmon, *Oncorhynchus kisutch*」49巻3-4号, 111-117, 2011

≪論文賞受賞≫ 内田裕会員(独立行政法人海洋研究開発機構)

「Absolute salinity measurements of standard seawaters for conductivity and nutrients」49巻3-4号, 119-126, 2011

15:50～16:30 学会賞受賞記念講演

神田穰太会員(東京海洋大学)「海洋における生物地球化学循環に関する研究」

17:00～19:00 懇親会(魚匠 恵比寿ガーデンプレイスにて)

3. 新入会員

氏名	所属	紹介者
國分 優孝	東京大学大気海洋研究所	小松輝久
高橋 秀行	独立行政法人 水産総合研究センター	小松輝久
渡邊 隆司	東京海洋大学 集団生物学研究室	渡邊精一
和 吾郎	株式会社 西日本科学技術研究所	木下 泉
脇田 昌英	独立行政法人 海洋研究開発機構 むつ研究所	内田 裕
戸口 和貴	東京海洋大学 環境測定学研究室	荒川久幸
中村 真由子	東京海洋大学 環境測定学研究室	荒川久幸
岡本 峰雄	東京海洋大学 環境テクノロジー学講座	小松輝久
田 關	東京海洋大学 環境テクノロジー学講座	小松輝久
岡安 章夫	東京海洋大学 環境テクノロジー学講座	吉田次郎

4. 退会

渡邊隼人, 小山尚之, 永延幹男, 松生治, Andreas A. Hutahaeta, 和田明, 謝旭暉, (賛助) テラ株式会社 中川一郎, 永田豊, 王歆

5. 所属および住所変更

氏名	新しい所属先
田上英明	〒759-6595 山口県下関市永田本町 2-7-1 (独)水産大学校
下田 徹	〒305-8686 茨城県つくば市オオワシ 1-1 国際農林水産業研究センター水産領域
小林 裕	〒295-0024 千葉県南房総市千倉町平磯 2492 千葉県水産総合センター資源研究室 上席研究員
谷口 旭	〒103-0012 東京都中央区日本橋堀留町 1 丁目 3-17 三洋テクノマリン株式会社 生物生態研究所 所長
黒田 寛	〒085-0802 北海道釧路市桂恋 116 (独)水産総合研究センター 北海道区水産研究所

No.49-50

KOREA INSTITUTE OF OCEAN SCIENCE&TECHNOLOGY; Annual Report2012
PROGRESS IN FISHERY SCIENCES (中国水産学会);
第 34 卷 Vol.34 第 1 期 No.1, 第 3 期 No.3
中国海洋大学学报; 第 43 卷第 7 期-第 43 卷第 8 期

6. 寄贈図書および資料

Ship & Ocean Newsletter (海洋政策研究財団);
No.302-310
Ocean Newsletter (海洋政策研究財団); No.311-316
海洋政策研究財団; 海洋白書 2013 日本の動き 世界の動き
Ocean Breeze (東京大学大気海洋研究所); 第 12 号
東京大学大気海洋研究所 50 年史 1962-2012
東京大学大気海洋研究所要覧・年報 2013
FRAN NEWS (水産総合研究センター); No.34-36
東海大学海洋研究所研究報告; 第 34 号
東海大学紀要海洋学部; 2013 Vol.10 No.3
神奈川県立博物館研究報告自然科学 (神奈川県立生命の星・地球博物館); 42 号
増養殖研究レター (水産総合研究センター); 第 3 号
RESTEC News (一般財団法人リモート・センシング技術センター); 第 2 号-第 3 号
農工研ニュース (農村工学研究所); No.84-86
農村工学研究所報告 (農村工学研究所); 第 52 号
農村工学研究所成果情報・地域資源活用研究他場所成果情報 (農村工学研究所); 平成 24 年度
なつしま (JAMSTEC); 323-330
国立科学博物館研究報告 A 類 (動物学); 第 39 巻第 1-2 号, 増補 7
独立行政法人 産業技術総合研究所 地質調査情報センター 地質・衛星情報アーカイブ室; 野間岬沖表層堆積図 (CD-R), 奥尻島北方表層堆積図 (CD-R), 日高舟状海盆表層堆積図 (CD-R)
水産技術 (独立行政法人水産総合研究センター); 第 5 巻第 2 号
水産総合研究センター研究報告; No.37
PROGRESS IN FISHERY SCIENCES (中国水産学会);
第 34 巻 1
Techno-ocean News (テクノオーシャンネットワーク);

(資料1)

平成24年度収支決算

収入の部				
費目	予算額(A)	決算額(B)	増減(B)-(A)	摘要
前年度繰越金	1,053,229	1,053,229	0	
正会員会費	936,000	720,000	-216,000	8,000円×90名
特別会員	60,000	36,000	-24,000	6,000円×6名
学生会員会費	16,000	12,000	-4,000	4,000円×3名
賛助会員会費	130,000	110,000	-20,000	7社(10,000円×11口)
学会誌売上金	150,000	222,288	72,288	
広告費	20,000	20,000	0	
別刷り代等	500,000	49,700	-450,300	別刷り, 超過頁, カラー印刷費
掲載料	700,000	350,000	-350,000	50,000円×7編
雑収入	100,000	88,268	-11,732	学術著作権使用料他
寄付金	0	100,000	100,000	笹川財団
収入合計	3,665,229	2,761,485	-903,744	

支出の部				
費目	予算額(A)	決算額(B)	増減(B)-(A)	摘要
学会誌印刷費	1,800,000	807,170	-992,830	50巻1-2号 50巻3-4号
送料・通信費	100,000	78,595	-21,405	
事務費	700,000	532,373	-167,627	人件費, 事務用品, 事務員交通費他
交通費	20,000	6,060	-13,940	日仏会館
会議費	15,000	2,262	-12,738	
学会賞経費	50,000	17,336	-32,664	賞状他
50周年記念事業	0	0	0	
雑費	25,000	25,060	60	振込み手数料他
次年度繰越	955,229	1,292,629	337,400	
支出合計	3,665,229	2,761,485	-903,744	

(資料2)

平成 25 年度予算 (案)

収入の部				
費 目	25 年度予算(A)	24 年度予算(B)	増減(A)-(B)	摘 要
前年度繰越金	1,292,629	1,053,229	239,400	
正会員会費	984,000	936,000	48,000	123 名 (8,000 円×123 名)
特別会員	72,000	60,000	12,000	12 名 (6,000 円×12 名)
学生会員会費	4,000	16,000	-12,000	1 名 (4,000 円×1 名)
賛助会員会費	80,000	130,000	-50,000	8 社 (10,000 円×8 口)
学会誌売上金	150,000	150,000	0	
広告費	20,000	20,000	0	※51 (1.2) は広告掲載無し
別刷り代等	200,000	500,000	-300,000	別刷り, 超過頁, カラー印刷費
掲載料	500,000	700,000	-200,000	10 編×50,000 円
雑収入	100,000	100,000	0	
寄付金	1	0	1	
収入合計	3,402,630	3,665,229	-262,599	

支出の部				
費 目	25 年度予算(A)	24 年度予算(B)	増減(A)-(B)	摘 要
学会誌印刷費	1,350,000	1,800,000	-450,000	3 冊×450,000 円
送料・通信費	100,000	100,000	0	
事務費	700,000	700,000	0	人件費, 事務用品, 事務員交通費他
交通費	20,000	20,000	0	
会議費	5,000	15,000	-10,000	
学会賞経費	30,000	50,000	-20,000	賞状他
雑費	25,000	25,000	0	振込み手数料他
次年度繰越 (予備費)	1,172,630	955,229	217,401	
支出合計	3,402,630	3,665,229	-262,599	

日仏海洋学会誌「うみ」投稿規定

1. 「うみ」(欧文誌名 La mer)は日仏海洋学会の機関誌として、和文または欧文により、海洋学および水産学ならびにそれらの関連分野の研究成果を発表する学術雑誌であり、同時に研究者間の情報交換の役割をもつことを目的としている。
2. 「うみ」は、原則として年4回発行され、投稿(依頼原稿を含む)による原著論文、原著短報、総説、学術資料、書評その他を、編集委員会の審査により掲載する。これらの著作権は日仏海洋学会に帰属する。
3. 投稿は日仏海洋学会会員、および日仏海洋学会正会員に準ずる非会員からとする。共著者に会員を含む場合は会員からの投稿とみなす。
4. 用語は日、仏、英3カ国語のいずれかとする。ただし、表および図の説明の用語は仏文または英文に限る。原著論文には約200語の英文または仏文の要旨を別紙として必ず添える。なお、欧文論文には約500字の和文要旨も添える。ただし、日本語圏外からの投稿の和文要旨については編集委員会の責任とする。
5. 原稿はすべてワードプロセッサを用いて作成し、本文・原図とも2通(正、副各1通)ずつとする。副本は複写でよい。本文原稿はすべてA4判とし、白紙にダブル・スペース(和文ワープロでは相当間隔)で記入する。表原稿および図の説明原稿は本文原稿とは別紙とする。
6. 投稿原稿の体裁形式は「うみ」最近号掲載論文のそれに従う。著者名は略記しない。記号略号の表記は編集委員会の基準に従う。引用文献の表示形式は、雑誌論文、単行本分載論文(単行本の一部引用も含む)、単行本などの別による基準に従う。
7. 原図は版下用として鮮明で、縮尺(版幅または1/2版幅)に耐えられるものとする。
8. 初稿に限り著者の校正を受ける。
9. 会員に対しては10印刷ページまでの掲載を3,000円/ページとする。会員の投稿で上記限度を超える分および非会員投稿(依頼原稿を除く)の印刷実費はすべて著者負担(1万円/ページ)とする。ただし、カラー印刷を含む場合には、別に所定の費用(9万円/ページ)を著者(会員、非会員とも)負担とする。
10. 別刷りは50部単位で有料で作製される。別刷り請求用紙は初稿校正と同時に送付される。
11. 原稿の送り先は下記の通りとする。なお著者(共著の場合は代表者)連絡先のe-mailアドレス並びにFAX番号を付けることとする。

〒108-8477 東京都港区港南4-5-7

東京海洋大学海洋科学部海洋環境学科(吉田 次郎気付)

日仏海洋学会編集委員会

e-mail: jjiroy@kaiyodai.ac.jp

執筆要領

1. 原稿

- (1) 和文原稿の場合:ワードプロセッサを使用し、A4版の用紙におよそ横30字、縦25行を目安に作成すること。
- (2) 欧文原稿の場合:ワードプロセッサを使用し、A4版の用紙にダブルスペース25行でタイプし、十分な英文添削または仏文添削を経て提出すること。
- (3) 和文原稿、欧文原稿いずれの場合も、要旨、表原稿および図版説明原稿はそれぞれ本文原稿とは別紙とする。
- (4) 最終原稿提出の際に、印刷原稿とともに原稿、表、図版が保存されたフロッピーディスク、CD-R/RW、MO等での提出を依頼する。この場合、原稿はMicrosoft WORD、Just System 一太郎、PDFの原稿のみに限る。また、表、図版はこれら原稿ファイルの中に取り込むか、bmp、jpg等の一般的な画像ファイルに保存したものに限る。なお、電子媒体は返却しない。

2. 原稿記載の順序

- (1) 原著(和文原稿):原稿の第1ページ目に表題、著者名、研究の行われた所属機関、所在地、郵便番号を和文

と英文で記載する。研究終了後所属機関が変わった場合は現所属機関も記載する。連絡先（共著の場合は連絡先とする著者を明示する）の住所、電話番号、ファックス番号、E-mail アドレスも記す。最後にキーワード（4語以内）、ランニングヘッドを英文で記載すること。第2ページ目に欧文要旨（欧文表題、著者名を含む）を200語以内で記す。本文は第3ページ目から、「緒言」「資料」「結果」「考察」「謝辞」「文献」「図版の説明」などの章立てあるいは項目で順に記載する。基本的には最近号掲載論文の体裁形式を参考にして投稿原稿を作成すること。原稿には通しのページ番号を記入すること。

- (2) 原著（欧文原稿）：原稿の第1ページ目に表題、著者名、研究の行われた所属機関、所在地、郵便番号を記載する。研究終了後所属機関が変わった場合は現所属機関も記載する。最後にキーワード（4語以内）、ランニングヘッドを記載すること。第2ページ目に欧文要旨（欧文表題、著者名を含む）を200語以内で記す。本文は第3ページ目からとする。「Introduction」「Data」「Results」「Discussion」「Acknowledgement」「References」「Figure Caption」などの章立てで順に記載する。基本的には投稿原稿の体裁形式は最近号掲載論文を参考にして作成すること。最終ページに和文の表題、著者名、連絡先著者住所、電話番号、ファックス番号、E-mail アドレスおよび約500字以内の和文要旨を添える。原稿には通しのページ番号を記入すること。
- (3) 原著短報、総説：和文ならびに欧文原稿とも原著論文に準ずる。
- (4) 学術資料、書評：特に記載に関する規定はないが、すでに掲載されたものを参考にすること。

3. 活字の指定

原稿での活字は10.5 pt～12 ptを目安に設定し、英数字は半角フォントを用いること。学名はイタリック、和文原稿での動植物名はカタカナとすること。句読点は（。）および（，）とするが、文献リストでは（.）および（,）を用いること。章節の題目、謝辞、文献などの項目はボールドまたはゴシックとする。

4. 文献

文献は本文および図表に引用されたもののすべてを記載しなければならない。和文論文、欧文論文共に筆頭著者のアルファベット順（同一著者については、単著、共著の順とし、それぞれ発表年の古い順）にまとめ、以下の例に従って記載する。

(1) 論文の場合

有賀祐勝, 前川行幸, 横浜康継 (1996): 下田湾におけるアラメ群落構造の経年変化. *うみ*, **34**, 45–52.

YANAGI, T. T. TAKAO and A. MORIMOTO (1997): Co-tidal and co-range charts in the South China Sea derived from satellite altimetry data. *La mer*, **35**, 85–93.

(2) 単行本分載論文（単行本の一部引用の場合）

村野正昭 (1974): あみ類と近底層プランクトン. *海洋学講座 10 海洋プランクトン* (丸茂隆三編), 東京大学出版会, 東京, p.111–128.

WYNNE, M. J. (1981): Pheophyta: Morphology and classification. *In the Biology of Seaweeds*. LOBBAN, C. S. and M. J. WYNNE (eds.), Blackwell Science, Oxford, p.52–85.

(3) 単行本の場合

柳 哲雄 (1989): 沿岸海洋学—海の中でのものはどう動くか—. 恒星社厚生閣, 東京, 154pp.

SVERDRUP, H. U., M. W. JOHNSON and R. H. FLEMING (1942): *The Oceans: Their Physics, Chemistry and General Biology*. Prentice-Hall, Englewood Cliffs, New York, 1087pp.

(4) 本文中での文献の引用

本文中での文献の引用方法はすでに発行された雑誌を参考にすが、基本的には次の形式に従う。

① GREVE and PARSONS (1977)

② (AVIAN and SANDRIN, 1988),

③ YANAGI *et al.* (1997) は…… (3名以上の共著の場合)

④ ……示されている (例えば, YANAGI *et al.*, 1997) (3名以上の共著の場合)

5. 図, 表および写真

- (1) 図, 表および写真とその説明はすべて英文または仏文を用いる。
- (2) 図, 表はそのまま写真製版用の草稿となるような明瞭なもので, A4 版の上質紙に作製したもの(写真は, 正原稿についてもオリジナルとは別に A4 版の用紙にコピーしておくことが望ましい)のみを受け付ける。カラー図を希望する場合はその旨明記する。この場合, 別に所定の費用を著者負担とする。
- (3) 写真は光沢平滑印画紙に鮮明に焼き付けたものを受け付ける。カラー写真の印刷を希望する場合はその旨明記する。この場合, 別に所定の費用を著者負担とする。
- (4) 図, 表および写真は刷り上がり時に最大横が 14 cm, 縦が 20 cm (説明文を含む) 以内であることを考慮して作製すること。
- (5) 図(写真を含む)には, Fig. 1, Fig. 2, ……のように通し番号をつけ, 一つの図中に複数の図を含む場合は Fig. 3 (a), Fig. 3 (b), ……のように指定する。本文中での引用は和文原稿の場合も「Fig. 1 にみられるように……」のようにすること。
- (6) 表には, 表題の次(表の上のスペース)に説明をつけ, 表ごとに別紙とし, Table 1, Table 2, ……のように通し番号をつけること。
- (7) 図, 表および写真は 1 枚ごとに著者名, 通し番号をつけること。また, 本文中での挿入箇所を最終提出原稿の該当箇所右欄外に朱書きすること。
- (8) 図, 写真の説明は別紙にまとめること。
- (9) 地図にはかならず方位と縮尺または緯度, 経度を入れること。

6. 単位系

原則として SI 単位を用いること。塩分は実用塩分単位 (Practical Salinity Unit : psu または PSU) を用いる場合は単位なしとする。

賛 助 会 員

J F E アドバンテック株式会社	兵庫県神戸市西区井吹台東町 7-2-3
株式会社 イーエムエス	兵庫県神戸市中央区東川崎町 1-3-3 神戸ハーバーランドセンタービル 13F
有限会社 英和出版印刷社	東京都北区中里 2-14-8 シャンボール駒込 101
信幸建設株式会社	東京都千代田区神田司町 2-2-7 パークサイド 18 階
ケー・エンジニアリング株式会社	東京都台東区浅草橋 5-14-10
公益財団法人海洋生物環境研究所	東京都新宿区山吹町 347 藤和江戸川橋ビル 7 階
いであ株式会社	東京都世田谷区駒沢 3-15-1

日仏海洋学会入会申込書

(正会員・学生会員)

	年度より入会	年	月	日申込
氏名				
ローマ字		年	月	日生
住所 〒				
勤務先 機関名				
電話	E-mail:			
自宅住所 〒				
電話	E-mail:			
紹介会員氏名				
送付金額	円	送金方法		
会誌の送り先 (希望する方に○をつける)		勤務先 自宅		

(以下は学会事務局用)

受付	名簿	会費	あて名	学会
	原簿	原簿	カード	記事

入会申込書送付先：〒150-0013 東京都渋谷区恵比寿 3-9-25

(財) 日仏会館内

日 仏 海 洋 学 会

郵便振替番号：00150-7-96503

賛 助 会 員

J F E アドバンテック株式会社	兵庫県神戸市西区井吹台東町 7-2-3
株式会社 イーエムエス	兵庫県神戸市中央区東川崎町 1-3-3 神戸ハーバーランドセンタービル 13F
有限会社 英和出版印刷社	東京都北区中里 2-14-8 シャンボール駒込 101
信幸建設株式会社	東京都千代田区神田司町 2-2-7 パークサイド 18 階
ケー・エンジニアリング株式会社	東京都台東区浅草橋 5-14-10
公益財団法人海洋生物環境研究所	東京都新宿区山吹町 347 藤和江戸川橋ビル 7 階
いであ株式会社	東京都世田谷区駒沢 3-15-1

日仏海洋学会入会申込書

(正会員・学生会員)

	年度より入会	年	月	日申込
氏名				
ローマ字		年	月	日生
住所 〒				
勤務先 機関名				
電話				E-mail:
自宅住所 〒				
電話				E-mail:
紹介会員氏名				
送付金額	円	送金方法		
会誌の送り先 (希望する方に○をつける)		勤務先	自宅	

(以下は学会事務局用)

受付	名簿 原簿	会費 原簿	あて名 カード	学会 記事
----	----------	----------	------------	----------

入会申込書送付先：〒150-0013 東京都渋谷区恵比寿 3-9-25

(財) 日仏会館内

日 仏 海 洋 学 会

郵便振替番号：00150-7-96503